MRI for Technologists

4712-101

MRI of the Brain and Spine

PROGRAM INFORMATION

MRI for Technologists is a training program designed to meet the needs of radiologic technologists entering or working in the field of magnetic resonance imaging (MRI). These units are designed to augment classroom instruction and on-site training for radiologic technology students and professionals planning to take the review board examinations, as well as to provide a review for those looking to refresh their knowledge base in MR imaging.

Original Release Date: **May 2004**

Review Date: **August 2018**

Expiration Date: **May 1, 2021**

This material will be reviewed for continued accuracy and relevance. Please go to www.icpme.us for up-to-date information regarding current expiration dates.

OVERVIEW

The skill of the technologist is the single most important factor in obtaining good quality diagnostic images. A successful MRI examination is the culmination of many factors under the direct control of the technologist.

MRI of the Brain and Spine introduces the learner to the concepts and techniques used in neuroradiological imaging, including surface coil technology, imaging applications, pulse sequences, disease processes, and protocols.

EDUCATIONAL OBJECTIVES

- Describe current surface coil technology, field strength and gradient power, and pulse sequences that drive MRI of the central nervous system
- Characterize specific applications of MR brain imaging, including demyelinating disease, primary brain tumors, and vascular disease
- Explain the techniques of MR angiography and venography
- Discuss why MRI of the fetal brain is superior to ultrasound
- Describe various differential diagnoses including infections, inflammation, and vascular disease and the role of MRI in narrowing the diagnosis
- Apply the correct imaging pulse sequence, plane, and coverage for the major clinical indications for brain MRI
- List the main clinical indications for spinal MRI
- Discuss the most common disease processes evaluated by MRI of the spine
- Describe the most common pulse sequences used for spine imaging
- Explain fundamental imaging requirements for spine imaging

EDUCATIONAL CREDIT

This program has been approved by the American Society of Radiologic Technologists (ASRT) for 3.0 ARRT Category A continuing education credits.

HOW TO RECEIVE CREDIT

Estimated time to complete this activity is 3 hours. The posttest and evaluation are required to receive credit and must be completed online.

- In order to access the posttest and evaluation, enroll in the online course at icpme.us
- Read the entire activity.
- Log in to your account at icpme.us to complete the posttest and evaluation, accessible through the course link in your account.
- A passing grade of at least 75% is required to be eligible to receive credit.
- You may take the test up to three times.
- Upon receipt of a passing grade, you will be able to print a certificate of credit from your online account.
- Your credit certificate will remain in your account as a permanent record of credits earned with ICPME

FACULTY

Thomas R. Schrack, BS, ARMRIT
Manager, MR Education and Technical Development
Fairfax Radiological Consultants, P.C.
Fairfax, VA

Currently serving as Manager of MR Education and Technical Development at Fairfax Radiological Consultants in Fairfax, VA, Thomas Schrack served as Adjunct Faculty Instructor for Northern Virginia Community College from more than 10 years, teaching MR physics and clinical procedures. He serves on the Board of Examiners of the American Registry of Magnetic Resonance Imaging Technologists (ARMRIT) and in 2013 was elected to the Board of Directors. Mr. Schrack is also the Co-Founder and Program Director of the Tesla Institute of MRI Technology, a school offering certification in MRI for radiologic technologists and others interested in entering the field of MRI.

Mr. Schrack is the author of *Echo Planar Imaging: An Applications Guide,* GE Healthcare, 1996, and contributing author, *Magnetic Resonance Imaging in Orthopaedics & Sports Medicine* with David Stroller, MD, 1997. Working with International Center for Postgraduate Medical Education, Mr. Schrack has authored or co-authored several units of the *MRI for Technologists* series, including *MRI Systems and Coil Technology, MR Image Postprocessing and Artifacts, Patient and Facility Safety in MRI, MRI Contrast Agent Safety, Advanced MRI Neurological Applications, MRI of the Brain and Spine, Musculoskeletal MRI, Clinical Magnetic Resonance Angiography, MRI of the Body, and Cardiac MRI.*

Mr. Schrack is a graduate of The Pittsburgh NMR Institute, James Madison University, and Northern Virginia Community College.

CONFLICT OF INTEREST DISCLOSURE

ICPME is committed to providing learners with high-quality continuing education (CE) that promotes improvements or quality in healthcare and not a specific proprietary business interest of a commercial interest.

A conflict of interest (COI) exists when an individual has both a financial relationship with a commercial interest and the opportunity to control the content of CE relating to the product or services of that commercial interest. A commercial interest is defined as any proprietary entity producing healthcare goods or services with the following exemptions: (1) governmental agencies, eg, the NIH; (2) not-for-profit organizations; and (3) CE honoraria received by the faculty or advisors, planners and managers, or their spouse/life partner.

The following faculty, planners, advisors, and managers have NO relationships or relationships to products or devices they or their spouse/life partner have with commercial interests related to the content of this CE activity:

Tom Schrack, BS, ARMRIT

Jacqueline Bello, MD, FACR

Kate Latimer, BSRS, RT (R)(MR)(CT)

Linda McLean, MS

Victoria Phoenix, BS

ACKNOWLEDGMENTS

For their insightful review of this material, special thanks go to:

Jacqueline Bello, MD, FACR
Director of Neuroradiology
Professor of Clinical Radiology and Neurosurgery
Montefiore Medical Center
Albert Einstein College of Medicine
Bronx, NY

Kate Latimer, BSRS, RT (R)(MR)(CT)
Clinical Education Coordinator for MRI
Health Technologies Division
Forsyth Technical Community College
Winston-Salem, NC

Recognition is also due the author of the original material, Gordon Sze, MD, for his significant and lasting contributions.

PROVIDED BY

DISCLAIMER

Participants have an implied responsibility to use the newly acquired information to enhance patient outcomes and their own professional development. The information presented in this activity is not meant to serve as a guideline for patient management. Any procedures, medications, or other courses of diagnosis or treatment discussed or suggested in this activity should not be used by clinicians without evaluation of their patient's conditions and possible contraindications on dangers in use, review of any applicable manufacturer's product information, and comparison with recommendations of other authorities

FDA Drug Safety Communication: FDA warns that gadolinium-based contrast agents (GBCAs) are retained in the body; requires new class warnings

https://www.fda.gov/Drugs/DrugSafety/ucm589213.htm Accessed June 14, 2018.

05-16-2018 Update

In addition to approving the updated prescribing information concerning the gadolinium retention safety issues described in the Drug Safety Communication below, FDA has also approved new patient Medication Guides for all GBCAs.

Health care professionals and patients can access the patient Medication Guides according to the GBCA drug name* on the Medication Guides webpage, or the latest prescribing information by searching in Drugs@FDA.

All MRI centers should provide a Medication Guide the first time an outpatient receives a GBCA injection or when the information is substantially changed. In general, hospital inpatients are not required to receive a Medication Guide unless the patient or caregiver requests it. A health care professional who determines that it is not in a patient's best interest to receive a Medication Guide because of significant concerns about its effects may direct that it not be provided to that patient; however, the Medication Guide should be provided to any patient who requests the information.†

*The brand names of the GBCAs can be found in Table 1 below.
†For more information on distribution of Medication Guides, see the Guidance Document, the Drug Info Rounds Video, or the Code of Federal Regulations at 21 CFR 208.26.

This is an update to the FDA Drug Safety Communication: FDA identifies no harmful effects to date with brain retention of gadolinium-based contrast agents for MRIs; review to continue issued on May 22, 2017.

12-19-2017 Safety Announcement

The U.S. Food and Drug Administration (FDA) is requiring a new class warning and other safety measures for all gadolinium-based contrast agents (GBCAs) for magnetic resonance imaging (MRI) concerning gadolinium remaining in patients' bodies, including the brain, for months to years after receiving these drugs. Gadolinium retention has not been directly linked to adverse health effects in patients with normal kidney function, and we have concluded that the benefit of all approved GBCAs continues to outweigh any potential risks.

However, after additional review and consultation with the Medical Imaging Drugs Advisory Committee, we are requiring several actions to alert health care professionals and patients about gadolinium retention after an MRI using a GBCA, and actions that can help minimize problems. These include requiring a new patient Medication Guide*, providing educational information that every patient will be asked to read before receiving a GBCA. We are also requiring manufacturers of GBCAs to conduct human and animal studies to further assess the safety of these contrast agents.

GBCAs are used with medical imaging devices called MRI scanners to examine the body for problems such as cancer, infections, or bleeding. GBCAs contain gadolinium, a heavy metal. These contrast agents are injected into a vein to improve visualization of internal organs, blood vessels, and tissues during an MRI, which helps health care professionals diagnose medical conditions. After being administered, GBCAs are mostly eliminated from the body through the kidneys. However, trace amounts of gadolinium may stay in the body long-term. Many GBCAs have been on the market for more than a decade.

Health care professionals should consider the retention characteristics of each agent when choosing a GBCA for patients who may be at higher risk for gadolinium retention (see Table 1 listing GBCAs). These patients include those requiring multiple lifetime doses, pregnant women, children, and patients with

inflammatory conditions. Minimize repeated GBCA imaging studies when possible, particularly closely spaced MRI studies. However, do not avoid or defer necessary GBCA MRI scans.

Patients, parents, and caregivers should carefully read the new patient Medication Guide* that will be given to you before receiving a GBCA. The Medication Guide explains the risks associated with GBCAs. Also tell your health care professional about all your medical conditions, including:

- If you are pregnant or think you might be pregnant
- The date of your last MRI with gadolinium and if you have had repeat scans with gadolinium
- If you have kidney problems

There are two types of GBCAs based on their chemical structures: linear and macrocyclic (see Table 1 below). Linear GBCAs result in more retention and retention for a longer time than macrocyclic GBCAs. Gadolinium levels remaining in the body are higher after administration of Omniscan (gadodiamide) or OptiMARK (gadoversetamide) than after Eovist (gadoxetate disodium), Magnevist (gadopentetate dimeglumine), or MultiHance (gadobenate dimeglumine). Gadolinium levels in the body are lowest after administration of Dotarem (gadoterate meglumine), Gadavist (gadobutrol), and ProHance (gadoteridol); the gadolinium levels are also similar across these agents.

*The Medication Guide will be posted once it is approved.

Table 1. FDA-Approved GBCAs*

Brand name	Generic name	Chemical Structure
Dotarem†	gadoterate meglumine	Macrocyclic
Eovist	gadoxetate disodium	Linear
Gadavist†	gadobutrol	Macrocyclic
Magnevist	gadopentetate dimeglumine	Linear
MultiHance	gadobenate dimeglumine	Linear
Omniscan‡	gadodiamide	Linear
OptiMARK‡	gadoversetamide	Linear
ProHance†	gadoteridol	Macrocyclic

*Linear GBCAs result in more gadolinium retention in the body than macrocyclic GBCAs.
†Gadolinium levels remaining in the body are LOWEST and similar after use of these agents.
‡Gadolinium levels remaining in the body are HIGHEST after use of these agents.

To date, the only known adverse health effect related to gadolinium retention is a rare condition called nephrogenic systemic fibrosis (NSF) that occurs in a small subgroup of patients with pre-existing kidney failure. We have also received reports of adverse events involving multiple organ systems in patients with normal kidney function. A causal association between these adverse events and gadolinium retention could not be established.

We are continuing to assess the health effects of gadolinium retention in the body and will update the public when new information becomes available. We are requiring the following specific changes to the labeling of all GBCAs:

- A *Warning and Precaution*
- Changes related to gadolinium retention in the *Adverse Reactions, Pregnancy, Clinical Pharmacology*, and *Patient Instructions* sections

We urge patients and health care professionals to report side effects involving GBCAs or other medicines to the FDA MedWatch program.

MR Imaging of the Brain

Bolded items can be found in the glossary

After completing this educational material, the learner will be able to:

- Describe current surface coil technology, field strength and gradient power, and pulse sequences that drive MRI of the central nervous system
- Characterize specific applications of MR brain imaging, including demyelinating disease, primary brain tumors, and vascular disease
- Explain the techniques of MR angiography and venography
- Discuss why MRI of the fetal brain is superior to ultrasound
- Describe various differential diagnoses including infections, inflammation, and vascular disease and the role of MRI in narrowing the diagnosis
- Apply the correct imaging pulse sequence, plane, and coverage for the major clinical indications for brain MRI

INTRODUCTION AND OVERVIEW

The brain continues to be the most frequently imaged organ by MR imaging (**Figure 1**). Technological developments in computer design and processing speeds as well as hardware developments have enabled significant growth in MR brain imaging. This growth is evident in the broad spectrum of brain applications, postprocessing techniques, and increased spatial resolution of images. Beyond simple anatomical imaging of the brain, advanced techniques now include functional MRI (fMRI), such as blood oxygen-level dependent (BOLD) imaging and 3D proton spectroscopy, diffusion tensor imaging (DTI), perfusion imaging, and volumetric measurements. However, basic techniques remain the foundation for all MR brain imaging.

This material reviews MR brain imaging surface coils, explains standard MR techniques for imaging the brain, explores the more advanced brain applications, and offers standard MR brain imaging protocols.

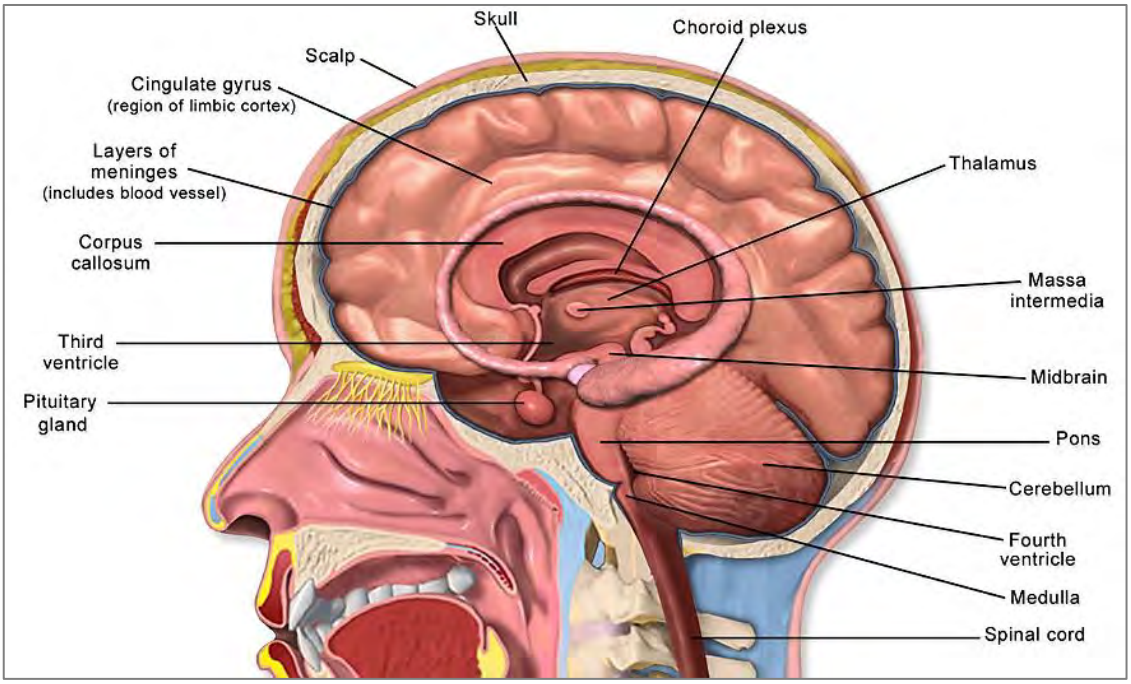

Figure 1. Anatomy of the brain.
Courtesy of Bruce Blausen. Available at Wikimedia Commons

CURRENT SURFACE COIL TECHNOLOGY

In MR imaging, the use of surface coils near the area of interest greatly boosts the **signal-to-noise ratio** (SNR). Surface coils for brain imaging usually consist of two types: single-channel transmit/receive coils and high-channel phased array coils.

Single-Channel Transmit/Receive Head Coils

Single-channel transmit/receive coils are a whole volume "bird-cage" design that surrounds the entire head to below the level of C2 or C3 (**Figure 2**). This type of coil usually employs a quadrature design to further boost SNR, and the coil serves as both a transmit and receive antenna. The transmit field is well-tuned and directed to the head area, reducing the **specific absorption rate** (SAR) — the amount of RF energy in kilowatts (kW) permitted to be transmitted to the patient.

Figure 2. Single-channel transmit/receive head coil. *Courtesy of GE Healthcare.*

This whole volume design provides adequate SNR for most general brain applications when small detail is not required as in tumor imaging, stroke evaluation, and ventricular assessment. However, in order to visualize very small pathology such as small MS lesions or pituitary micro-adenomas, scan times can become unacceptably long in order to attain the required SNR. The development of phased array technology has addressed this issue.

High-Channel Phased Array Coils

The development of phased array technology addressed both SNR issues and concerns about anatomical coverage. The higher SNR provided by high-channel brain phased array coil design allows for imaging with higher spatial resolution — smaller voxels, thinner slice acquisitions, and small fields-of-view for greater detection of small pathology and small-vessel **stenoses**.

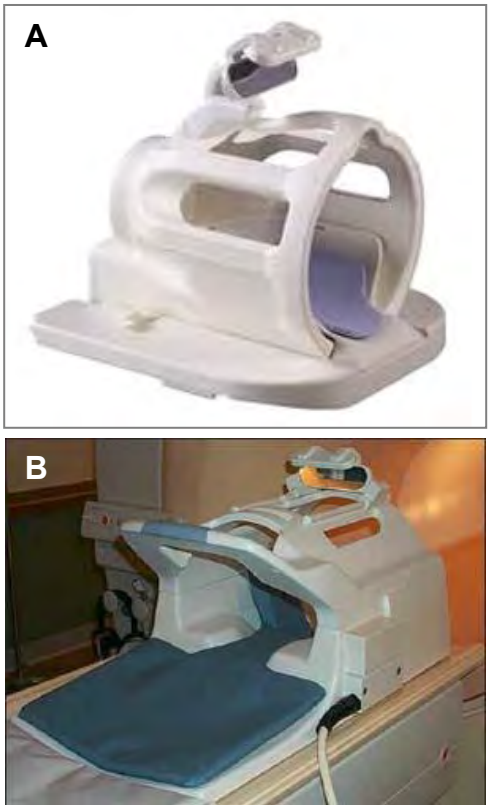

Figure 3. (A) Eight-channel phased array head coil. (B) Neurovascular phased array coil. *Courtesy of Philips Healthcare.*

Contrast-enhanced MR angiography (MRA) allowed for assessing not only intracranial vasculature but the extracranial carotid and vertebral arteries. In order to image the vessels of the brain and the neck without exchanging the head coil for a neck coil, a combined head/neck coil was needed. However, as a single-channel, the coil element would be too large to yield adequate SNR. The development of the phased array head/neck coil with numerous elements permitted large coil coverage with small coil SNR. In addition, head-only coils benefited from phased array coil design by greatly increasing the SNR as compared to the same design using a single-coil element (**Figure 3**).

FIELD STRENGTH AND GRADIENT POWER

Since the early 2000s, the growth of higher field strength MRI systems has been accelerating. Prior to 2000, “high field” MRI systems in clinical use were typically 1.5 **tesla** (15,000 **Gauss**). Today, clinical 3.0T MRI systems are common. A 3.0T MRI system uses a main magnetic field 2x as great as a 1.5T unit and 4x greater than most of the open MRI systems.

In MRI, protons are the essential ingredient that fuels SNR — the more protons that can be excited, the greater the SNR yield (all other factors remaining the same). In other words, the higher the field strength, the greater the number of excited protons for a given sample. 3.0T MRI systems yield far greater SNR than lower field strength systems per unit of time spent scanning, allowing for faster scan times, higher spatial resolution, or a combination of the two. Neurologic and musculoskeletal applications have particularly benefited from these higher field MRI systems (**Figure 4**).

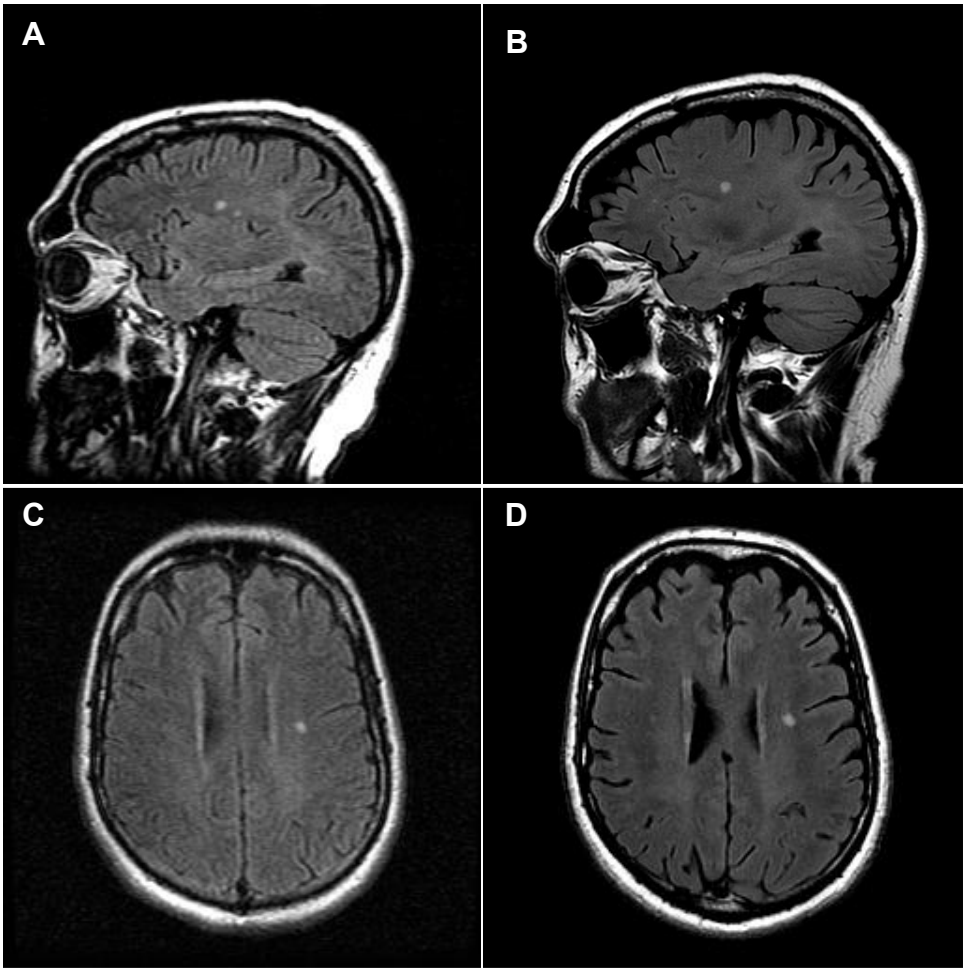

Figure 4. Sagittal and axial FLAIR images from the same patient one year apart. Images A and C were scanned on a 1.5T single-channel head coil. Images B and D were scanned on an 8-channel phased array head coil on a 3.0T system. Overall signal-to-noise ratio and visual sensitivity is greater on Images B and D, demonstrating technical advantages of phased array coils and higher field strength imaging.

An MRI system's "engine" is the gradient subsystem; gradient power drives neuro-based MRI applications. In order to excite a very specific area of tissue and spatially encode the data, the main magnetic field ($\mathbf{B_0}$) must be altered along a very rigid coordinate. Six pairs of cabled windings (two in each **orthogonal** direction of x, y, and z) add to, or take away from, the B_0 field, which changes the processional frequencies of excited protons. The magnitude of change in the B_0 field is the gradient **amplitude** and is measured in millitesla/meter (mT/m). The time to achieve this change is **rise time** and is measured in microseconds (µs or 1/1000 millisecond). The slope of these two parameters is expressed in **slew rate** and measured in tesla/meter/sec. An MRI system with a more powerful gradient subsystem achieves:

- faster scanning (shorter minimum **repetition time** [TR])
- sharper, less distorted images (shorter minimum echo spacing)
- fewer flow-related artifacts (shorter minimum **echo time** [TE])
- thinner slice profiles
- smaller fields-of-view (FOV)

Clearly neurological MR imaging has benefited greatly from the technical developments of recent years. This evolution has not only improved long-existing neuro applications but has fueled the development of new applications like diffusion tensor imaging and perfusion imaging that use extremely fast echo planar (EPI) pulse sequences.

Techniques

Techniques used in head MRI are not written in stone. Each facility decides on the best method for imaging the brain based on their MRI system configuration, patient and referring physician needs, and prevailing academic literature. That being said, there is much common ground across facilities for routine brain imaging. Standards for imaging have emerged through the use of common protocols.

Routine MR brain imaging typically consists of T1-weighted sagittal images, T2-weighted axial images, and T2-weighted axial fluid-attenuated inversion recovery (FLAIR). With FLAIR images, pathology generally appears hyperintense due to the optimization of the **inversion time** (TI) required to null the signal of water. The **cerebrospinal fluid** (CSF) in FLAIR images appears to be of relatively low intensity compared to conventional proton density (PD) spin echo images. This offers a decided benefit since low-intensity CSF has two advantages. First, lesions directly adjacent to CSF, particularly in the periventricular region, are better differentiated from CSF. Second, lesions such as hemorrhage or infectious **exudates** may replace CSF in the sulci to appear hyperintense on FLAIR images but may be difficult to detect on conventional proton density spin echo images. For this reason, FLAIR imaging has largely replaced proton density-weighted imaging for many brain imaging indications.

For T2-weighted imaging, fast spin echo (FSE) or turbo spin echo (TSE) techniques are used. FSE or TSE techniques are widely used because of the reduction in scan time for these sequences. High-gradient power MR systems offer greater reduction of echo spacing so that FSE/TSE-associated blur is not as much of a concern. Moreover, reduced sequence time allows higher spatial resolution imaging.

In addition, axial diffusion-weighted imaging (DWI) has become common. Usually EPI-based, this sequence is extremely fast and especially useful for detecting areas of ischemia.

Axial T1-weighted images are also acquired in general brain imaging. However, the type of T1 sequence may vary from facility to facility. Four variations of T1 imaging are conventional spin echo, fast/turbo spin echo, spoiled gradient echo, and T1 FLAIR.

Conventional Spin Echo Imaging

Conventional spin echo (SE) imaging yields high-contrast T1 images that are generally free of flow motion artifacts when corrective measures such as presaturation pulses are employed. Compared to the other methods however, this method suffers from longer scan times, particularly when thin slices (<3.0mm) require extra imaging time to acquire the desired SNR and anatomical coverage.

Fast/Turbo Spin Echo Imaging

Fast/turbo spin echo imaging can also yield high-contrast T1 images with greatly reduced scan times, but more care is required. Since this method of scanning acquires echoes during the T2 decay cycle, each line of **k-space** may have a differing amount of T2 decay information, potentially resulting in image blur. Additionally, with FSE/TSE, more T2 information can be displayed. To reduce blur and excess T2 information, care must be taken to optimize the echo spacing (ESP) as well as the echo train length (ETL). The common methods for achieving this are to reduce the ETL while increasing the receive bandwidth of the MR system.

Spoiled Gradient Echo

Spoiled gradient echo (SPGR) T1 imaging is a well-understood imaging variation of gradient echo imaging (GRE). GRE imaging uses gradient-reversal to refocus the transverse magnetization. This pulse sequence is designed to be faster than standard spin echo imaging. However, GRE typically employs shorter TRs as compared to SE techniques. These very short TRs are often shorter than the T2 times of some tissues, for example, CSF. If TR is shorter than the T2 of a tissue, its transverse magnetization never decays completely. This residual transverse magnetization is problematic since the leftover transverse signal is from long T2 tissues. This means that as long as transverse magnetization exists, the image will always have significant T2 weighting (**Figure 5A**).

To remove the transverse magnetization, MR systems typically employ either a radiofrequency pulse or another gradient application to “spoil” the transverse magnetization. Along with an optimized TR and flip angle, the spoiler pulse in a GRE sequence yields excellent T1 weighting. SPGR can be both fast and effective in T1 imaging (**Figure 5B**). Moreover, SPGR is naturally effective at reducing artifacts from flowing blood because the gradient refocusing pulse acts as a flow compensator. However, all gradient echo-based pulse sequences fail to refocus spins that have decayed from susceptibility-related causes. These include **dephasing** caused by metal in the area of interest, eg, surgical clip; tissue-air interfaces, eg, brain-sinus; and compact bone-tissue interfaces, eg, **petrous** ridge-brain interface. This type of dephasing (termed T2’ [prime]) leaves a void in these areas, exacerbating signal loss compared to SE and FSE pulse sequences.

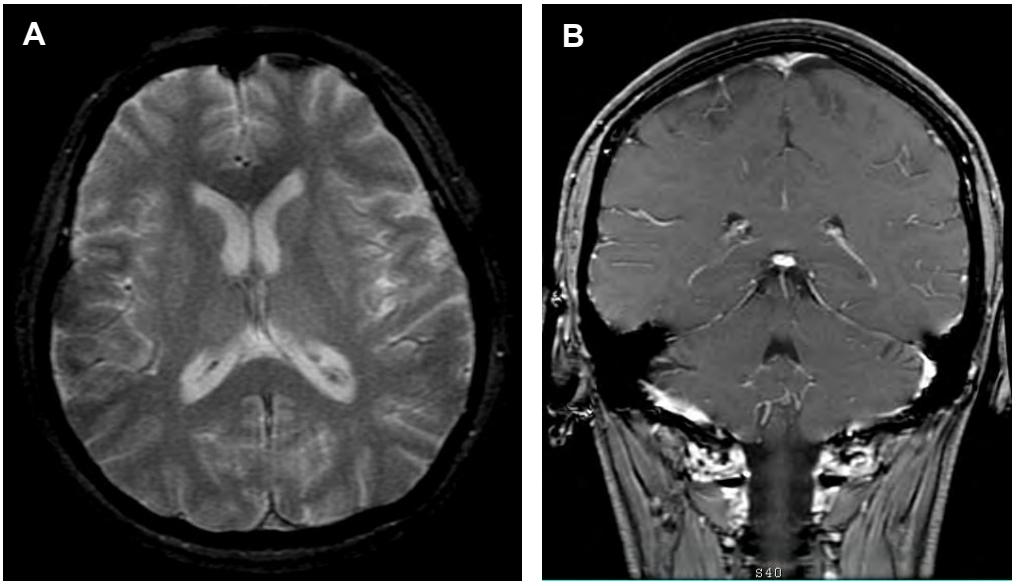

Figure 5. (A) Axial GRE. Note hyperintense cerebrospinal fluid demonstrating T2* contrast due to residual transverse magnetization. (B) Coronal SPGR. Demonstrates hypointense cerebrospinal fluid showing the "spoiling" of the residual transverse magnetization. (Hyperintense signal in the superior sagittal sinus and transverse sinuses is due to administration of gadolinium contrast).

T1 FLAIR

Fluid-attenuated inversion recovery, as the name implies, is an inversion recovery-based pulse sequence that utilizes a specific TI selection specifically set to provide maximum T1 contrast between tissues. The TI time is typically set to the null point of cerebrospinal fluid. Because CSF has such a long T1 time, it follows that the TR time is also long. For example, at 1.5T, the TI for a T1 FLAIR is approximately 2200 milliseconds. Such a relatively long TI time necessitates the use of a relatively long TR as well, typically 3500msec or longer. This long TR increases scan time as compared to FSE/TSE and GRE-based pulse sequences. However, the degree of T1 contrast in a T1 FLAIR compared to the three spin echo techniques may warrant the extra scan time because of the superior quality of T1 FLAIR (**Figure 6**).

Regardless of the T1-weighted pulse sequence selected, the axial plane is typically done both pre- and postcontrast administration.

The small collection of sequences just discussed forms the nucleus for the basic MR brain examination. When MRI originated, these sequences were all that were available. Needless to say, the number of potential techniques has multiplied dramatically since then, presenting the technologist with many sequence options.

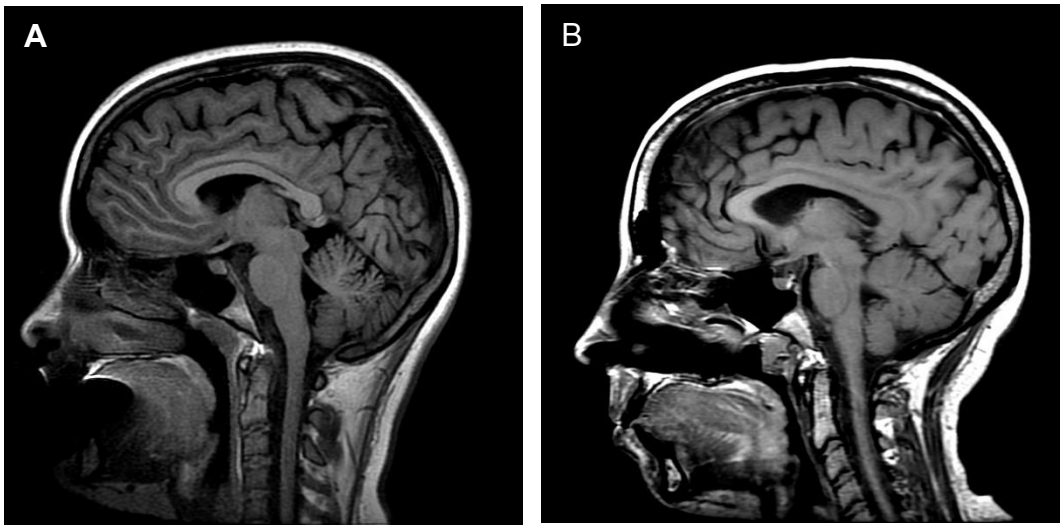

Figure 6. (A) Sagittal T1 FLAIR. Note the increased contrast between gray and white matter. (B) Sagittal fast/turbo spin echo. While both images demonstrate T1 weighting, T1 FLAIR often exhibits greater T1 contrast compared to the spin echo-based sequences.

Slice Thickness

Slice thickness is usually standardized in the basic examination, with the norm being 4.0-5.0mm sections separated by an interslice gap of 1.0mm thickness. If the lesions being considered are small, much thinner sections can be used with a reduced interspace gap or none at all. For example, if pituitary pathology is suspected, the initial sagittal sequence may consist of 3.0mm or thinner sections.

The **number of excitations** or **number of signal averages** (NEX/NSA) is generally kept to a minimum to balance SNR requirements with shorter scan time. However, if very thin sections are used and particularly if good signal-to-noise ratio is sought, an increased number of excitations may be employed. Repetition time and echo time for T1-weighted images are generally optimized to maximize T1 weighting. Similarly for T2-weighted spin echo images, repetition time is generally kept between 2,000msec-4000msec since the length of the scan is directly dependent upon the repetition time.

In specialized circumstances, three-dimensional T1-weighted spoiled gradient echo sequences are also useful. Three-dimensional techniques have the advantage of being able to section a block of excited tissue into very thin partitions, allowing for better spatial resolution. 3D techniques also tend to enhance gray matter-white matter differentiation. T1-weighted SPGR technique can be useful in clinical conditions in which very small structural abnormalities of gray matter, such as the hippocampi or cortical dysplasia are encountered, as in seizure cases. Since seizures typically involve the temporal lobe, imaging in the coronal plane is optimal.

Contrast Enhancement

Gadolinium-based contrast enhancement is useful in brain imaging. Physicians often believe that administration of contrast is indicated for all lesions. Three conditions must be met in order for contrast enhancement to occur:

1. An adequate blood supply to the lesion must exist
2. **Blood-brain barrier** (BBB) breakdown must be present
3. Sufficient extracellular space must be available for the contrast agent to localize after it has leaked out of the vasculature

In cases in which lesions do not enhance, the lack of enhancement in and of itself provides useful clinical information (**Figures 7 and 8**).

Especially because of its ability to assess the integrity of the blood-brain barrier, the use of contrast is useful for characterizing lesions. For example, high-grade gliomas tend to have greater blood-brain barrier disruption and therefore tend to display greater contrast enhancement than low-grade gliomas. Exceptions include juvenile pilocytic astrocytomas, which are low-grade tumors but which will generally enhance.

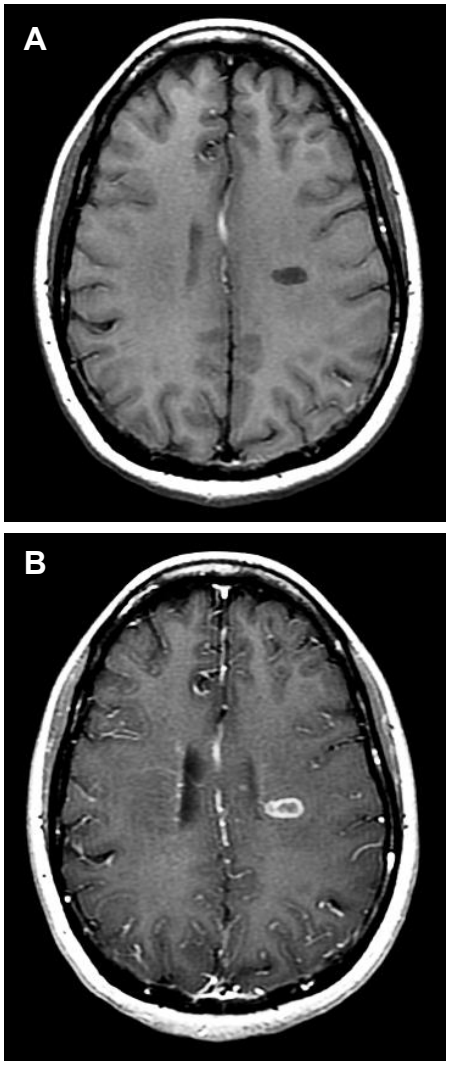

Figure 7. MS plaque. (A) Axial spin echo T1W image precontrast. (B) The same image location postcontrast.

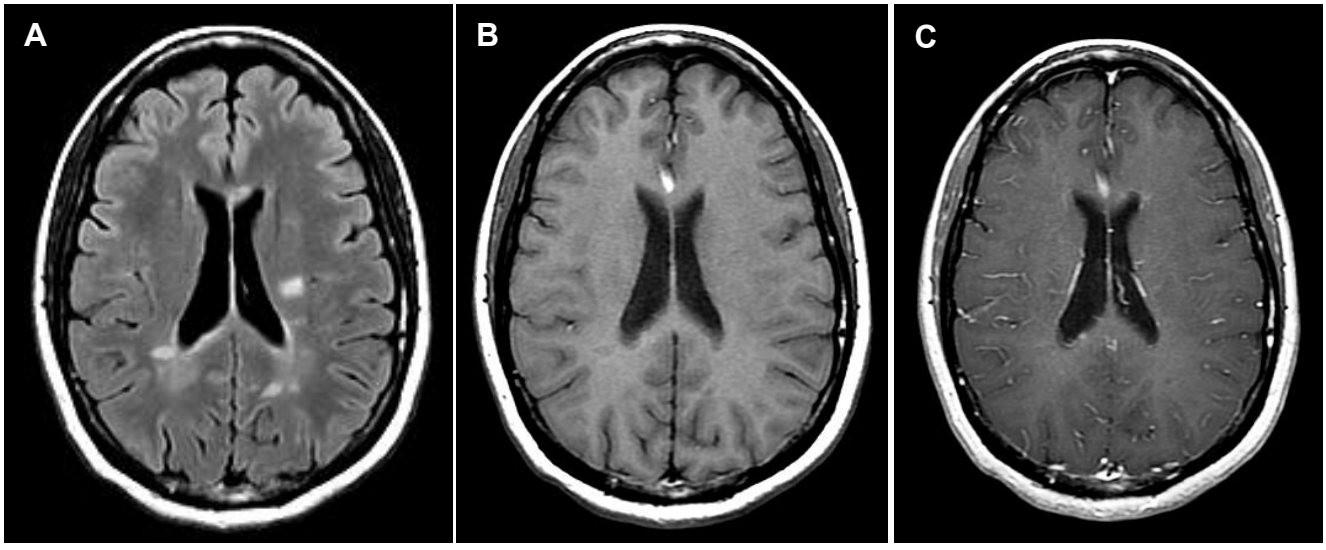

Figure 8. Demonstration of non-enhancing MS lesion. (A) Axial T2 FLAIR displaying several MS plaques in the periventricular white matter. (B) Precontrast spin echo T1W image of the same location. (C) Same location postcontrast spin echo T1; note the lack of contrast enhancement.

Similarly, active multiple sclerosis plaques tend to have greater blood-brain barrier disruption and tend to enhance as compared to chronic plaques. Thus, in patients with multiple sclerosis, T2-weighted and FLAIR imaging are essential for chronic, inactive plaque visualization (**Figure 9**).

Not only can the use of contrast demonstrate which plaques are more active, contrast aids in the staging of lesions. For example, areas of **infarct** only enhance a few days after occurrence, and enhancement generally lasts up to approximately two weeks. If a patient has a suspected infarct that demonstrates enhancement months after the event, then another etiology, such as an underlying tumor, must be considered.

Figure 9. (A) Coronal and (B) post-contrast axial T1W images demonstrating a large enhancing anterior midline meningioma.

BRAIN IMAGING FOR SPECIFIC INDICATIONS

Along with typical brain imaging discussed above, specific indications often require particular additions or changes to the imaging protocol. This section addresses many of the common indications in brain imaging.

Please note that the recommendations provided are only suggestions and should not be viewed as imaging technique requirements.

Imaging of Multiple Sclerosis

Some diseases occur almost exclusively in the white matter and are typically demyelinating diseases; the most common is multiple sclerosis.

Demyelinating Disease

MRI is particularly effective at detecting demyelinating disease and was the first imaging modality to effectively visualize demyelinating disease. Typically MS plaques occur anywhere in the periventricular white matter and are well seen on FLAIR or proton density images. The presence of plaque in structures that are not typically affected by small vessel disease, such as the corpus callosum, is very helpful in making the diagnosis. Active plaques will enhance, with ring-like or nodular patterns and after several weeks generally cease to enhance.

Because MS is a disease of both **demyelination** and **axonal** destruction, more chronic plaques usually display the “black hole” appearance. Due to destruction of the axons within the plaque, the center of the plaque frequently appears hypointense on T1 weighting.

In addition to the presence of plaque, multiple sclerosis is also characterized by brain volume loss (atrophy). Using techniques such as **magnetization transfer imaging** (MTI), even normal-appearing white matter can be found to have abnormalities in MS patients. The result of this process is the reduction of signal intensity in stationary tissues. Magnetization transfer is commonly used with intracranial MRA sequences to suppress signal in the brain, creating higher contrast between cranial arteries (bright) and surrounding brain tissue (dark).

Since MS is a disease that by nature undergoes remission and exacerbation, often it is not clear if patients under therapy are improving. Patients may symptomatically improve since the lesion causing the primary symptoms is improving, but simultaneously there may be lesions developing in the silent parts of the brain. MRI, particularly with contrast enhancement, is especially effective for lesion detection and characterization. That is, if a patient reports improvement while receiving one of the new immune modulation therapies but MR shows new enhancing plaques, therapy would be considered to be unsuccessful.

Although imaging of the brain specific to MS is similar to a routine brain protocol, there are a few important differences.

In addition to the more standard sagittal T1-weighted series, most facilities use a sagittal T2 FLAIR, which is extremely well-suited for visualizing the plaques associated with MS (**Figure 10**).

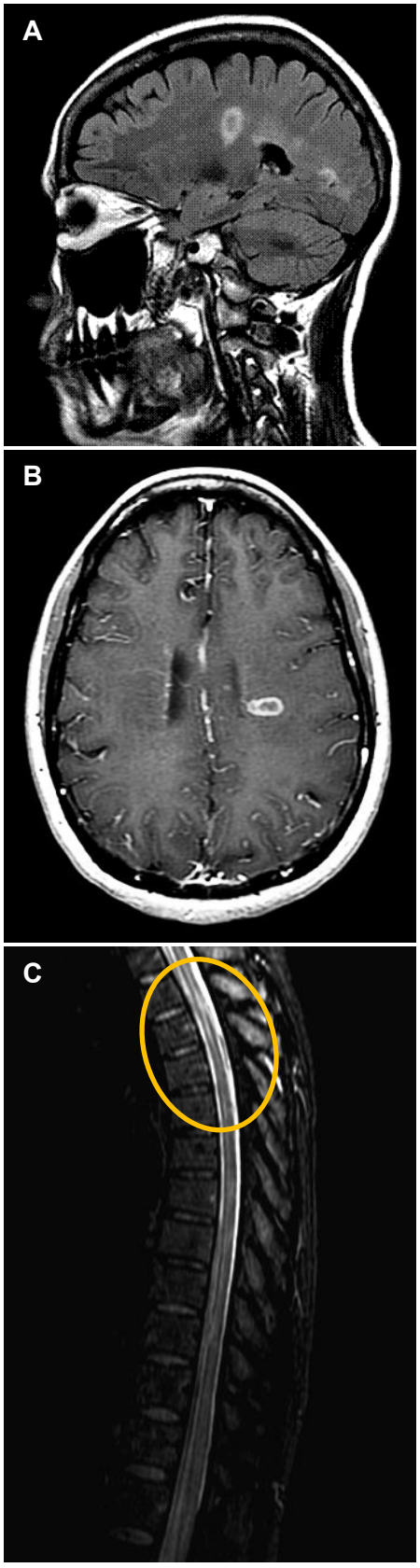

Figure 10. (A) Sagittal T2 FLAIR. (B) Axial T2 FLAIR. Both images demonstrate MS plaques in the periventricular white matter. (C) Sagittal STIR of the thoracic spine demonstrating plaque appearance (circle).

The plaques appear hyperintense against the white matter. It is important that the coverage for this series encompasses the entire brain as plaques can be widely dispersed throughout the white matter.

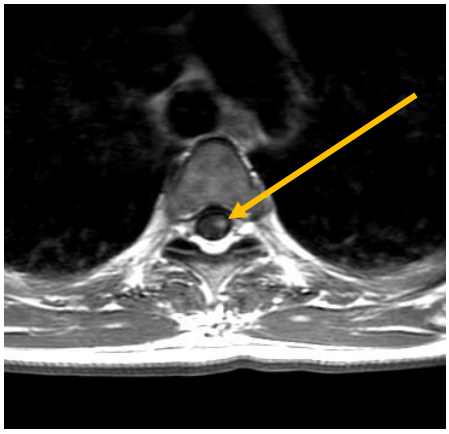

Figure 11. Postcontrast axial T1 demonstrating enhancement of the spinal cord in the thoracic spine.

Postcontrast imaging is considered standard of care when imaging demyelinating disease. One important difference in contrast-enhanced imaging of the routine brain versus demyelinating disease is the postcontrast pulse sequences. Specifically, axial T2 FLAIR is typically performed at least five minutes postcontrast administration. Compared to precontrast T2 FLAIR, many users report greater plaque visualization on T2 FLAIR postcontrast, provided the interval from time of injection to time of imaging is at least five minutes (**Figure 10 and Figure 11**).

Imaging of Primary Brain Tumors

Primary brain tumor imaging typically includes the routine pre- and postcontrast brain protocol but with important additions. It is important to note that adults and children typically present with different tumor types.

Intraaxial Tumors

Gliomas are common primary tumors that are **intraaxial**, meaning they occur inside the brain tissue itself. Gliomas are classified as Grade I, II, III, and IV; the higher the grade, the more malignant and aggressive the tumor. There are multiple types of gliomas, including astrocytomas, glioblastomas, and mixed neuronal-glial tumors such as oligodendrogliomas, gangliogliomas, and dysembryoplastic neuroepithelial tumors (DNET).

The protocol for primary brain tumor imaging is the same regardless of age. First, smaller tumors may require thinner slice acquisitions. Instead of the typical 4.0-5.0mm thickness, 3.0mm slice thicknesses or thinner may be needed to clearly define boundaries of the tumor in both the pre- and postcontrast series.

In children, the most common primary tumors — medulloblastomas, ependymomas, and juvenile pilocytic astrocytomas — typically occur in the posterior fossa. Because of the confinement of the posterior fossa, impingement on the fourth ventricle is frequently seen, and obstruction to CSF flow results in hydrocephalus.

Primary intraaxial tumors of the pineal gland can arise; these may be either germinomas or pineal cell tumors. Similarly, tumors of the pituitary also occur, especially pituitary adenomas. These tumors are best studied with imaging protocols tailored to the tumor's specific location. While contrast is typically given to define tumor enhancement, in the case of pituitary microadenomas, the contrast outlines relatively nonenhancing microadenoma. In other words, since the surrounding pituitary tissue lies outside of the blood/brain barrier (**Figure 12**), it shows marked enhancement, while the relatively nonenhancing microadenoma stands out by comparison. Imaging of the pituitary gland is discussed in detail later in this material.

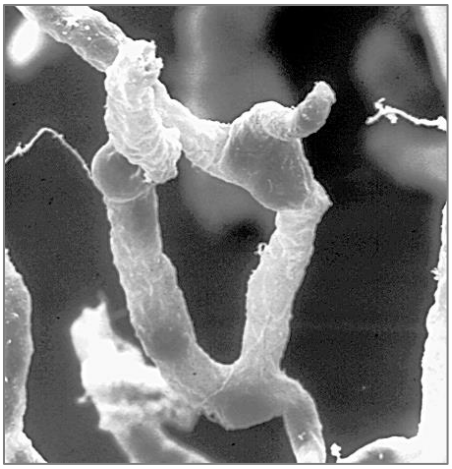

Figure 12. Part of the blood brain barrier. A network of capillaries supplies brain cells with nutrients. Tight seals in the capillary walls keep blood toxins, as well as beneficial drugs, out of the brain. *Courtesy of Dan Ferber*.[1]

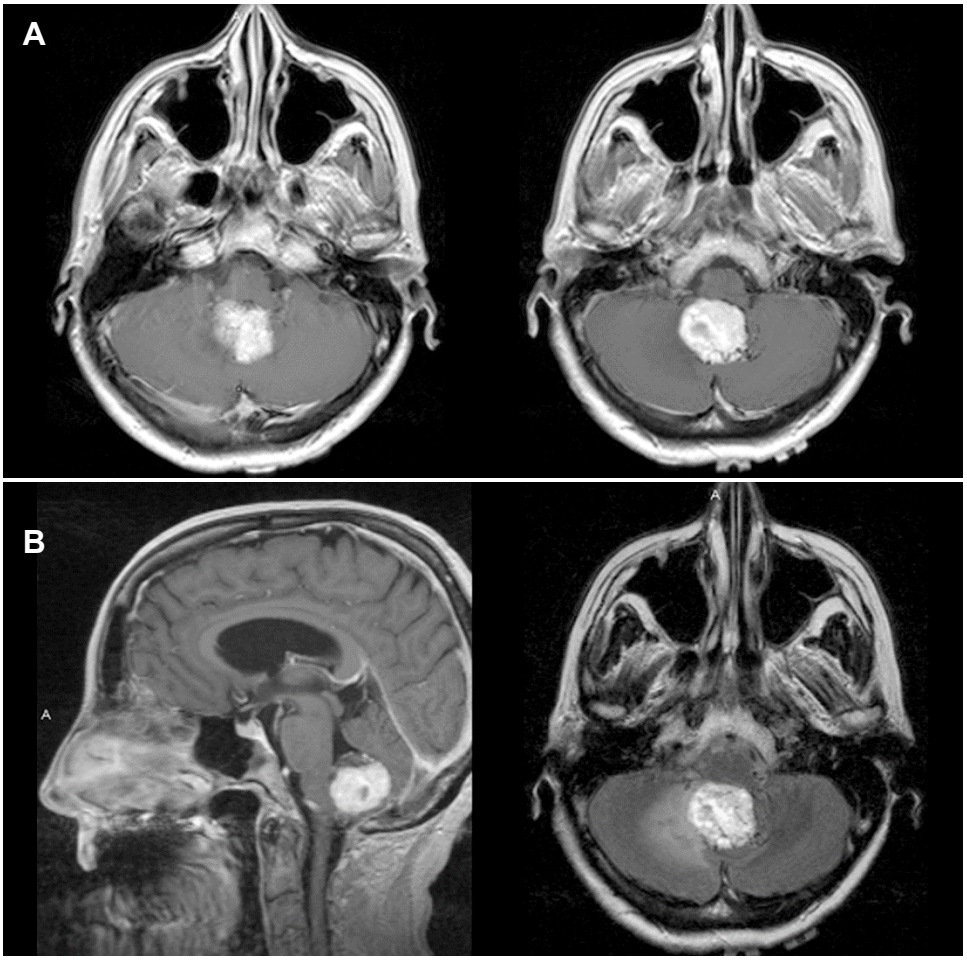

Figure 13. Hemangioblastoma. (A) Postcontrast axial T1. (B) Postcontrast axial and sagittal T1 proton density image.

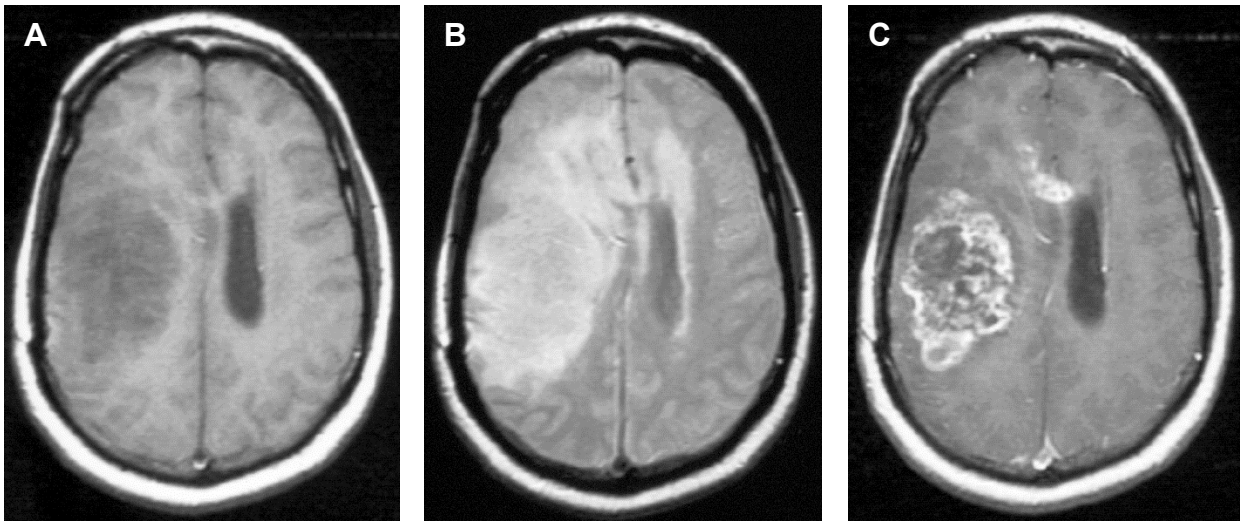

Figure 14. A 32-year-old patient with weakness and seizures. (A) Axial T1W image. (B) Axial proton density image. (C) Axial T1W image with contrast. The images show a glioma extending across the corpus callosum.

On MRI, **metastases** may appear similar to primary tumors. Metastatic tumors are slightly hypointense on T1-weighted images and hyperintense on proton density and T2-weighted images. However, there are some differences between primary and metastatic tumors. First, metastases are frequently associated with marked surrounding edema. Second, they are frequently, although not always, multiple. Third, metastases almost always enhance. Fourth, metastases are typically located at the gray matter-white matter junction. Therefore, multiple enhancing lesions in a patient with known breast or lung carcinoma are indicators of brain metastases (**Figures 13 and 14**).

Extraaxial Tumors

Extraaxial tumors are tumors that lie outside the brain tissue along the dura, within the subdural and epidural spaces, along the vasculature, or in the skull itself. These tumors are imaged using essentially the same protocols for intraaxial tumors. Examples of extraaxial tumors are meningiomas, pituitary adenomas, meningeal carcinomatosis, and acoustic neuromas/ vestibular schwannomas (**Figure 15**).

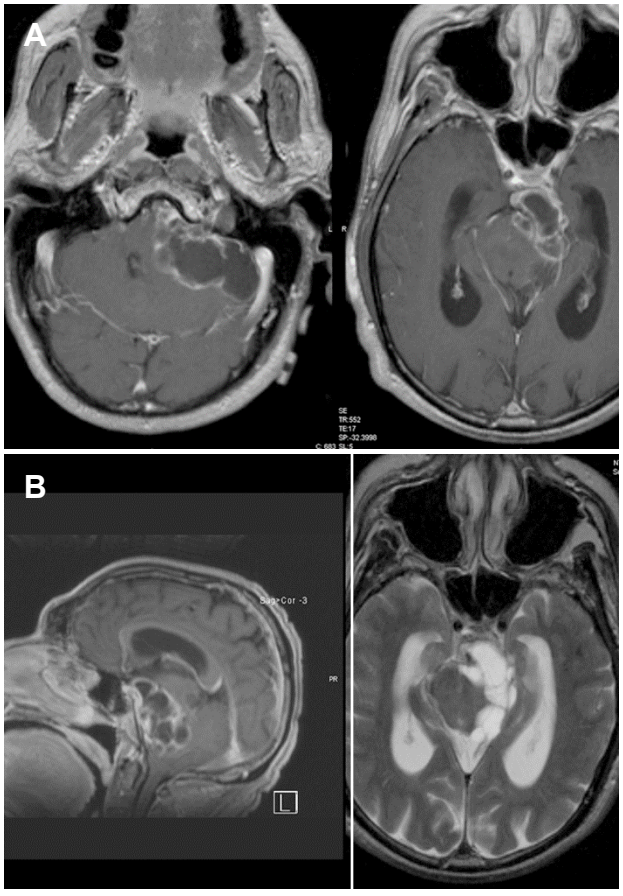

Figure 15. Schwannoma. (A) Axial T1W postcontrast images. (B) Sagittal T1W postcontrast image (left) and axial T2W image (right).

Spectroscopy in Brain Imaging

In some instances such as a suspected low-grade glioma that does not enhance, magnetic resonance spectroscopy (MRS) may be useful. Spectroscopy may help in differentiating tumor from edema or other pathology and in differentiating tumor recurrence from radiation **necrosis**. It is important to note that MRS can be highly subjective, and its success depends on numerous factors, some of which are beyond the control of the technologist. B_0 homogeneity must be excellent, and automated small-volume shimming has to be employed as well. Moreover, the lesion location needs to be a sufficient distance away from areas of high susceptibility, such as the parasinuses, skull base, and petrous ridges. Typical tumor signatures will show decreased N-acetyl-aspartate (Naa) peaks and increased choline (**Figure 16**).

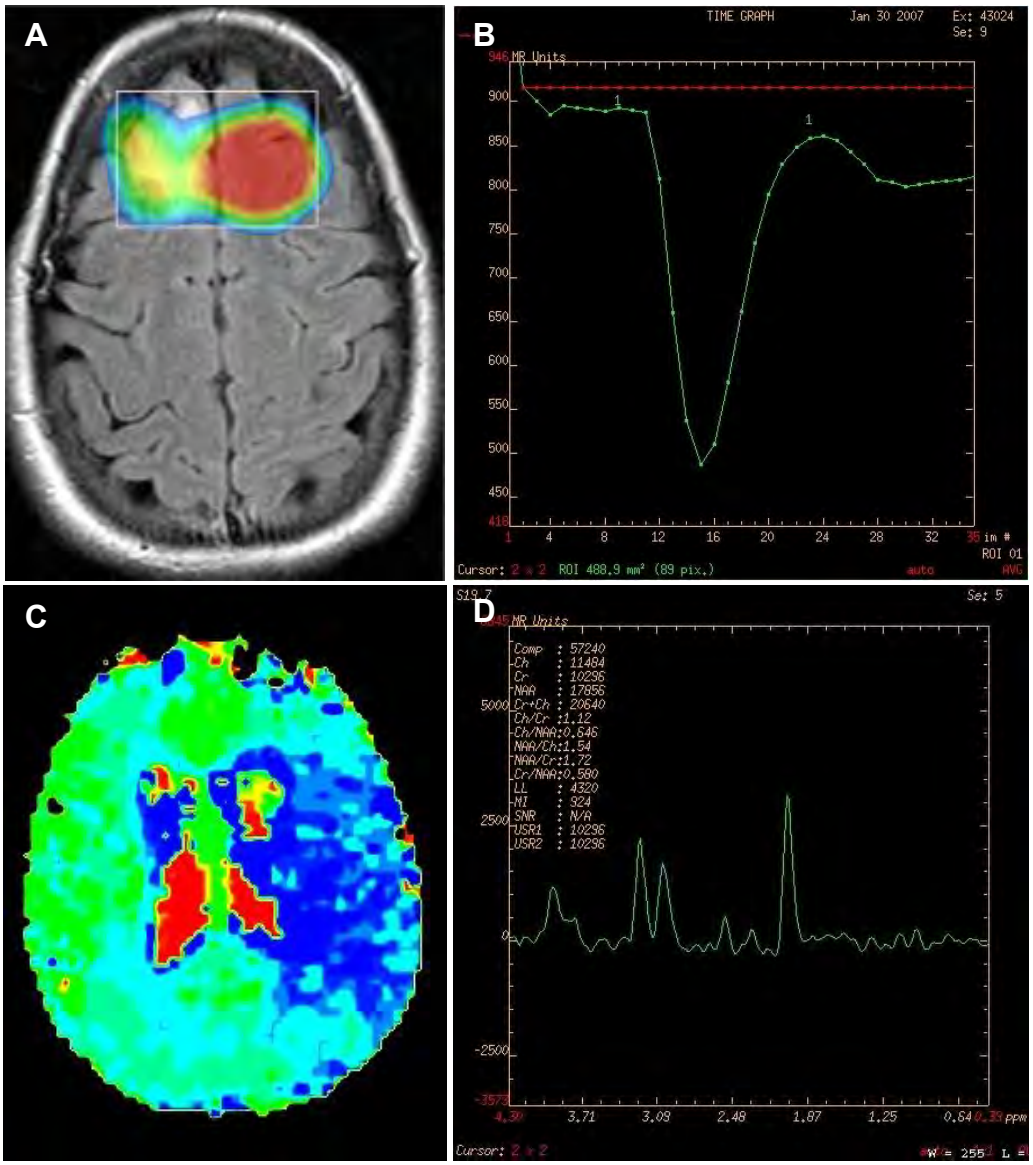

Figure 16. (A) Spectroscopy metabolite map reveals high concentrations of Naa (red) and abnormally low Naa levels (yellow). (B) Graphic spectrum. (C) Brain perfusion relative to rCBV showing lower blood volume on the left (dark blue) as compared to the right (light blue/green). (D) Wash-in/out time course graph.

Perfusion in Brain Imaging

MR perfusion is most often a single-shot EP-based sequence. Imaging is accomplished by very rapidly scanning the area in question over many phases during contrast administration. As discussed earlier, normal brain tissue prevents gadolinium from crossing the blood-brain barrier. In MR perfusion, imaging is done rapidly enough to observe and measure the relative cerebral blood volume (rCBV) and relative cerebral blood flow (rCBF). Postprocessing of the large data sets of hundreds of images yields maps that distinguish areas of low perfusion (indicating necrosis) from areas of normal perfusion to areas of very high perfusion (indicating possible recurrent tumor).

In the evaluation of tumor and recurrence, MR brain perfusion can be extremely useful, particularly following radiation therapy. Radiation therapy causes brain necrosis at the point where the radiation is concentrated, and necrotic tissue is often surrounded by edema. However, recurrent tumor can often produce edemic fluid. Thus, to differentiate between recurrent tumor and radiation necrosis, brain perfusion may be useful.

Imaging of the Sella Turcica

The **sella turcica**, a saddle-shaped depression in the sphenoid bone, contains the important pituitary gland, an endocrine gland that produces several hormones depending on sex, age, environment, etc. Among those hormones are thyroid hormone, growth hormone, prolactin, and sex hormones. Tumors of the pituitary gland typically fall into two categories: micro- and macroadenomas. These benign tumors are classified according to their size. An adenoma less than 10mm is considered a microadenoma, whereas a tumor greater than 10mm is a macroadenoma. Regardless of tumor type, MR imaging of the brain to exclude or characterize a pituitary adenoma is typically the same. Again, along with the routine brain protocol, there are several additional sequences designed not only to visualize the tumor but to characterize it by visualizing its function as well (**Figure 17**).

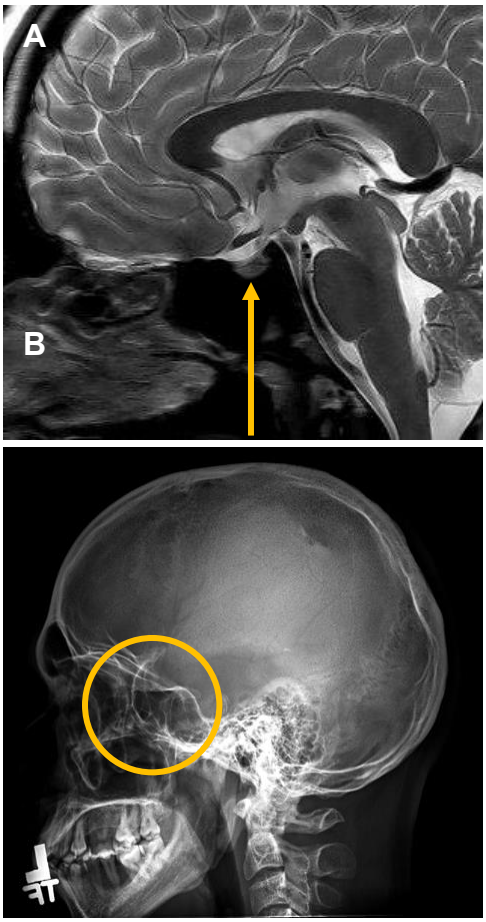

Figure 17. (A) Sagittal T2W high resolution image of the brain displaying the pituitary gland within the sella turcica, which is hypointense and invisible (arrow). (B) Lateral radiograph of the skull demonstrating the bony structure of the sella turcica (circle). *Courtesy of Toshiba America Medical Systems.*

Because the pituitary is a small gland, high spatial resolution is required. Thoroughly imaging the pituitary requires very thin slice acquisitions of 3.0mm or less and a relatively small **field-of-view** of 16-18cm.

Usually a series of coronal and sagittal T1W images is acquired both pre- and postcontrast administration (**Figure 18**). Utilizing both thin slice thickness and small FOV increases spatial resolution but also decreases SNR. To maintain SNR at levels that will yield acceptable image quality, the number of signal averages or number of excitations will need to be increased as well.

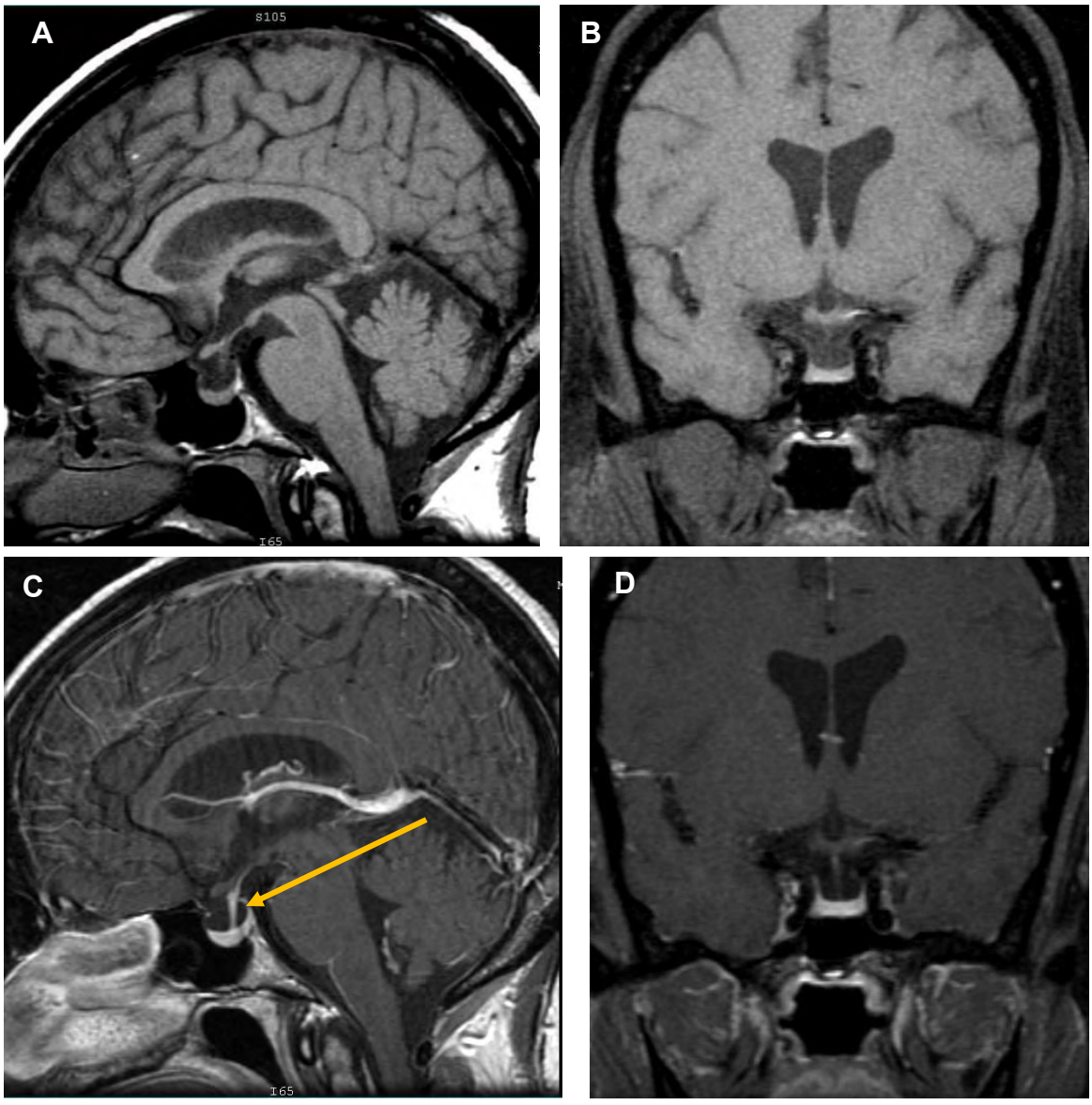

Figure 18. (A & B) Sagittal and coronal T1W images of the pituitary gland precontrast. (C & D) Postcontrast images demonstrate normal pituitary enhancement including the infundibulum (arrow).

In addition to pre- and postcontrast sagittal and coronal thin slice imaging, pituitary tumor evaluation usually includes a dynamic contrast uptake series, where slice acquisitions are obtained very rapidly while contrast is injected. The imaging must be fast enough to obtain images in several passes or phases. Typically there are 5-6 phases per slice location, and imaging is usually completed within 20-30 seconds per phase. The need for dynamic imaging arises from the rapid contrast uptake characteristics of normal versus abnormal pituitary gland. Since the normal pituitary gland lies outside the blood-brain barrier, it enhances quickly and earlier than abnormal pituitary gland. Thus, dynamic imaging allows the radiologist to visualize contrast uptake to distinguish normal from abnormal characteristics in this very small gland.

To avoid overwhelming the pituitary with contrast enhancement, one can inject half of the weight-based dose of contrast during the dynamic contrast series. The second half of the dose is given after the dynamic series to provide full dosage enhancement for the whole-brain portion of the exam that is part of the imaging protocol.

Imaging of the Orbits and Optic Nerves

Imaging of the optic nerves is required for various indications, including blurred vision and optic neuritis, which may be a complication of MS (**Figure 19**). Imaging of the orbits and optic nerves is usually, but not always, accompanied by a routine brain protocol. For the purpose of this discussion, we will assume that the brain is imaged along with the more specific orbital exam.

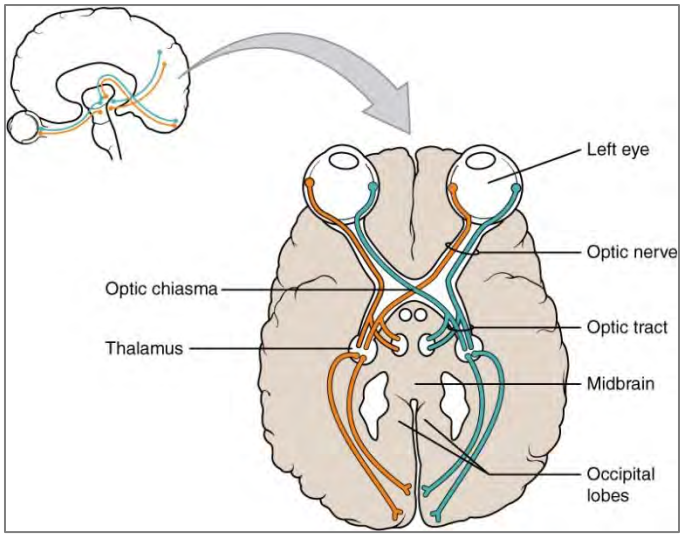

Figure 19. Anatomy of the orbit and optic nerve. *Courtesy of OpenStax. Available at* Wikimedia.

The optic nerves are surrounded by fatty tissue, which presents excellent intrinsic tissue contrast for nerve imaging. That said, it is important to suppress the hyperintense signal from fat in specific protocols for optic nerve imaging.

Typically, orbital and optic nerve imaging consists of thin slice axial and coronal planes with and without fat suppression (**Figure 20**).

Slice thickness for axial imaging is usually 3.0mm or less through the entire orbit, with attention to obtaining one slice directly through the optic nerve. Because of the orientation of the optic nerve, adjustment of the axial plane and/or sagittal **oblique** plane is often necessary. The axial acquisitions are T1 with fat saturation and with and without contrast, as well as a T2 sequence.

Coronal imaging is also routine for orbital and optical nerve imaging. T1W imaging with fat suppression and T2W imaging are typically done, extending from the dorsum sellae through the ocular lenses. Typically the slice thickness for coronal imaging is 4.0mm. Some imaging facilities prefer coronal STIR imaging because of the superior fat suppression that is insensitive to susceptibility effects due to tissue-air interfaces around the sinuses. However, the low spatial resolution and long scan times of STIR imaging, in addition to better local magnetic field shimming techniques, have given way to fat saturation techniques.

Finally, to reduce potential artifact and maintain patient safety, be sure to review these two important points with each patient. First, encourage the patient to keep their eyes closed during data acquisition. This reduces the potential for ghosting artifacts from orbital motion. Secondly, the patient should remove any eye make-up, as beauty products may contain small metallic flakes to provide "shine." These flakes can cause noticeable eye irritation and increase dephasing artifact, which may interfere with obtaining a high-quality image.

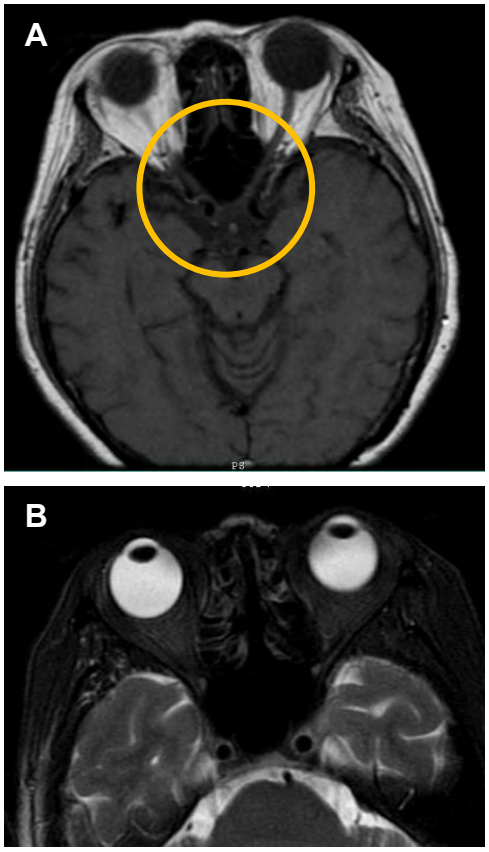

Figure 20. (A) Axial T1W image through the optic nerves. The optic chiasm is circled. (B) Axial T2W fat-suppressed image. The fluid-filled orbital globes are hyperintense; the ocular lenses are hypointense.

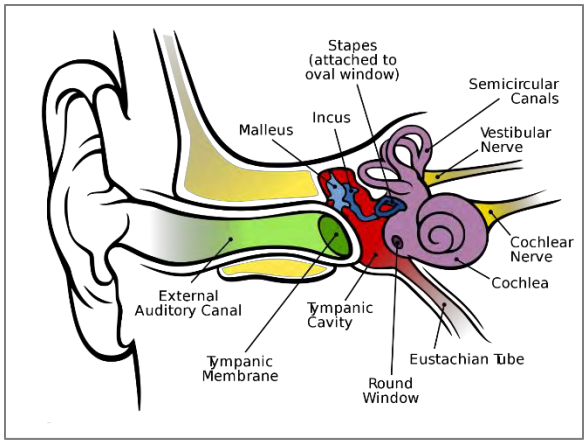

Figure 21. Anatomy of the internal auditory canal. (The length of the auditory canal is exaggerated in this image.) *Courtesy of Chittka L. Brockmann.* Available at *Wikimedia Commons*

Imaging of the Internal Auditory Canals and Cranial Nerves

Clinical symptoms of loss of balance or gait abnormalities, vertigo, **tinnitus**, and loss of hearing are symptoms often evaluated by MRI. MRI of the internal auditory canals (IACs) is one of the more common specialized brain MRI applications. Although "MRI of the brain for IACs" is a common request, it is a misnomer. In this exam, the IACs are not what is being assessed but rather the contents within the canals, namely the 7th (facial) and 8th (vestibular cochlear) cranial nerves and the middle and inner ear structures, including the cochlea, stapes, and semi-circular canals (**Figure 21**).

Along with routine brain imaging, imaging the IACs and cranial nerves usually consists of thin-slice T1W imaging in the coronal and axial planes pre- and postcontrast with fat suppression. The axial coverage is typically through the bony petrous ridges with a slice thickness of not more than 3.0mm. Coronal images, no thicker than 3.0mm, cover from the pituitary to the fourth ventricle. Axial ultra-high-resolution T2W imaging is also commonly done with a slice thickness of approximately 1.0mm for reformatting in other planes (**Figures 22 and 23**).

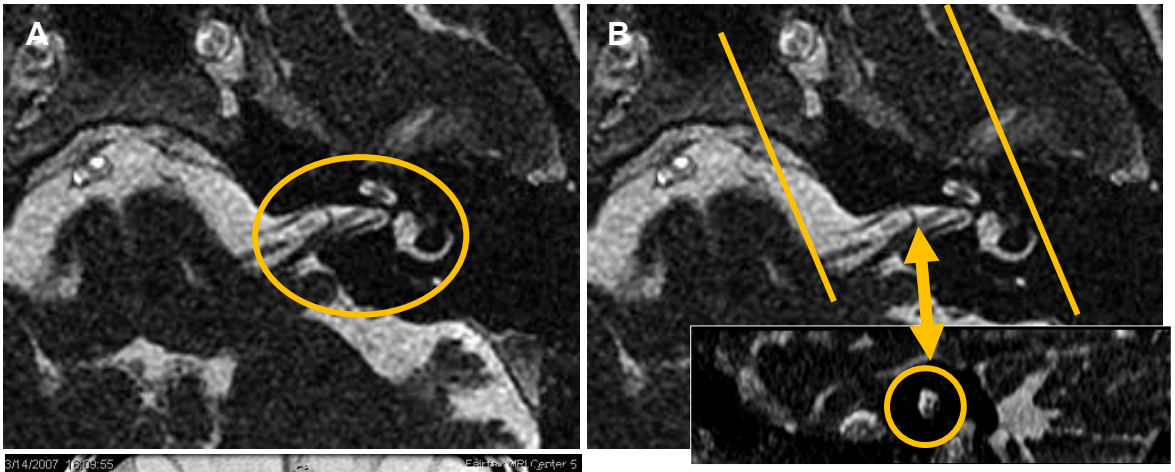

Figure 22. (A) Axial 3D FIESTA™ acquisition demonstrating the 8th cranial nerve, the vestibulocochlear nerve, and cochlea (circle). (B) 2D reformation of 3D axial acquisition indicating the reformatted plane is perpendicular to the plane of the nerve. The circled area within the reformatted image shows the acoustic nerves in a perpendicular view. (C) Coronal ultra-thin slice T1W image demonstrates each internal auditory canal.

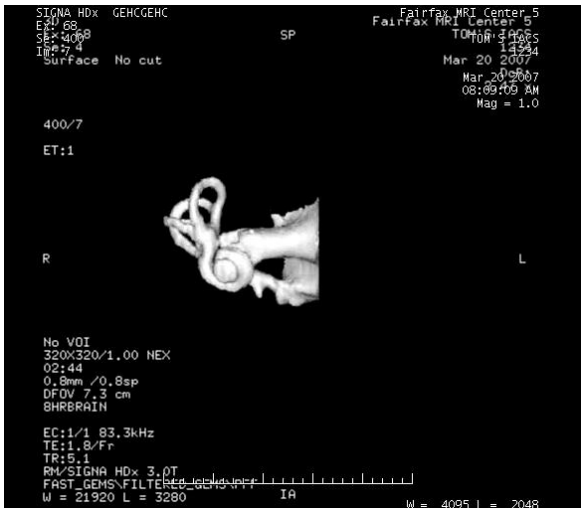

Figure 23. Movie of 3D volume-rendered model of the cochlea created from a 3D FIESTA™ acquisition. *Click here to view movie.*

Imaging Brain Hemorrhage

Whether to evaluate traumatic brain injury (TBI) or vascular pathology, magnetic resonance is effective in both detecting and characterizing hemorrhage. Hemorrhage is typically categorized into four chronologic stages. Each of these stages of hemorrhage has a distinctive appearance on T1W and T2W imaging due to the changing nature of blood breakdown products (**Table 1**).

Stage	Age of Hemorrhage	Blood Breakdown Products	Signal on T1	Signal on T2
Hyperacute (very early)	<24 hours	oxyhemoglobin	isointense	hyperintense
Early Acute	24–72 hours	deoxyhemoglobin	isointense	hypointense
Early Subacute (recent)	several days	intracellular methemoglobin	hyperintense	hypointense
Late Subacute (older)	up to 2 weeks	extracellular methemoglobin	hyperintense	hyperintense
Chronic (old)	many weeks	hemosiderin and ferritin	iso- to hypointense	iso- to hypointense

Table 1. Hemorrhage staging criteria.

Hyperacute Stage

In the hyperacute stage of hemorrhage, blood consists mostly of **oxyhemoglobin**. Here the area of hemorrhage appears brighter than CSF on T1W imaging and **isointense** to normal brain gray-white matter. In T2W imaging, hyperacute hemorrhage appears bright (hyperintense) compared to both CSF and normal brain tissue.

Early Acute Stage

In the early acute stage of hemorrhage, oxyhemoglobin is converted to **deoxyhemoglobin**, which appears isointense to brain on T1W imaging and is hypointense to brain on T2W imaging.

Early and Late Subacute Stages

In the early subacute stage, deoxyhemoglobin is converted to **methemoglobin** (intracellular), which is hyperintense on T1W imaging and hypointense on T2W imaging. In the late subacute stage, the red blood cells **lyse** and the methemoglobin becomes extracellular, appearing hyperintense on both T1W and T2W imaging (**Figure 24**).

Chronic Stage

Finally in the chronic stage of hemorrhage, the methemoglobin is converted into **hemosiderin** and ferritin. At this point almost all of the blood breakdown products have been reabsorbed by the body, with the exception of the iron constituents, hemosiderin and ferritin. The remaining iron creates an efficient magnetic susceptibility effect that causes significant dephasing in the area of the hemosiderin. Local field **inhomogeneity** due to hemosiderin and ferritin causes T2' (prime) dephasing. The combination of T2' and a tissue's true T2 greatly shorten dephasing times and are referred as T2* (star). The periphery of the hemorrhage consists of hemosiderin and ferritin and is iso- to hypointense on both T1W and T2W imaging. In this stage, the best pulse sequence for visualizing hemosiderin and ferritin is the gradient echo (GRE) sequence (**Figure 25**).

Utility of gradient echo imaging

GRE, by definition, does not rephase signal loss due to T2' effects. Magnetic susceptibility caused by the ferromagnetic components of deoxyhemoglobin, intracellular methemoglobin, and hemosiderin and ferritin cause local field dephasing and therefore signal loss. Spin echo sequences, especially long echo train FSE sequences, correct T2' susceptibility effects and recover signal loss. This is detrimental when trying to visualize the susceptibility effect of old hemorrhage. Today, specialized GRE sequences that accentuate susceptibility effects of hemorrhage are available.

The resultant images from this type of sequence are referred to as susceptibility-weighted images (SWI).

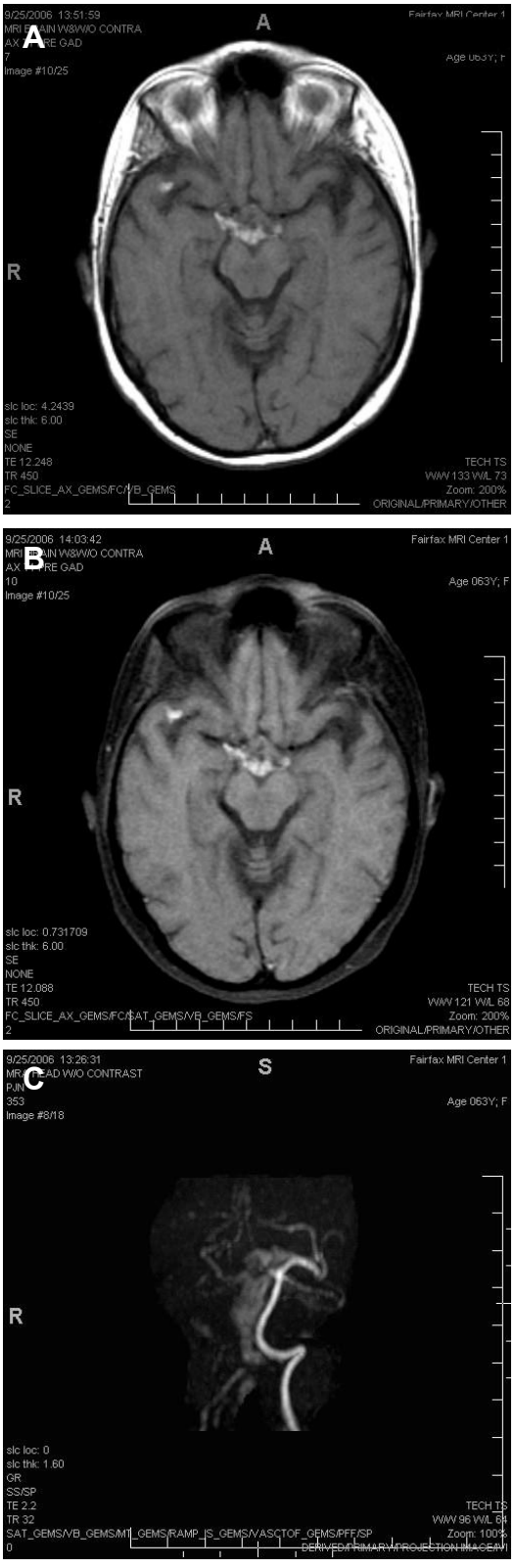

Figure 24. MRI appearance of an active bleed. Patient presented with history of headaches for two weeks. (A) Axial T1W image. The hyperintense area posterior to the Circle-of-Willis and the right frontal lobe indicate blood. (B) T1 with fat saturation to differentiate blood from fat. (C) 3D TOF MRA demonstrating hemorrhaging of the right posterior cerebral artery.

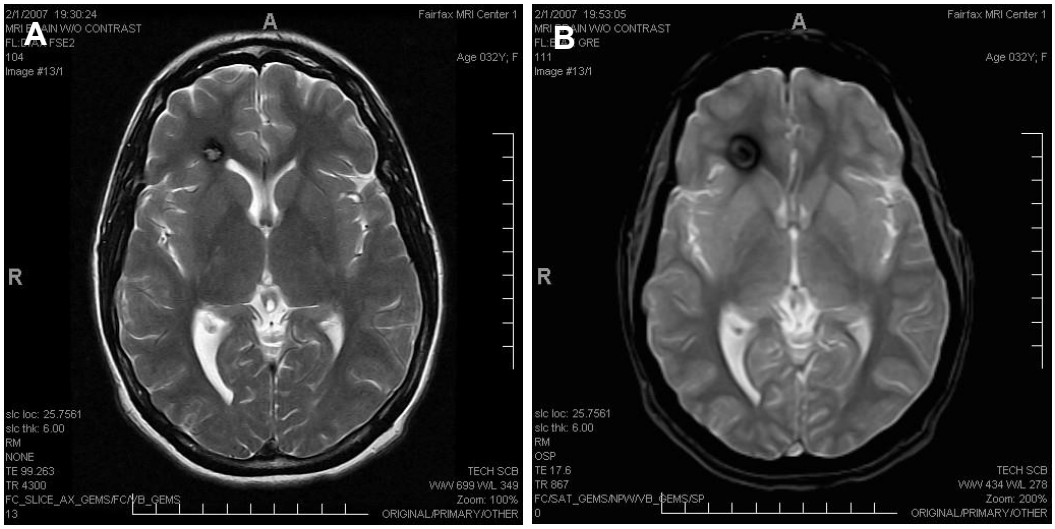

Figure 25. The use of gradient echo imaging to visualize hemosiderin. (A) Axial fast spin echo T2W image demonstrating a small area of hypointense signal due to the T2' (prime) dephasing effects of the iron- heavy hemosiderin. (B) Axial GRE T2* (star) image of the same location. Note the greater T2' effect.

Imaging Traumatic Brain Injury

With traumatic brain injury (TBI), other physiological changes may occur in addition to hemorrhage. Gross structural changes such as bony fractures are better visualized with CT. However, more subtle but important abnormalities are better seen with MR. By far the most common of these subtle findings is diffuse axonal injury (DAI), often a devastating type of TBI. Axons are nerve fibers that conduct impulses away from the nerve cell or neuron. DAI is common in TBI patients and is most often seen in the gray-white matter interface, corpus callosum, periventricular regions, and in the brain stem. In addition to the previously mentioned gradient echo imaging sequences, sagittal high-resolution T2W imaging is often performed to assess the corpus callosum for **shear injury** in TBI patients.

Utilizing the hemorrhage staging criteria defined, MRI is accurate for establishing the age of a hemorrhage. Particularly in elderly patients with subdural **hematomas**, blood of several different ages is seen simultaneously. This information is useful in cases of suspected child abuse in which hemorrhage of different stages is seen due to repeated injury over time.

MR ANGIOGRAPHY OF THE CENTRAL NERVOUS SYSTEM

MR angiography (MRA) has become a mainstay of brain MR imaging. MRA is typically performed either in the neck for examination of the carotid and vertebral arteries or intracranially to examine the Circle-of-Willis and the main cerebral arteries that arise from it (**Figures 26 and 27**).

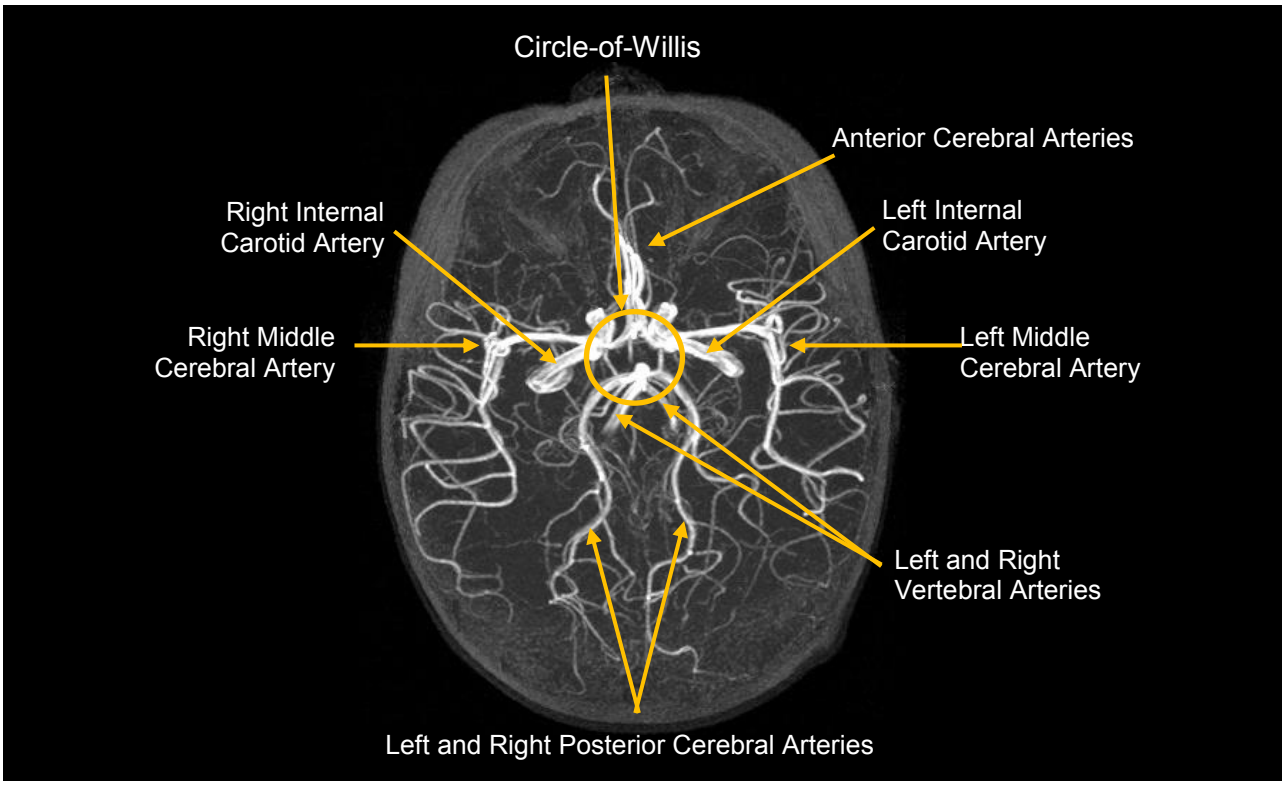

Figure 26. Axial maximum intensity pixel projection (MIP) 3D TOF of intracranial arterial tree showing normal vascular anatomy.

In the neck, contrast-enhanced MRA takes advantage of improved software and increased gradient strengths to allow reduction in MRA imaging time, as well as more precise timing of the injected bolus to capture the actual passage of contrast through the carotids in the arterial phase. Many radiologists believe contrast MRA to be superior to noncontrast 2D or 3D time-of-flight (TOF) sequences, particularly in patients who have significant disease.

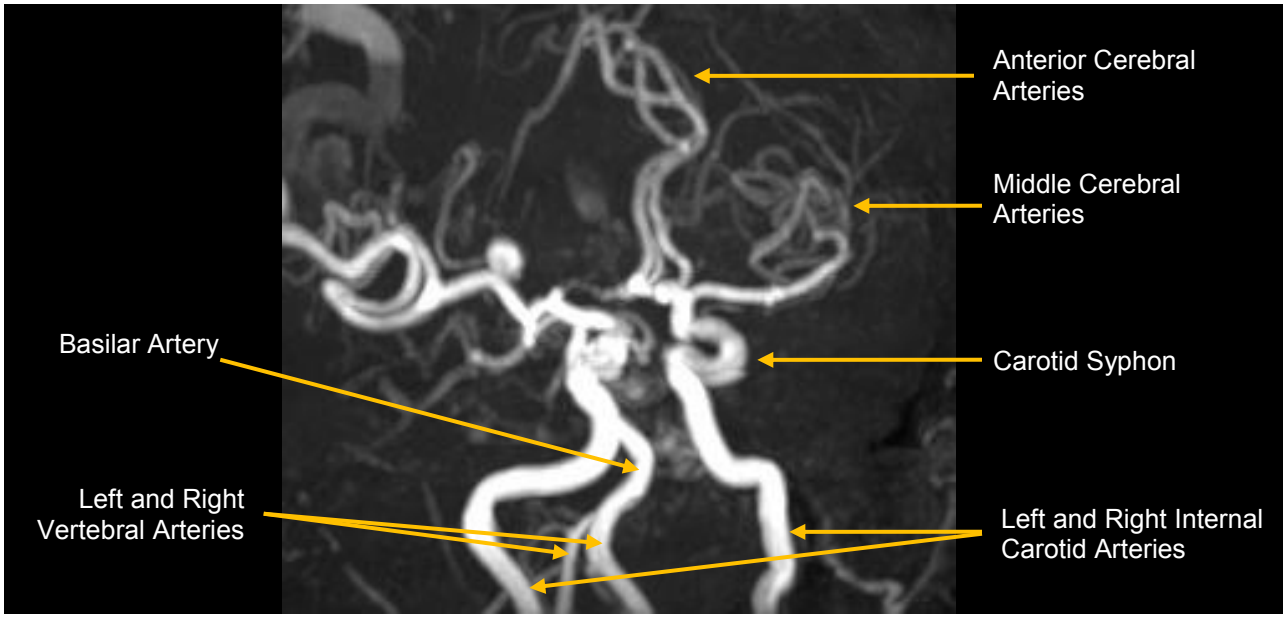

Figure 27. MIP projection 3D TOF of intracranial arterial tree showing vascular anatomical landmarks.

MRA of the Brain

Indications for MRA of the brain include history of known **aneurysm**, severe headache, ischemic symptoms and stroke, loss of vision, tinnitus, etc. In short, a variety of neurological symptoms arise from intracranial ischemia.

MR angiography is particularly useful in the evaluation of ischemia and infarction. In the evaluation of arterial infarction, conventional 3D TOF MRA covering the Circle-of-Willis is useful (**Figure 26**). This technique will not depict small penetrating arterial **thrombosis** but can detect thrombosis involving larger vessels, such as the middle cerebral artery (MCA), anterior cerebral artery (ACA), and posterior cerebral artery (PCA). If venous thrombosis is suspected, MR venography (MRV) can be useful. In both MRA and MRV, thrombosis is generally seen as an area of cutoff or signal loss within a vessel.

The typical pulse sequence for MRA is a 3D TOF sequence, as opposed to MRV. 3D TOF MRA is typically done in one or several “blocks” or “slabs” of excited tissue. These slabs of data undergo a second set of phase encoding steps at the end of the data acquisition in the slice-select direction. This second series of phase encoding steps reconstructs the slabs into discrete thin slice images. Zero-filling of k-space allows slices to be reconstructed with negative overlaps, just as with CT data. For example, a single 20cm slab of excited tissue can be reconstructed into twenty 2.0mm thin slice images every 1.0mm. In many instances, the reconstructed images can be submillimeter in thickness. When multiple slabs are prescribed, the slabs are typically overlapped to avoid interslab boundary artifact. Saturation pulses are also used superiorly to “null” venous flow from the super sagittal sinus. Used in conjunction with high-SNR phased array head coils, the result is high quality MR angiography of the intracranial arteries, including the Circle-of-Willis, internal carotid arteries, basilar artery, and anterior, middle, and posterior cerebral arteries.

Figure 28. Movie of 3D TOF MRA of the brain.
Click here to view movie.

Unlike MRA of the neck, most radiologists believe that when imaging the arteries of the brain, noncontrast 3D TOF methods are optimal. When contrast is used, enhancement of venous structures and normal nonvascular structures affect visualization of the arterial vasculature.

In essence, with IV contrast, MRA of the brain may become a "bowl of spaghetti," making it difficult to delineate individual vascular structures (**Figures 26-29**). The exception to this rule is evaluation of the intracranial arteries following placement of an intracranial aneurysm clip.

For many years, the existence of an implanted intracranial aneurysm clip was an absolute contraindication for MRI. Indeed, patient death due to torque by the magnetic field of the aneurysm clip has been documented. (See FDA Safety Notification, Nov. 1992.[2]) Today, however, it is rare to find a non-MRI safe intracranial aneurysm clip. With prudent and careful screening and verification, many patients with clip placement can, and have, undergone safe and diagnostic MRI examinations.

For patients with intracranial aneurysm clips, routine 3D TOF imaging may be inadequate. This is because the usually titanium-based clip, while **non-ferrous**, creates a significant metal-related artifact that completely obscures visualization of blood flow in the region of the clip. Fortunately, IV gadolinium administration significantly reduces this artifactual signal drop-out.

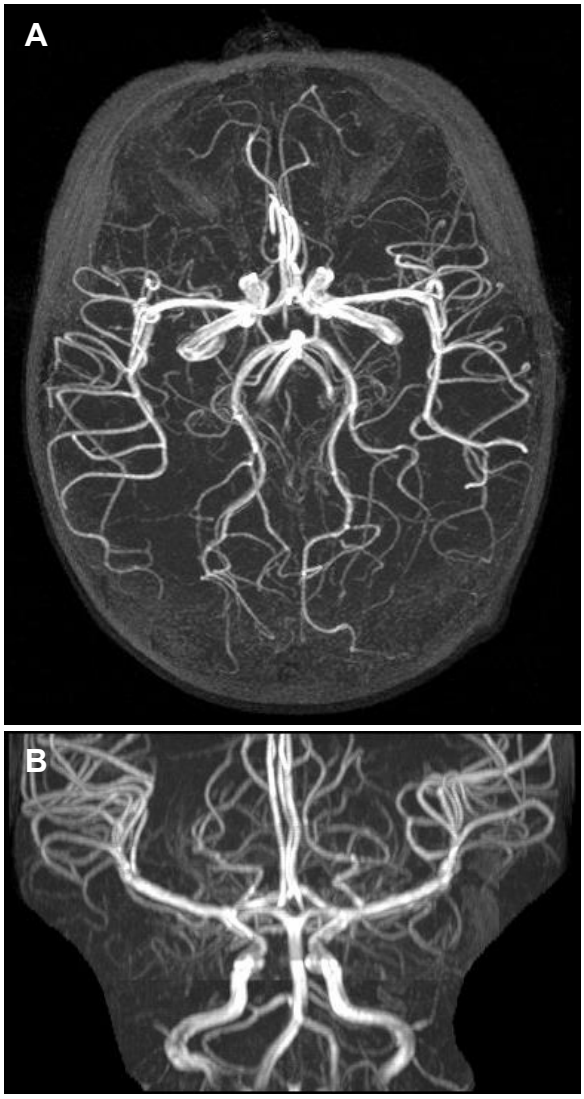

Figure 29. Intracranial MR angiography. Both images are projections of a 3D TOF multi slab acquisition. (A) Axial collapsed MIP. (B) Coronal MIP. Images were acquired without the use of contrast.

MRA of the Neck

For many of the above-mentioned indications, MRA of the neck is required to assess **patency** of the (**Figures 30-33**):

- origins of the three branches of the aortic arch (left subclavian artery, left common carotid artery, and the brachiocephalic, or innominate, artery that bifurcates into the right subclavian and the right common carotid arteries)
- right and left carotid artery bifurcation into the internal and external carotid arteries
- right and left vertebral arteries
- basilar artery

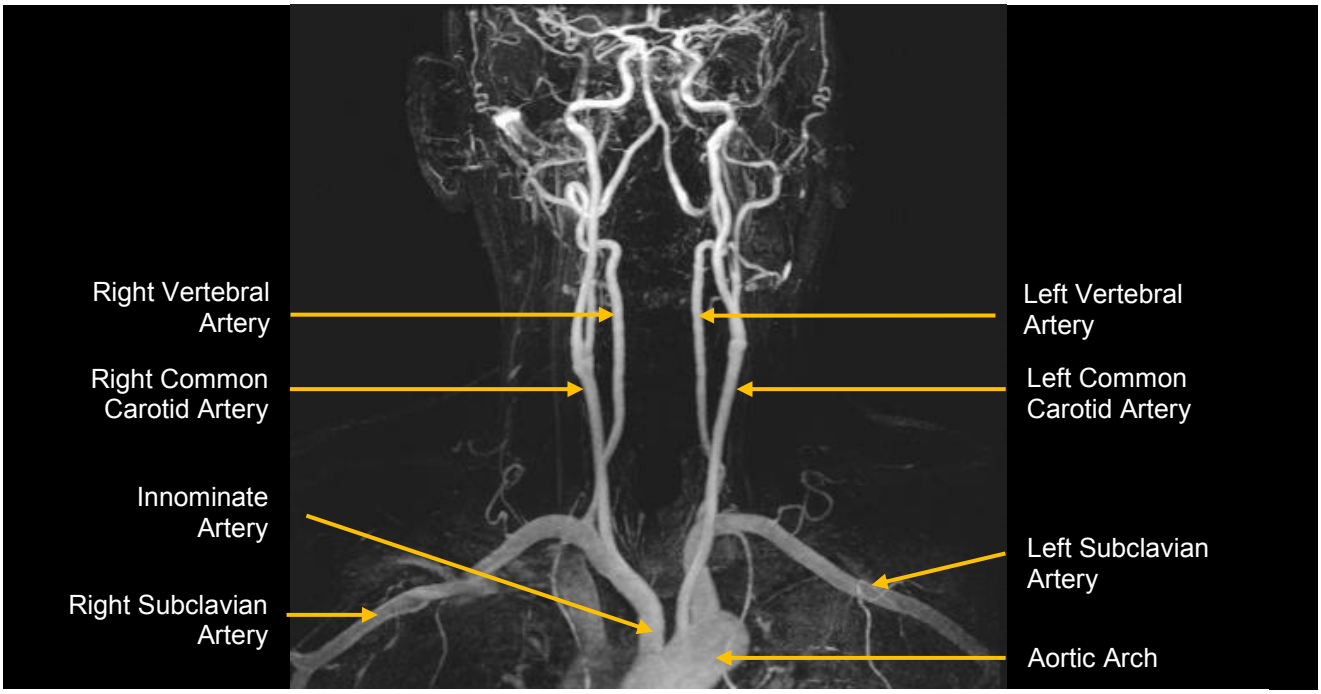

Figure 30. Normal vasculature of the neck.

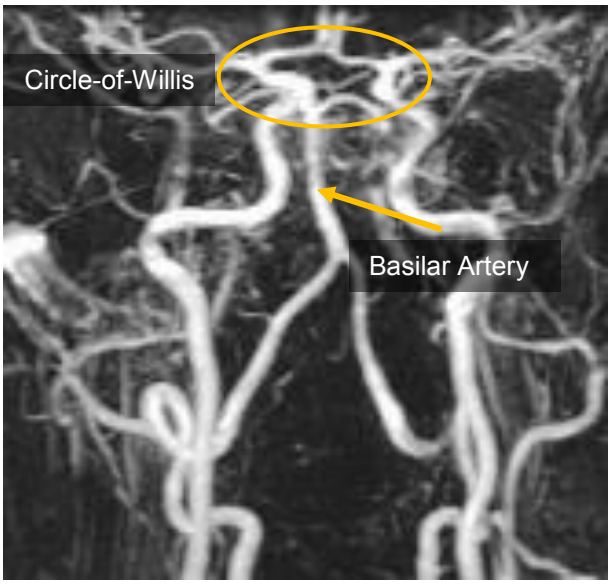

Figure 31. Intracranial vasculature.

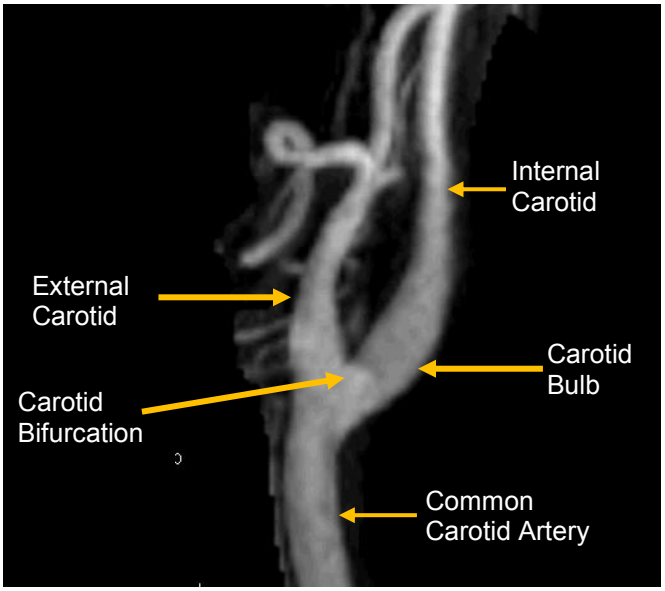

Figure 32. Normal carotid vessel.

MRA of the neck is typically performed using contrast-enhanced 3D fast gradient echo imaging. Timing data acquisition to the peak filling of vessels with contrast is achieved by various timing methods that range from manual bolus timing runs to automated bolus detection software, visual detection of the bolus (often called MR fluoroscopy), and extremely rapid imaging through several phases of bolus filling.

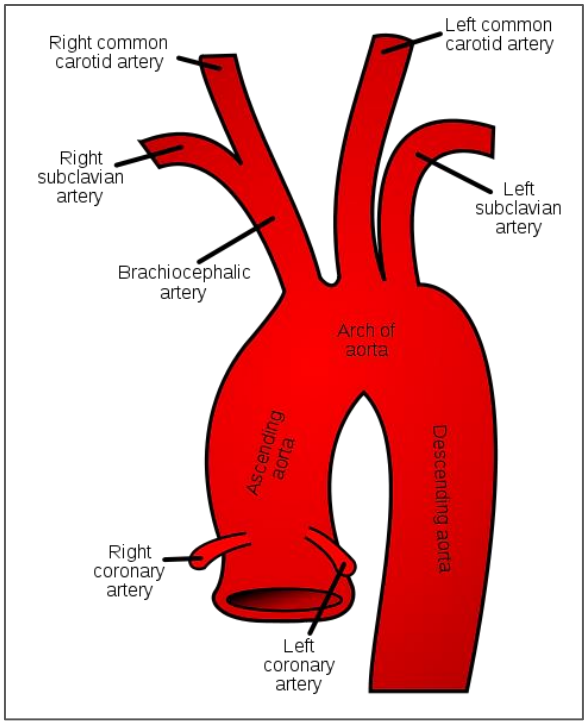

Figure 33. Normal anatomy of the neck and thorax.
RHcastilhos reproduction of illustration from the 20th U.S. edition of Gray's Anatomy of the Human Body, 2000.

The primary advantage of contrast-enhanced MRA of the neck versus 2D and 3D TOF imaging is the known over-estimation of carotid bifurcation **stenosis** by TOF — a result of signal loss from **vortex flow** in the carotid bulb. Contrast alleviates this phenomenon. TOF images the flow of the blood, but in contrast-enhanced MRA, the blood itself is imaged. With contrast in the vessel, the direction of the flow and complex flow dynamics are irrelevant. However, timing of the bolus is critical since contrast in the jugular veins appears equally as bright as in the arteries (**Figures 34 and 35**).

Figure 34. Movie of MR angiogram. **Cine** MIP rotation of a contrast-enhanced 3D TOF of the neck. Aortic arch is demonstrated with three branches extending intracranially to the Circle-of-Willis. Contrast bolus injection was timed to maximize arterial enhancement while minimizing venous contamination. A significant stenosis is seen in the left internal carotid artery immediately distal to the carotid bifurcation. Click here to view movie.

Figure 35. Movie of MR angiogram. A targeted cine loop of the same 3D TOF series segmented to show only the bifurcation of the left common carotid artery into the internal and external carotid arteries. These rotational views more precisely demonstrate a near 90% stenosis of the internal carotid artery.
Click here to view movie.

MR Venography

Assessment of the veins of the brain is often indicated for symptoms arising from occlusion of the major cerebral veins or venous thrombosis. MR venography (MRV) assesses the superficial (cortical) and deep cerebral veins, as well as the major dural sinuses including the superior sagittal sinus, transverse sinus, sigmoid sinus, and jugular bulb (**Figure 36**).

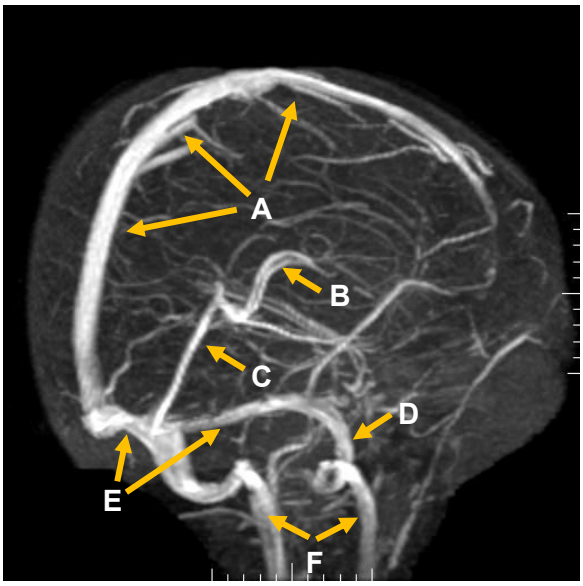

Figure 36. 2D MIP TOF MRV oblique sagittal view.
A. Superior sagittal sinus
B. Vein of Galen
C. Straight sinus
D. Sigmoid sinus
E. Left and right transverse sinuses
F. Left and right internal jugular veins

Venous angioma is a common, generally asymptomatic malformation. These cases represent anomalous venous drainage. Normally, venous malformations progress from the **ependymal** surface of the ventricle toward the periphery of the brain and are characterized by a **caput medusae** or tangle of abnormal medullary veins, converging into a prominent draining vein. Developmental venous anomalies (DVAs) are particularly visible after the administration of contrast. They tend not to bleed and lack **mass effect**. Not infrequently, cavernous malformations may be associated with venous angiomas and result in hemorrhage in the bed of the venous angioma (**Figure 37**).

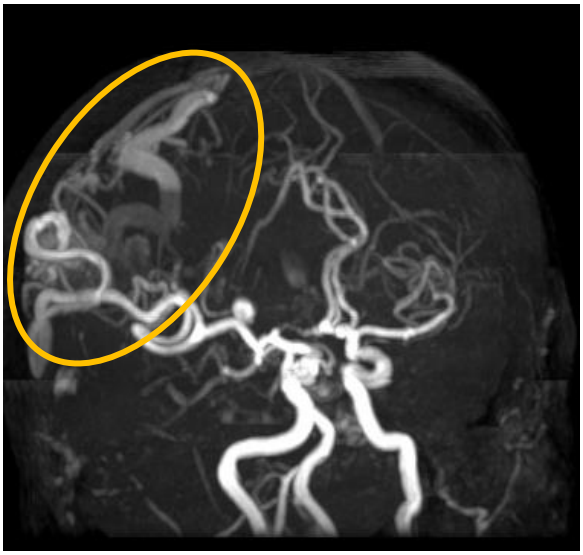

Figure 37. MRA/MRV of large posterior venous malformation (circle).

While techniques vary, TOF imaging is typically employed for MRV and in some cases contrast enhancement is used. However, TOF techniques suffer from artifacts that mimic thrombus when slow venous flow is in the same direction as the slice acquisition. For this reason, TOF techniques are often performed twice: once in the coronal direction (y axis) to assess the left and right transverse sinuses and superior sagittal sinus in the AP direction and secondly in the axial projection (z axis) to assess the sagittal sinus in the superior-to-inferior direction.

Bolus timing is far less critical with contrast enhancement methods for MR venography. Since arterial enhancement is not desired, a long delay is programmed between the injection and data acquisition. Some arterial contamination is always present, but the lack of artifact from slow venous flow usually overrides this concern.

MRI OF THE FETAL BRAIN

At birth, cerebral anomalies account for approximately 9% of all isolated anomalies and 16% of all multiple malformations. With an increase in surviving premature neonates, the need to diagnose, characterize, and potentially treat fetal anomalies is apparent. Ultrasonography poorly visualizes the corpus callosum and cerebral sulci and renders biometric measurements difficult. Lacking ionizing radiation and providing excellent visualization and characterization of tissue, MR significantly contributes to fetal brain imaging.[3]

With regard to safety of the fetus during imaging, no adverse effect has been found related to fetal MRI. Nevertheless, the National Radiological Protection Board & the Food and Drug Administration do NOT recommend imaging during the first trimester.[4]

MR imaging of the fetus takes advantage of recent significant technological advancements in MR technology. Faster gradient activation as well as extremely sophisticated pulse sequences enable motion-free imaging with high detail and tissue contrast in intervals short enough for the mother to hold her breath. Powerful gradient systems allow for extremely short TRs and TEs, which keeps imaging time short and reduces motion and susceptibility effects. Typical pulse sequences include single-shot fast spin echo techniques as well as ultra-short gradient echo sequences such as FIESTA™ (GE) and True FISP™ (Siemens) (**Figure 38**).

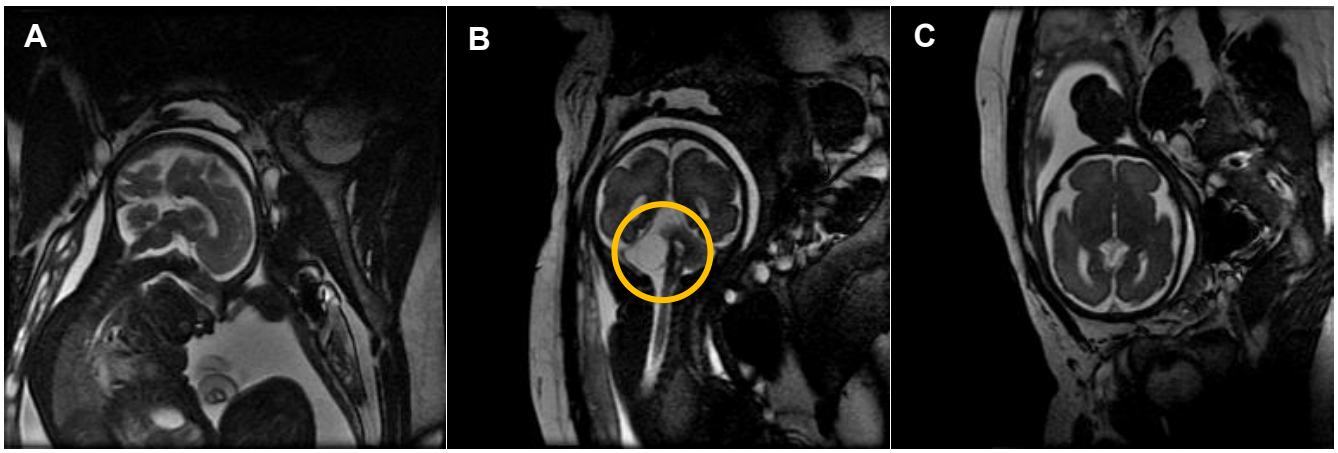

Figure 38. MR images of 30-week-old fetus. (A) Sagittal. (B) Coronal. (C) Axial FIESTA™. Note the cystic posterior fossa lesion on the coronal image (circle).

Single-shot techniques have the benefit of being motion-insensitive and provide truer proton density or T2-weighted contrast (**Figure 39**). However, with very long echo trains, specific absorption rate is a concern even with relatively short scan times. Ultra-short gradient echo sequences, while being far less SAR-intensive and excellent in demonstrating sulcal detail, are prone to more susceptibility effects and heavier T2* weighting.

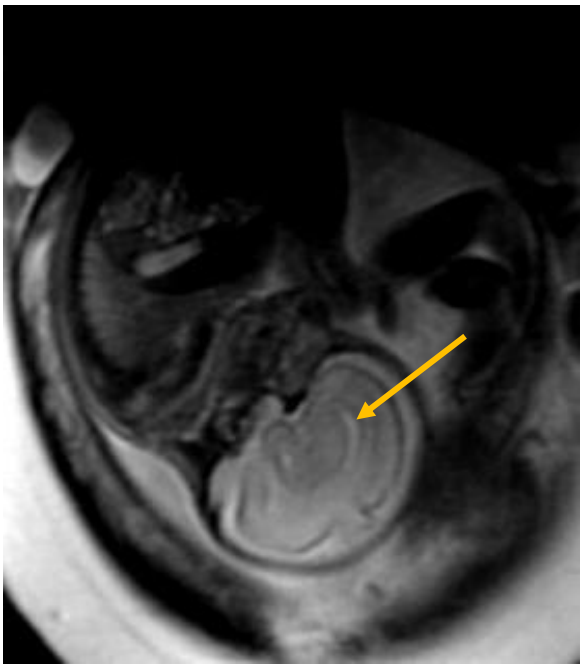

Figure 39. Oblique sagittal T2 single-shot fast spin echo scan of normally developing corpus callosum (arrow) in a 31-week-old fetus.

Fetal imaging is performed quickly in both set-up and execution. Since most imaging is done when the mother is well into her second trimester and often into the third, the patient will most likely be uncomfortable lying supine for a long period of time.

Figure 40. Sagittal T1W image of agenesis of the corpus callosum (circle).

Typically, imaging begins with a large FOV localizer scan in three planes to visualize the position of the fetus. Once the location of the head of the fetus is determined another localizer, based on the location of the head, is obtained to place the imaging plane as close to orthogonal as possible. From this point forward, each successive scan is based on the previous scan, minimizing the likelihood of fetal movement. Fetal repositioning from one scan to the next decreases with increased gestational age. In other words, the earlier the gestational age, the greater the likelihood of fetal repositioning between each scan. In setting up each series of imaging, the technologist prescribes from the most recent scan; all three orthogonal planes to the fetal head are typically acquired.

Agenesis of the corpus callosum is commonly seen and best viewed on sagittal scans (**Figure 40**). However, there are a large number of lesions that are best seen in other planes, especially on axial images. These lesions are generally due to disorders of brain development.

In the process of embryology, the cortex of the brain forms by migration of cells from the periventricular region outward. If normal migration of these cells is arrested at some point in the embryo's development, malformations will result. One such malformation is gray matter **heterotopia**, where remnants of gray matter remain in an abnormal position. If gray matter fails to migrate at all, it may remain in the periventricular region. However, if migration is arrested midway, then collections of gray matter may be seen in white matter regions, for example, the centrum semiovale.

Since the abnormalities are composed of gray matter, these lesions are differentiated from other types of pathology because their signal intensity is identical to those of normal gray matter on all MR pulse sequences.

General lack of knowledge regarding MR imaging of developing brain as well as the appearance of specific pathology has slowed the wide-spread use of fetal MR. Current research interest focuses on how to acquire T1-weighted images without fetal motion artifact during relatively long scan times. Other areas of research include diffusion-weighted imaging and spectroscopy, both of which show early promise in increasing the specificity of fetal brain imaging.

INFECTION AND INFLAMMATORY DISEASE

Intraaxial Space

Multiple infectious agents and inflammatory processes affect the brain. Infectious agents include bacteria, viruses, fungi, and parasites.

Bacteria

Bacterial infections of the brain traverse a well-defined sequence of events. First, the infectious agent invades a localized area of the brain causing **cerebritis**, typified by mass effect and swelling. The area involved appears slightly hypointense on T1-weighted images and hyperintense on proton density and T2-weighted images. Frequently there is mass effect on the adjacent lateral ventricles. After the administration of contrast, either no or scattered enhancement is seen. As infection progresses, the body tends to wall off the infection by creating a fibrous capsule, the beginning of an abscess. Over time, generally from ten days to two weeks, the interior content of the abscess liquefies and becomes necrotic while by comparison the abscess capsule is well visualized on imaging. The capsule wall is usually thin, well defined, and surrounded by edema. The capsule surrounds a lesion that appears slightly hypointense on T1, hyperintense on T2, and demonstrates restriction on diffusion-weighted imaging. After the administration of contrast, enhancement of the abscess rim is seen (**Figure 41**).

Clearly the appearance of an abscess can mimic that of tumor, and there is no absolute way to differentiate the two radiographically. Abscesses tend to have a thin capsule wall compared with tumors which often have thick, irregular walls. As noted, diffusion-weighted imaging may be useful for differentiating cystic tumor from abscess.

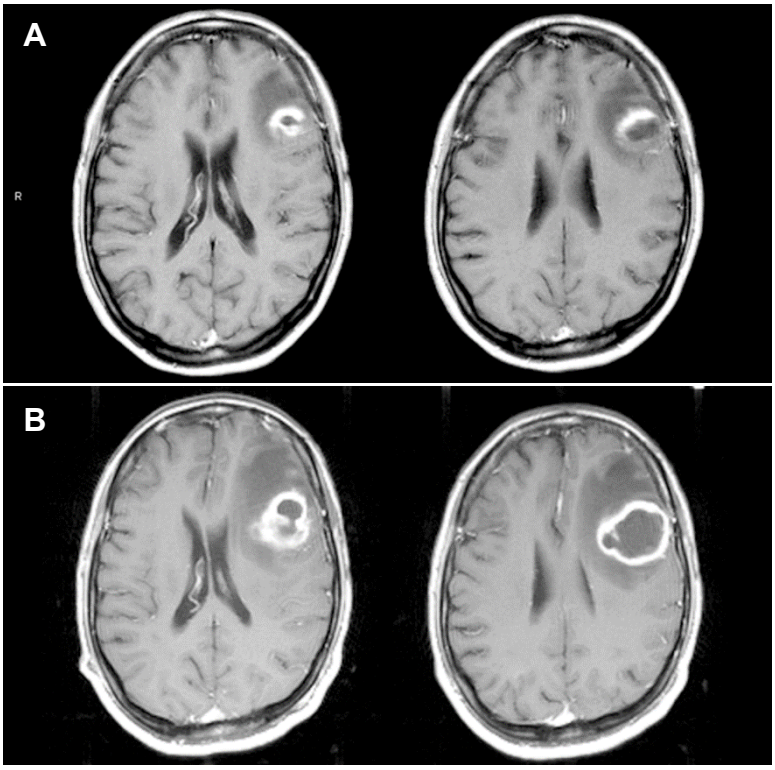

Figure 41. (A) Abscess on axial T1 postcontrast image. (B) Five days later, axial T1 postcontrast image.

Viruses

Unlike infections caused by bacteria, viral infections tend to lead to **encephalitis** rather than cerebritis and abscess formation. Encephalitis is pathologically similar to the cerebritis stage of bacterial infection but may be much more diffuse or scattered.

Most cases of encephalitis are difficult to differentiate, but there are a few specific types of encephalitis that have a characteristic imaging appearance. Chief among these is herpes simplex encephalitis which, in adults, classically affects the medial temporal lobes. It is believed that herpes virus travels in a **retrograde** fashion from the 5th cranial nerve in the face into the cavernous sinus and the adjacent medial temporal lobes. Thus, bilateral involvement of the medial temporal lobes is virtually **pathognomonic** for herpes simplex encephalitis.

On MR imaging, herpes simplex encephalitis is typified by mass effect and hypointensity on T1, with corresponding hyperintensity on T2. Early on there may be little contrast enhancement, but as the disease progresses, contrast enhancement will increase. Herpes simplex encephalitis is typically associated with **petechial** hemorrhage, which may appear hyperintense on noncontrast T1W imaging (**Figure 42**).

The early diagnosis of herpes simplex encephalitis is critical since immediate administration of acyclovir has proven to minimize the **sequelae** of this devastating disease.

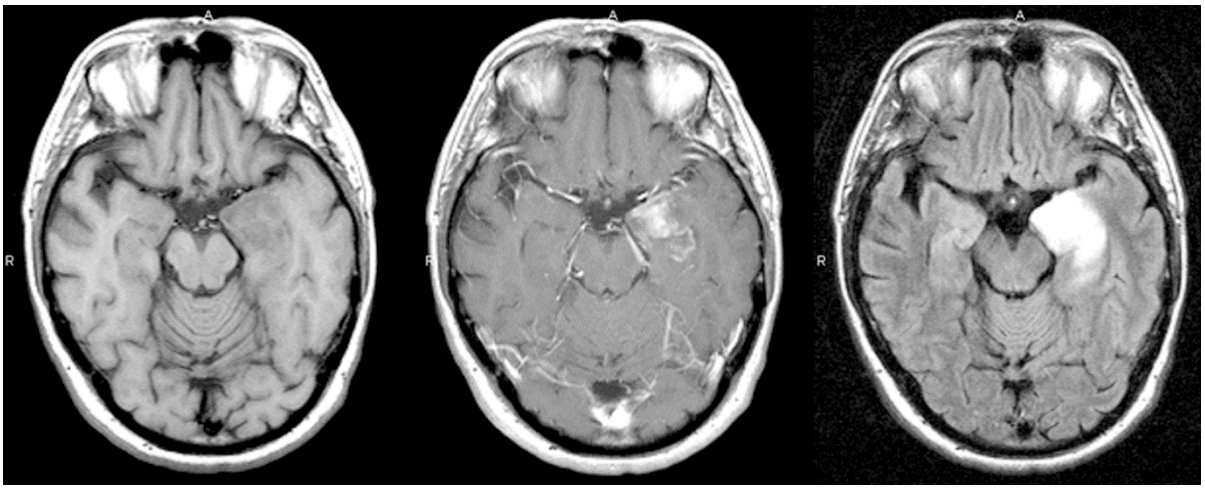

Figure 42. Herpes encephalitis. (A) Axial T1W precontrast administration. (B) Axial T1 postcontrast administration. (C) Axial FLAIR imaging.

Progressive multifocal leukoencephalopathy (PML) is another type of encephalitis with a characteristic appearance. PML is due to reactivation of papova virus, which typically occurs as an asymptomatic childhood infection. Because the papova virus attacks oligodendrocytes, PML is predominantly characterized by white matter involvement. PML is most often seen in immunocompromised states as in HIV/AIDS or transplant patients.

On MR imaging, PML has a characteristic appearance. Lesions are typically subcortical, multifocal, slightly hypointense on T1 and very hyperintense on T2, and limited to the white matter. Usually lesions show no mass effect, hemorrhage, or contrast enhancement (**Figure 43**). With time, they tend to increase in size and **coalesce**.

A few other unusual encephalitidies have a typical appearance. For example, equine encephalitis and Japanese encephalitis tend to center in the basal ganglia. However, the remaining encephalitidies tend not to have any characteristic appearance.

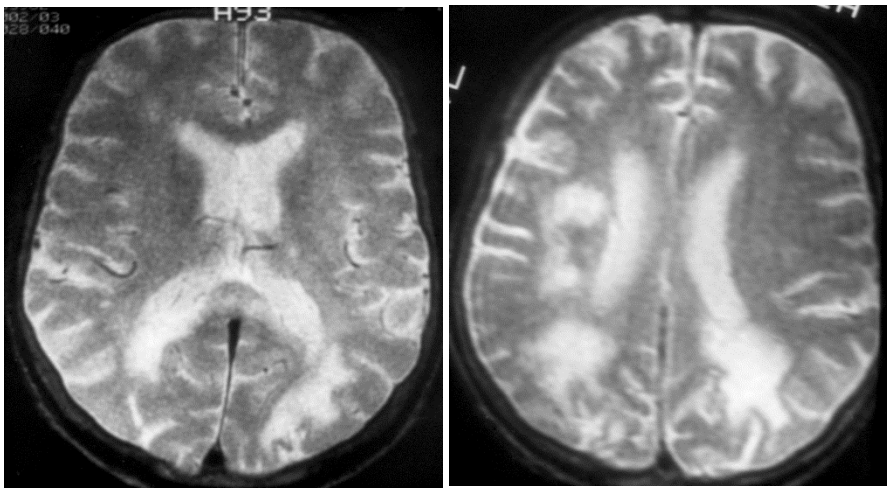

Figure 43. Axial T2 images of PML occur primarily in white matter and have very little mass effect.

Fungi

A large number of fungal agents can affect the brain. These include aspergillus, cryptococcus, and candida. While they most commonly occur in immunocompromised patients, fungal infections occur in non-immunosuppressed people as well.

Fungal lesions typically appear as well-circumscribed within the brain **parenchyma**. Typically multiple lesions are present, appearing slightly hypointense on T1 and hypo- or hyperintense on T2. These lesions typically enhance after contrast administration.

A few fungi are known for associated sequelae. Aspergillus in particular is known for involving the arterial vessels supplying the brain and thus can be associated with infarction and/or hemorrhage.

Parasites

In non-immunosuppressed patients, the only parasitic disease that commonly affects the brain in the United States is cysticercosis. Cysticercosis, caused by the larvae of the taenia solium tapeworm, is most common in its intraparenchymal form and is acquired from ingesting improperly cooked pork. The larvae migrate to the brain parenchyma where they cause small cystic lesions. In some cases, the scolex of the cyst can be seen. These lesions usually appear to be similar to CSF signal intensity (**Figure 44**). However, as the organisms die, the fluid within the lesion often becomes **turbid**. In these cases, the fluid becomes more hyperintense on both T1 and T2 as compared to normal CSF. In addition, an inflammatory reaction often surrounds the cyst at this stage. The final stage of cysticercosis shows **punctate** calcifications.

In immunosuppressed patients, especially those with HIV/AIDS, toxoplasmosis can occur. This parasite is transmitted by insufficiently cooked meat or by contact with contaminated cats or their feces. While the infection is usually mild, fetal damage can occur.

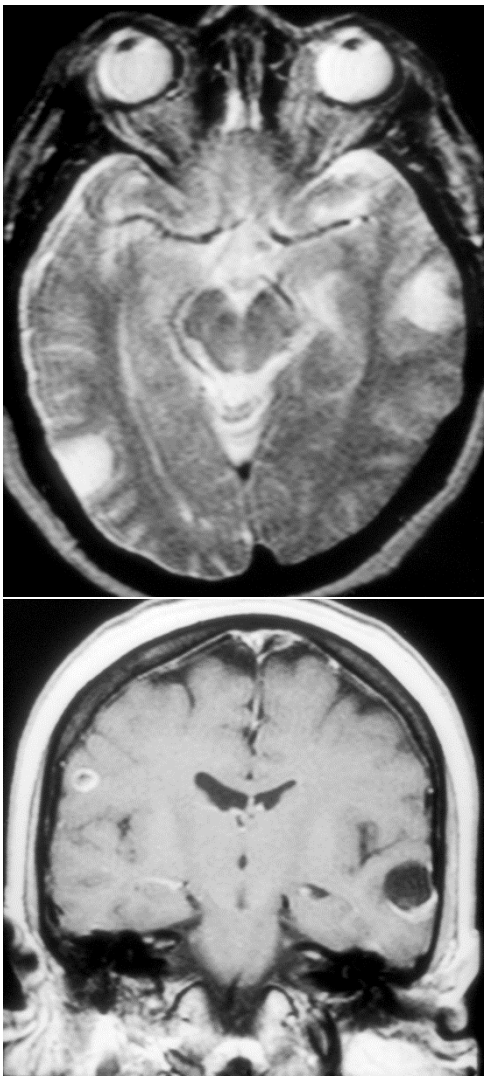

Figure 44. A 33-year-old man with seizures due to cysticercosis. The signal intensity of these lesions is similar to that of CSF. (A) T2W axial image. (B) Postcontrast T1W coronal image.

The parasite tends to favor the basal ganglia, although lesions may occur in all regions of the brain. Typically, scattered areas of hyperintense signal with mass effect are seen on T2-weighted images. After the administration of contrast, irregular enhancement is usual. The frequency of toxoplasmosis in the United States has decreased markedly due to both prophylactic treatment for toxoplasmosis and marked improvement in antiretroviral therapy for HIV/AIDs.

Extraaxial Spaces

Infectious and inflammatory lesions can also affect the extraaxial spaces. **Osteomyelitis** of the skull is unusual; however, infection involving the extraaxial space within the skull is not, where epidural and subdural **empyemas** occur. The epidural space is formed when the periostium is torn off the inner table of the skull. The subdural space occurs between the arachnoid and the dura. Because the periostium is very adherent to the inner table of the skull, epidural lesions tend to be lenticular in shape. Epidural empyemas are usually more **quiescent**, probably because they are somewhat limited in their ability to affect the underlying brain due to the thick and tough dura. In comparison, subdural lesions tend to have an elongated, **lentiform** shape with tapered edges. Subdural empyemas tend to be neurosurgical emergencies since they may result in underlying brain involvement.

While both epidural and subdural lesions were common in the pre-antibiotic era, today they are primarily seen in the post-surgical state. On T1-weighted images, an area of fluid is visualized. The signal of this fluid, however, does not resemble CSF, but is slightly hyperintense to CSF on T1 and proton density images. After the administration of contrast, there may be some enhancement around its rim.

Infection can also affect the CSF, as in meningitis, with secondary involvement of the arachnoid and pia. In these cases, the diagnosis is usually made clinically when the patient presents with a high fever and stiff neck. Lumbar puncture is performed to examine the CSF for white blood cells and culture. On MRI, no abnormalities may be seen in very mild cases, such as with viral meningitis even after contrast administration. However, in more severe cases, diffuse enhancement of the leptomeninges is seen (**Figure 45**). This appearance may be very similar to that of leptomeningeal seeding of a brain tumor or with leptomeningeal carcinomatosis.

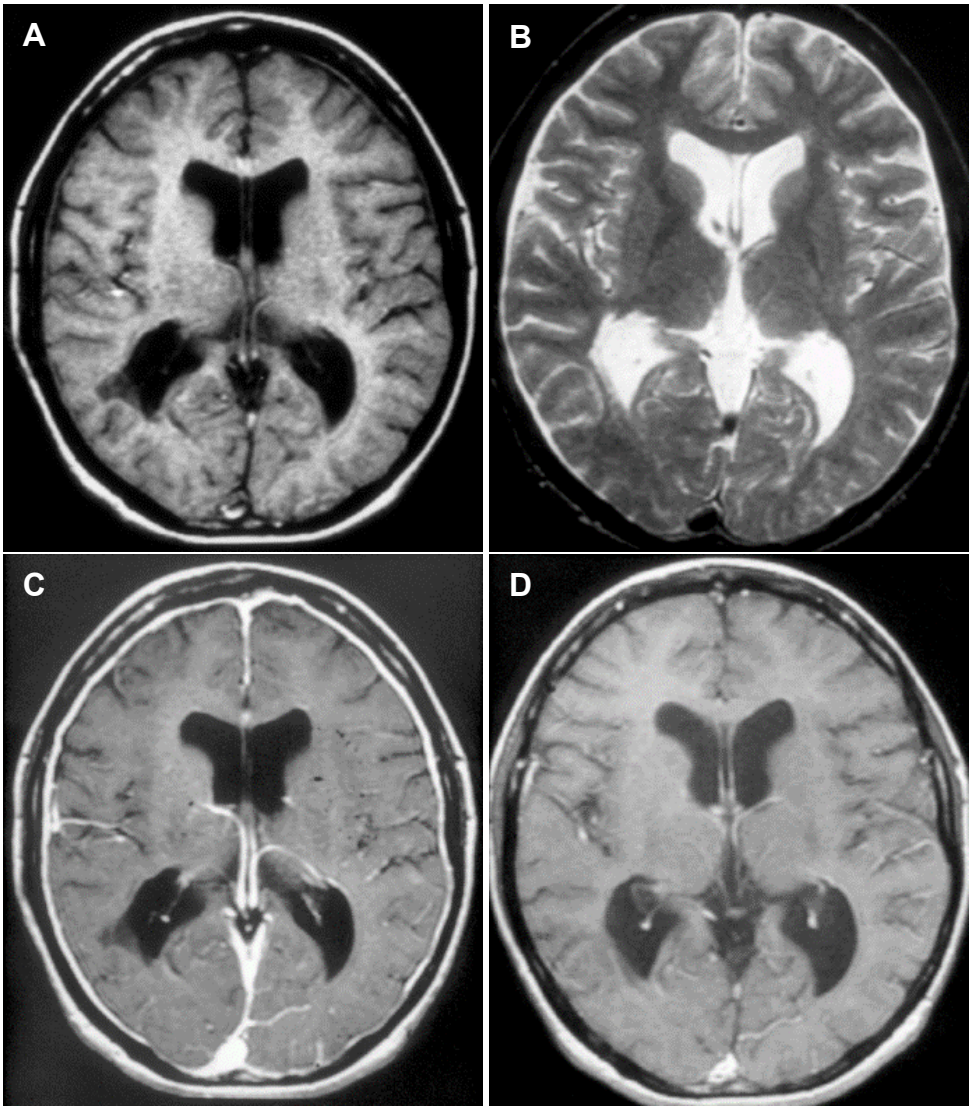

Figure 45. A 35-year-old woman with headache, diagnosed with meningitis. (A) Axial T1W image. (B) Axial T2W image. (C) Axial T1W postcontrast image demonstrating meningeal enhancement. (D) Axial T1W postcontrast image one month later showing resolution of meningitis.

SUMMARY

To a great extent, MRI has superseded CT imaging of the brain. Multiplanar capabilities provide exquisite demonstration of subtle pathology, making MRI the procedure of choice in the evaluation of suspected brain lesions. In addition, MR angiography has allowed evaluation of cervicocerebral vessels with or without contrast media. Diffusion and perfusion imaging techniques have permitted a physiologic or functional look at the brain. Finally, immense improvements in MR imaging techniques have made it possible to tailor MR protocols to optimally scan the entire brain anatomy for suspected pathology through high-quality diagnostic images.

MR Imaging of the Spine

After completing this material, the learner will be able to:

- List the main clinical indications for spinal MRI
- Discuss the most common disease processes evaluated by MRI of the spine
- Describe the most common pulse sequences used for spine imaging
- Explain fundamental imaging requirements for spine imaging

INTRODUCTION AND OVERVIEW

MRI of the spine, as well as MRI of the head, are among the oldest and best understood of all MR imaging applications. The usefulness of MRI for evaluation of spinal pathology was quickly realized early in the development of MRI technology. While growth in specialized pulse sequences and imaging techniques for MR imaging of the spine has not progressed as quickly as other MRI imaging applications, spinal MRI has benefited from developments in hardware, including phased array coil technology, and in software, such as faster pulse sequences and increased image resolution.

PRIMARY SPINE CONDITIONS

Pathology of the spine typically presents as one of two clinical scenarios: **radiculopathy** and **myelopathy**. Radiculopathy is characterized by pain radiating away from the source in the spine. A common cause of spinal radiculopathy is a **herniated nucleus pulposus** (HNP) or, in more common terms, a herniated vertebral disk.

Myelopathy is related to disease of the spinal cord itself. Common causes of myelopathy include tumor, multiple sclerosis, and **syrinx**, which is an abnormal collection of fluid within the spinal cord.

Radiculopathy and myelopathy differ in symptoms and treatment. However, they are evaluated using the same imaging parameters with some specific differences. For example, in cases of known or suspected **demyelinating** disease, intravenous contrast administration is typically administered. For radiculopathy due to suspected HNP, contrast is not typically indicated unless the exam is performed post-laminectomy. Axial imaging for myelopathy covers the cord continuously whereas axial scans for radiculopathy might be prescribed only through disk spaces.

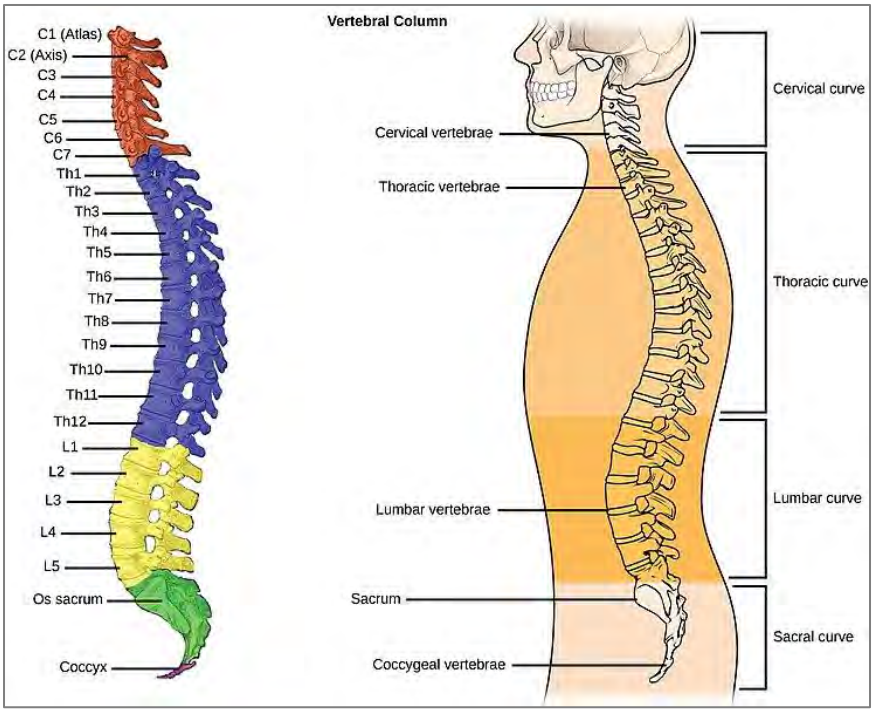

Figure 46. Illustration of spinal vertebra and position in the body. *Courtesy of CNX OpenStax. Available at https://Wikimedia Commons*

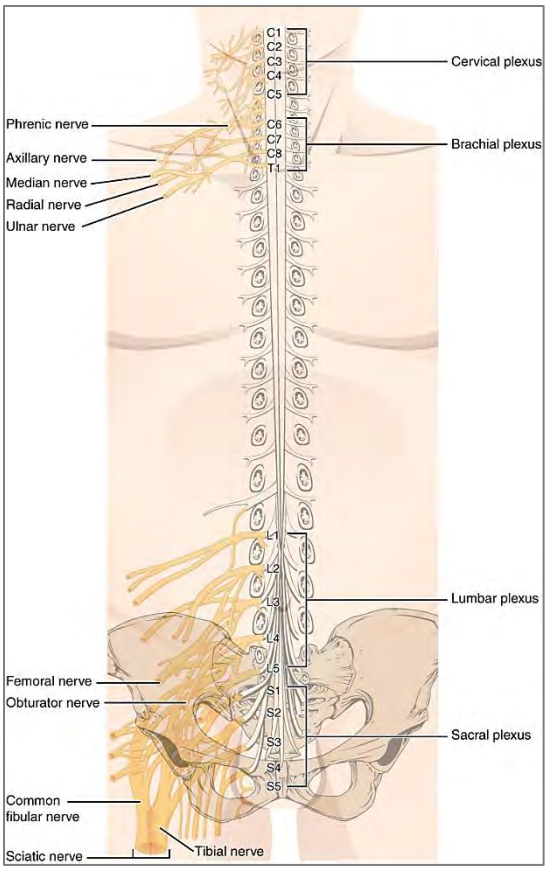

Figure 47. Illustration of the spinal plexuses, networks of intersecting nerves, of the back. *Available at https://Wikimedia.*

ANATOMY OF THE SPINE

The spine is divided into four distinct segments (**Figure 46**). Superiorly, the **cervical spine** is comprised of the first seven vertebrae. The **thoracic spine**, the longest of the four segments, encompasses the next 12 vertebrae and supports the rib cage. The next five vertebrae constitute the **lumbar spine**, which supports most of the body weight above the waist. Finally, the **sacrum** and **coccyx** represent the most inferior part of the spine. Thirty-one pairs of nerve roots exit the central nervous system from the spinal cord (**Figure 47**).

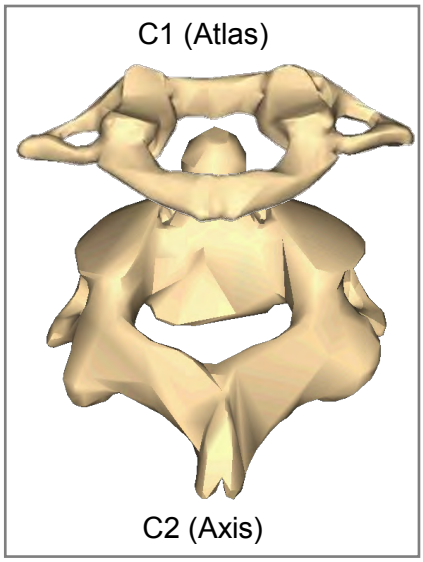

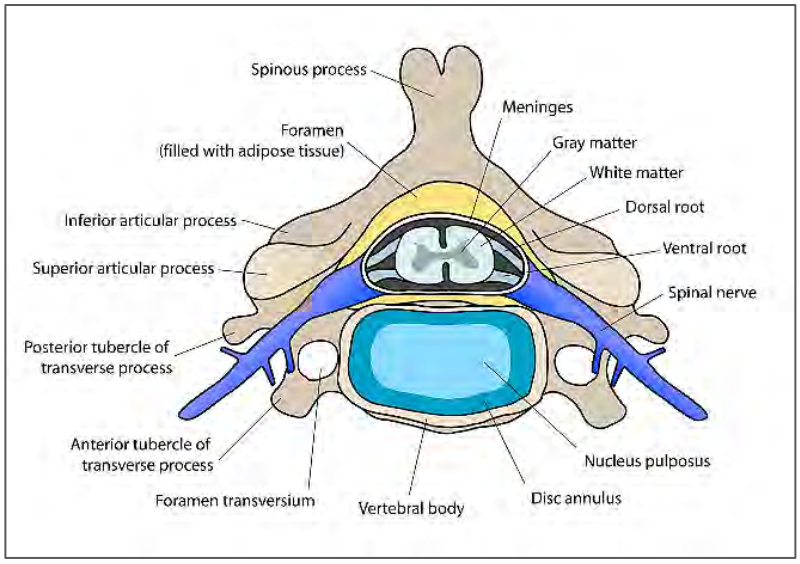

Figure 48. (Left) Illustration of C1 and C2, also called the atlas and axis. Together, the atlas and axis form the joint that connects the head and spine. *Courtesy of Anatomography.*
Animations available at Wikimedia Commons.

Figure 49. (Right) Illustration of cervical vertebra; note the spinous process. *Courtesy of Debivort.*
Available at Wikimedia Commons.

Cervical Spine

The cervical vertebrae – C1 through C7 – extend from the skull base to the thoracic inlet. The brain stem exits the skull through the foramen magnum at the medulla and becomes the spinal cord at the level of C1, the only vertebra without a body. It consists only of a ring of bone that serves as a platform on which the skull rests. The prominent feature of C2 is an upward protuberance of bone called the **odontoid process**, also known as the "dens" (**Figure 48**). The remaining five cervical vertebrae (C3-C7) are distinguished from other spinal vertebrae by their **bifid** spinous processes (**Figure 49**). See **Figures 50-52** for MRI and CT images of the cervical spine.

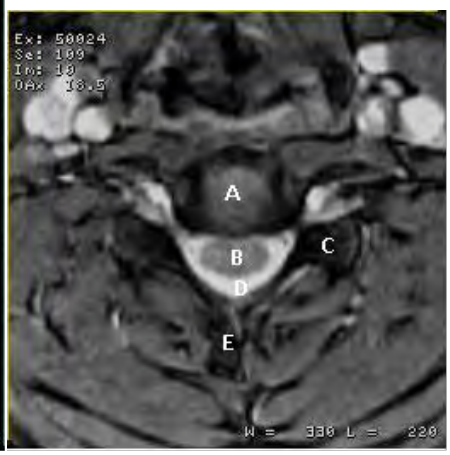

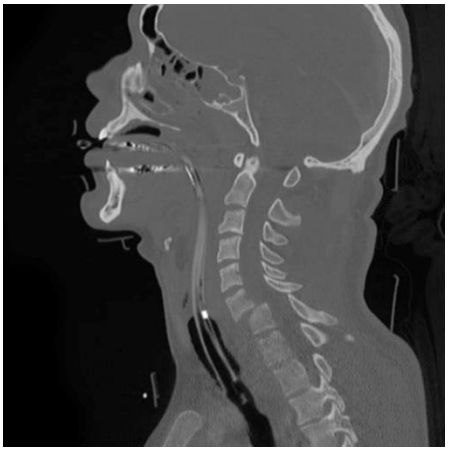

Figure 50. (Left) Sagittal T2 of the cervical spine.

Figure 51. (Center) Axial T2* of the cervical spine. (A) vertebral body (B) cord (C) transverse process (D) cerebral spinal fluid (E) spinous process.

Figure 52. (Right) CT of the cervical spine. Note the fracture dislocation at C6-C 7.
Courtesy of Frank Gaillard. Available at Wikimedia Commons

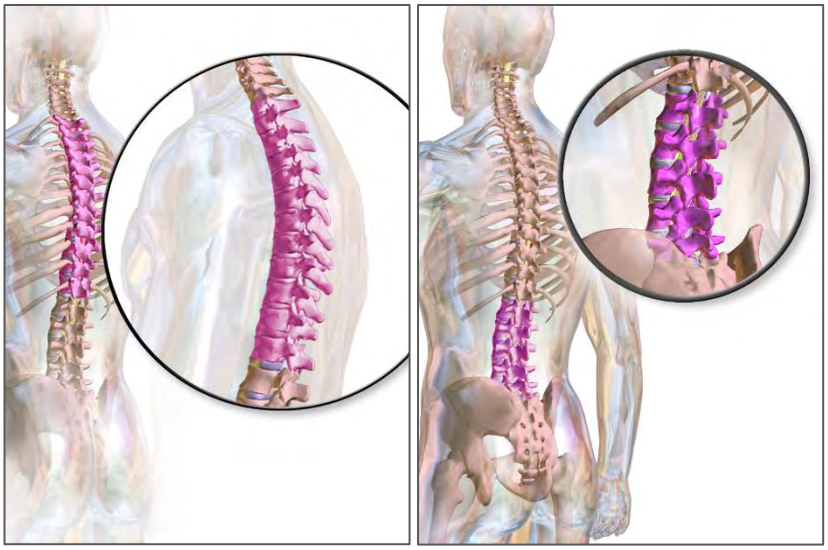

Figure 53. (Left) Illustration of the anatomy of the thoracic spine. Note the costo-vertebral articular facets for joining with the ribs.
Courtesy of BruceBlaus. Available at Wikimedia Commons.

Figure 54. (Right) Illustration of anatomy of the lumbar spine. Note the larger size compared to the thoracic and cervical vertebrae.
Courtesy of Blausen.com staff (2014). "Medical gallery of Blausen Medical 2014". WikiJournal of Medicine 1 (2). DOI:10.15347/wjm/2014.010. ISSN 2002-4436. Available at Wikimedia Commons.

Thoracic Spine

The thoracic spine, inferior to the cervical spine, is comprised of 12 vertebrae, T1 through T12. These vertebrae differ from cervical vertebrae in that their bodies are larger and become progressively larger as they descend. A notable characteristic of the thoracic vertebral bodies is the presence of costovertebral articular facets for joining with the ribs (**Figure 53**).

Lumbar Spine

The last five vertebrae, L1 through L5, comprise the lumbar spine. The lumbar vertebral bodies are the largest of all vertebrae (**Figure 54**). This segment of the spinal column supports the vast majority of the body weight above the waist. The spinal cord typically terminates at the L1 level as the conus medullaris (**Figure 55**), which gives rise to the **cauda equina**, the nerve root bundle that continues down the spinal canal. Because of the weight-bearing nature of the lumbar spine it is the most common location for degenerative disease, including HNP, typically at the L3-L4, L4-L5, and L5-S1 levels.

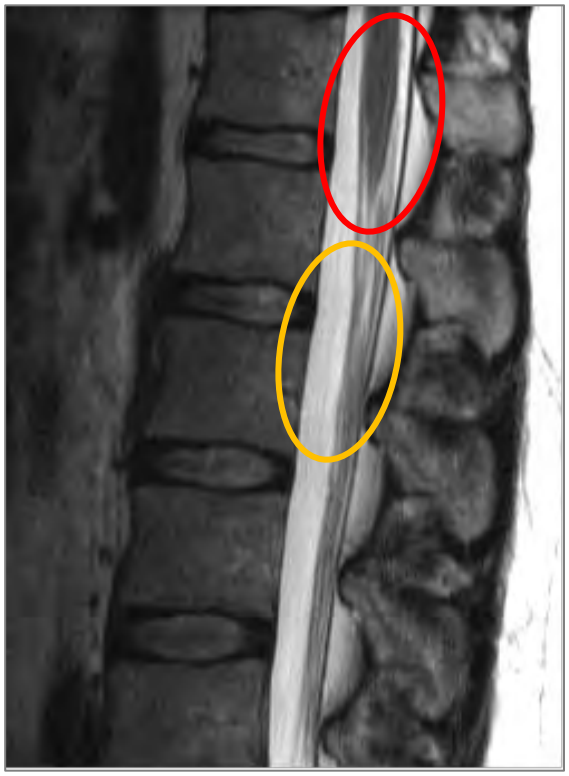

Figure 55. Sagittal T2 image demonstrating that conus medullaris (red circle) and the cauda equina (yellow circle).

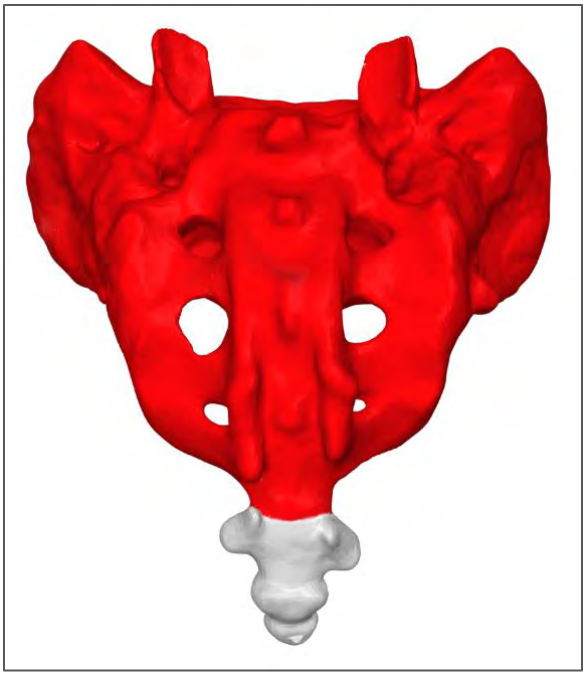

Figure 56. (Left) Illustration of sacrum (in red) and coccyx (in grey) in the lateral view. *Courtesy of BodyParts3D. Available at Wikimedia Commons.*

Figure 57. (Right) Illustration of sacrum (in red) and coccyx (in grey) in the posterior view. *Courtesy of BodyParts3D.* Available at Wikimedia Commons.

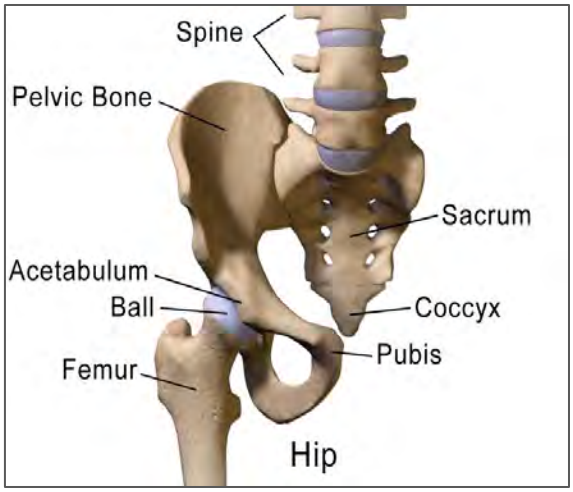

Figure 58. Illustration of hip anatomy; note articulation of the sacrum with the iliac (pelvic) bone. *Courtesy of BruceBlaus. Available at https://Wikimedia Commons.*

Sacrum and Coccyx

The most inferior portion of the spinal column consists of the sacrum and coccyx (**Figures 56 and 57**).

Composed of five segments, S1 through S5, the sacrum articulates with the iliac bones of the pelvis (**Figure 58**). The five sacral segments are large, fused vertebral bodies that form a singular, large triangular bone that is wider superiorly and gradually narrows to an apex inferiorly. The sacrum is curved in a concave manner, with the curvature more pronounced in females. Four pairs of **foramina** in the sacrum allow spinal nerves to pass through to the sacrum, constituting the **lumbosacral plexus**.

Typically the coccyx or tailbone is made up of four small, fused vertebrae, though common variants include one less or one more vertebral body in this segment. Like the sacrum, the coccyx is wider superiorly and narrows inferiorly to a small apex at its tip.

Intervertebral Disk

The superior and inferior surfaces of each vertebral body are abutted by thick cartilage consisting of a semi-gelatinous material called the nucleus pulposus, commonly known as the disk (**Figure 59**). This material is contained within a thick, fibrous perimeter called the **annulus fibrosus**. Excessive downward pressure on an intervertebral disk may cause it to herniate into the spinal canal where the spinal cord and its exiting nerve roots reside. Small herniations may be asymptomatic but larger herniations may exert pressure on the spinal cord or nerve roots causing pain, numbness, and tingling that may radiate over the shoulders or hips and down the arms or legs. If the herniation is more lateral, involving one side of the vertebral foramen, the symptoms may be restricted to that side. In severe cases, herniations may cause the annulus to rupture, allowing free fragments of the nucleus pulposus to compress nerves and cause weakness in the legs or arms.

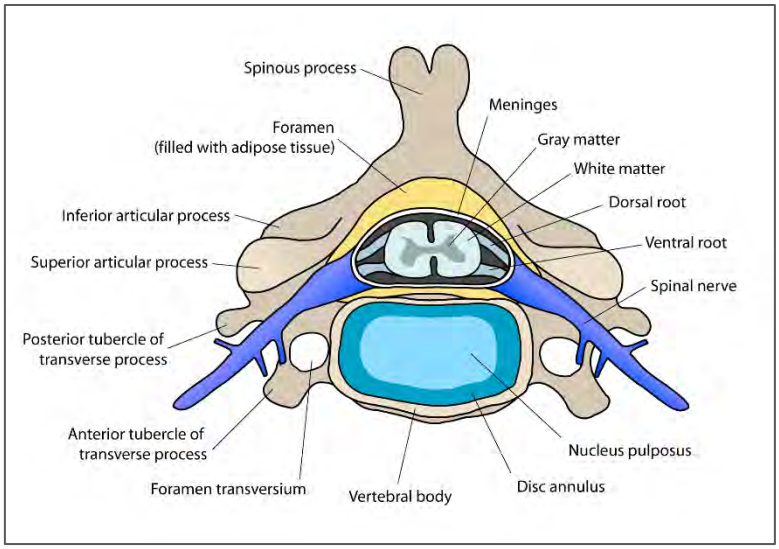

Figure 59. Illustration of cervical vertebra; note the disk annulus, which contains the nucleus pulposus, a semi-gelatinous material. *Courtesy of Debivort. Available at Wikimedia Commons.*

GENERAL IMAGING OF THE SPINE

In general, imaging of any spinal segment is essentially the same.

Surface Coils

Imaging of any spinal segment requires the use of a surface coil. Developments in surface coil technology over the past 25 years have greatly improved the speed and quality of spinal MR imaging. Initial surface coil technology consisted of simple single channel linear coils that produced poor signal-to-noise ratio and required long scan times to obtain diagnostic quality images.

The development of quadrature coils greatly increased image quality, but it was the development of phased array coil technology that provided a significant boost in SNR. Today, all spine imaging is done with phased array coil technology.

The particular phased array coil configuration used is determined by the area of the spine to be imaged and may vary by facility as well as manufacturer. Typically, the smallest coil configuration for the area of interest is used. For example, in imaging the cervical spine, a 2-3 phased array coil configuration may suffice, while for the thoracic spine a 3-4 phased array coil configuration may be necessary.

Surface Coil Intensity Correction

The increasing availability of clinical 3.0T scanners, as well as the development of 8, 16, and 32 receiver systems, has resulted in increased visualization of high signal intensity in the tissue closest to the surface coil (**Figure 60**).

The coil design heightens the brightness of the tissue closest to the coil, resulting in a haloed appearance of the entire image. The peripheral anatomy closest to the coil appears brighter than the anatomy toward the center of the image. This appearance may be distracting to the radiologist, and adjusting the window/level to create a more uniform image is virtually impossible since setting the brightness and contrast optimal to the spinal column and cord makes the posterior fat so bright that it is distracting.

Figure 60. Phased array coils.

(Top) 16-channel cardiac coil used for chest and cardiac imaging; also useful for imaging the hip.

(Center) 16-channel body coil used to image the chest-abdomen, abdomen-pelvis and thighs-lower legs depending on where the coil is placed on the patient.

(Bottom) 32-channel head, neck, and full spine coil used to image the head, neck, upper chest, brachial plexus and any segment of the spine.

Courtesy of GE Healthcare.

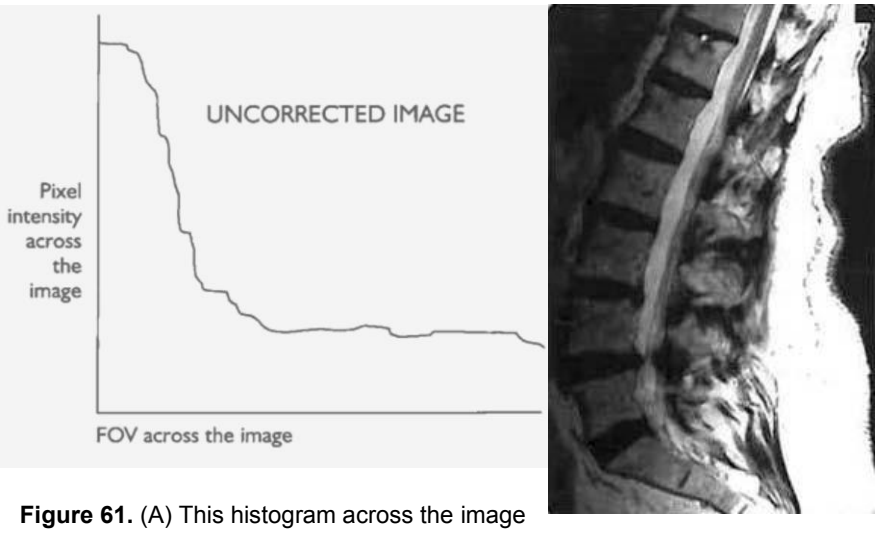

Figure 61. (A) This histogram across the image shown demonstrates the uncorrected high variation in signal intensity across the image. (B) Sagittal T2 of the lumbar spine displays characteristic very bright signal from fat posterior and proximate to the spine phased array coil. The extremely bright signal can be visually distracting to the radiologist.

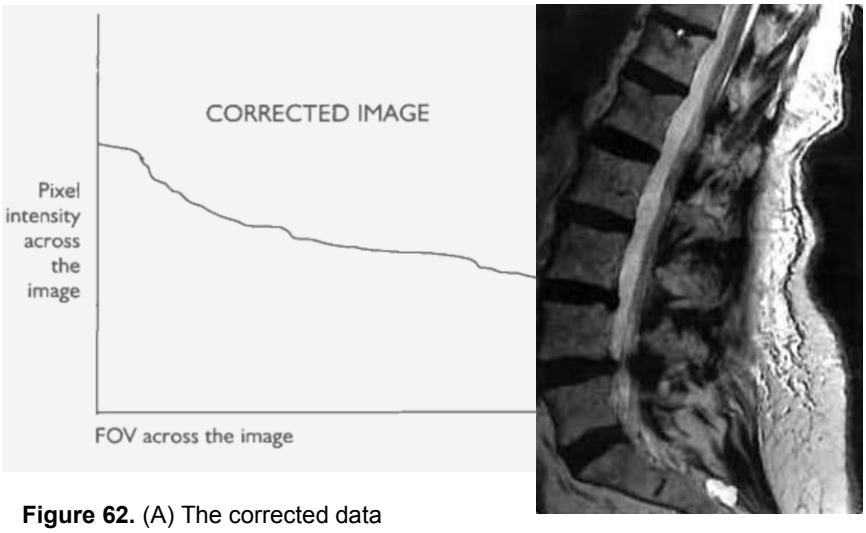

Figure 62. (A) The corrected data corresponding to the filtered image. (B) The same lumbar spine image after correction using an image intensity filter. Note the suppression of the excessive fat signal. The images shown in Figures 61 (B) and 62 (B) have exactly the same brightness and contrast levels.

For example, imaging a sagittal lumbar spine using a phased array spinal coil will demonstrate extremely bright signal posteriorly in the superficial fat closest to the coil, yet spinal structures further from the spinal coil and deep into the fat will appear less bright (**Figure 61**). The resulting significant difference in contrast can make it difficult to window/level the image for optimal brightness and contrast. Adjusting the window/level to optimize evaluation of the spinal cord may result in the posterior fat appearing so bright as to distract the radiologist. Conversely, adjusting the window/level to “dampen” the extremely bright fat signal may result in the spinal contents appearing too dark for adequate evaluation.

To correct, or at least reduce, excessive brightness near the coil, MRI manufacturers have instituted several surface coil intensity correction algorithms that are implemented into the reconstruction process or as a post-processing feature. The simplest and most common method uses software to view a pixel intensity histogram across the image (**Figures 61 and 62**). In the lumbar spine example given above, the histogram shows very high signal intensity superficially in the image, which then sharply drops off in the anatomy farther from the coil. The computer then reorganizes the image data to reduce the brighter signal intensity and increase the darker intensity. Finally, the data are reconstructed to display an image with uniform intensity across the image.

Patient Positioning

Positioning for spine imaging is typically supine, head first or feet first depending on the coil design, and in some cases patient preference. The patient is positioned straight on the table. To make the patient as comfortable as possible and reduce pressure in the lumbar region, a wedge sponge or pillow may be placed under the patient's knees. Although uncommon, some MRI designs allow images to be obtained while the patient is standing or sitting. These options produce weight-bearing images, though the usefulness of this scanning technique for obtaining high-resolution images is unclear. Supine positioning remains the standard technique.

Patient Positioning and Comfort

Most patients undergo MR imaging of the spine for some type of pain, from mild to extreme. Technologists must try to make the patient as comfortable as possible to limit motion and ensure a high-quality image.

- Position the patient as straight as possible on the exam table
- Place a wedge under the patient's knees to take pressure off the patient's back
- For cervical spine exams, place a small roll under the patient's neck

CLINICAL INDICATIONS FOR MRI OF THE SPINE

Degenerative Disease

MR has become the modality of choice for the evaluation of degenerative disease in the spine. The availability of direct multiplanar sequences is ideal for the visualization of disk protrusions and herniations and other degenerative changes (**Figure 63**).

Tumor

MR is superb for delineating tumors of the bony spine, making MRI the modality of choice for the evaluation of suspected spinal cord compression due to metastases in patients with known primary neoplasms, the impact of which affects outcome by expediting diagnosis and treatment (**Figure 64**).

Figure 63. T2-weighted image of a spinal disk protrusion at L5 level compressing the left central nerve root (circle).
Available at Wikipedia.

Figure 64. Sagittal lumbar spine and lower thoracic spine metastasis. (A) T2 demonstrating hypo-intense signal just above the conus (circle) (B) T1 demonstrating bony metastasis in the vertebral bodies of T12, L2, and L3. (C) T1 postcontrast with fat suppression demonstrating enhancement of the vertebral metastasis (circles), as well as the tumor in the spinal cord (arrow). *Available at Radiology Picture of the Day.*

Figure 65. Sagittal view of C4 fracture and dislocation, and spinal cord compression. *Courtesy of Андрей Королев 86. Available at Wikimedia Commons.*

Trauma

The real value of MRI in trauma cases is in the detection of soft tissue sequelae, as well as spinal cord injury. Plain films and CT exams remain superior for fracture detection. However, if epidural hematoma or traumatic disk herniation is suspected, MRI optimizes visualization of these sequelae (**Figure 65**).

Because MR imaging is not sensitive for diagnosing vertebral fractures and because trauma patients are often unstable, MRI is not usually performed in the acute setting of trauma. However, MRI can be very useful for spinal cord assessment, which is of great prognostic value.

MRI can be used to assess vertebral fracture in a non-acute trauma setting, for example in osteoporotic patients and/or patients undergoing steroid therapy with increased risk of compression fractures.

Congenital Anomalies

MRI is well-suited for the evaluation of congenital anomalies. Pediatric patients may present with a tethered cord, often associated with **spina bifida** (**Figure 66**). Tethered cord occurs when the conus medullaris fails to migrate to its normal L1-L2 location and is stretched beyond its normal T12-L2 location. Symptoms of a tethered cord may vary from low back pain, to weakness in both legs, to bowel and/or bladder incontinence. The most severe form of spina bifida involves formation of a **myelomeningocele** and is usually associated with a tethered cord. A myelomeningocele is a condition in which neural elements and meninges exit a dysraphic (incomplete closure) spinal canal in a pouch beyond the vertebral column.

Figure 66. Sagittal T2 of the lumbar spine demonstrating a tethered cord (white arrows) with an attached cystic lesion inferiorly (black arrows).

IMAGING PLANES AND SEQUENCES

Imaging in the Sagittal Plane

In the sagittal plane, an odd number of slice locations is performed to ensure that one slice is directly centered on the spinal cord, assuming the spine is not scoliotic. For tissue contrast, T2 and T1 imaging is routinely used, and sagittal STIR imaging is also useful. Each of these sequences provides valuable information for evaluating spinal pathology.

T2 imaging, typically using fast or turbo (FSE/TSE) spin echo, yields high resolution, high SNR images with bright cerebrospinal fluid (CSF) and dark spinal cord. The T2 FSE/TSE sequence is useful for evaluation of HNP, cord lesions such as MS and syrinx, and intervertebral disk space hydration status.

T1 imaging, usually using a lower echo-train FSE/TSE sequence, yields high spatial resolution and high SNR images with dark CSF and a brighter spinal cord. T1 imaging best demonstrates marrow replacement by bone metastases in the vertebrae and is also useful for evaluating HNP.

Particularly at 3.0T field strengths, T1 FLAIR provides excellent T1 contrast by utilizing long TI times (~2200msec) to increase the variance in T1 recovery of various tissues such as CSF, spinal cord, and bone.

STIR imaging results in bright CSF signal with robust fat suppression, though usually at lower spatial resolution. STIR is useful for evaluating bone marrow pathology, cord signal abnormality, vertebral body neoplasms, and disk hydration status. Typical slice thickness ranges from 3.0mm for the cervical spine, 3.0mm-4.0mm for the thoracic spine, to 4.0mm for the lumbar spine. (See protocol recommendations at the end of this unit.)

Imaging in the Axial Plane

Axial imaging typically employs both T1W and T2W imaging sequences. The degree of obliquity, if any, can either be angled through the intervertebral disk spaces to demonstrate HNP with the least distortion, or performed continuously through the disk spaces and vertebral bodies to allow for complete coverage of the spinal canal and spinal cord as well as the vertebral bodies. It is not uncommon for imaging facilities to obtain images using a combination of approaches.

POSTCONTRAST IMAGING

Intravenous gadolinium contrast administration is indicated for certain spinal applications, including spinal canal and cord neoplasm, multiple sclerosis, intramedullary inflammatory and vascular lesions, and syrinx. Contrast may also help distinguish benign etiologies of compression fractures from pathologic compression fractures due to metastatic disease. Following laminectomy, contrast enhancement helps differentiate post-surgical scarring from recurrent disk herniation (**Figure 67**). **Scar tissue** typically enhances with contrast, while disk material does not. Postcontrast T1W imaging is typically performed with fat suppression when extramedullary, non-spinal cord pathology is suspected, such as with vertebral body metastatic disease. When spinal cord pathology is suspected, as with multiple sclerosis, fat suppression is typically not performed as this reduces the contrast between cord and surrounding CSF.

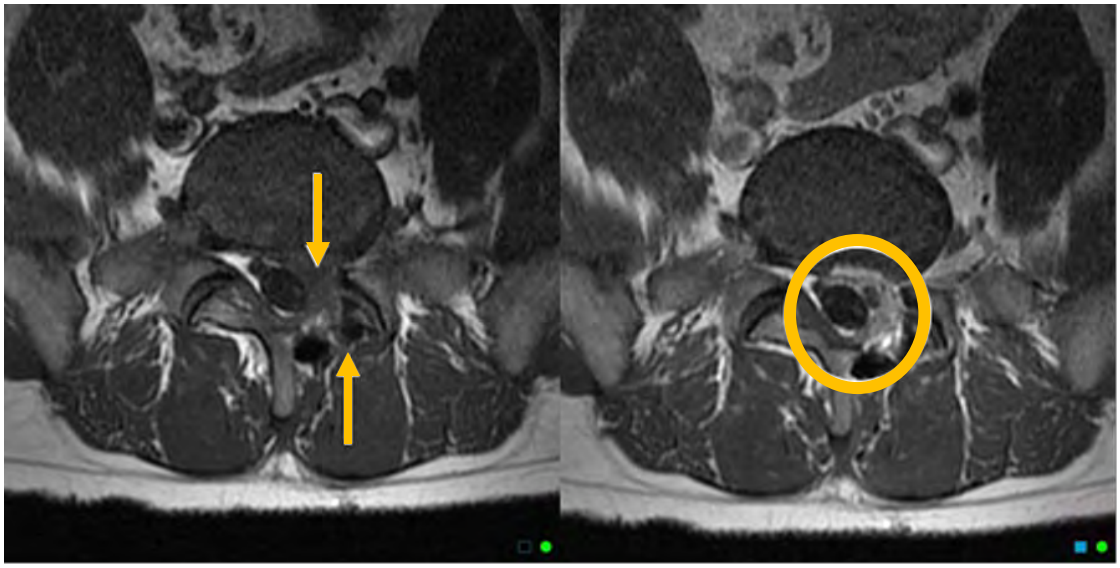

Figure 67. Postoperative axial T1 of the lower lumbar spine. (A) Precontrast image demonstrating low signal intensity in the subdural space on the left side (upper arrow) just anterior to the site of a laminectomy (lower arrow). (B) Postcontrast image demonstrating marked enhancement of the subdural space indicating scar tissue (circle).

MR NEUROGRAPHY

MR neurography is magnetic resonance imaging of specific peripheral nerves to evaluate the signal characteristics of the targeted peripheral nerves and surrounding fat. While standard MRI pulse sequences are used, it is the slice orientation and contrast mechanisms that differentiate MR neurography from other imaging applications. Pathology such as inflammation, swelling, and compression due to trauma or tumor alter the signal characteristics of the nerve, either at the site of the injury or at some distance along the nerve. The most frequently targeted nerves include the brachial plexus, the lumbosacral plexus, the pudendal nerve, ulnar nerve, and popliteal nerve (**Figures 68-70**).

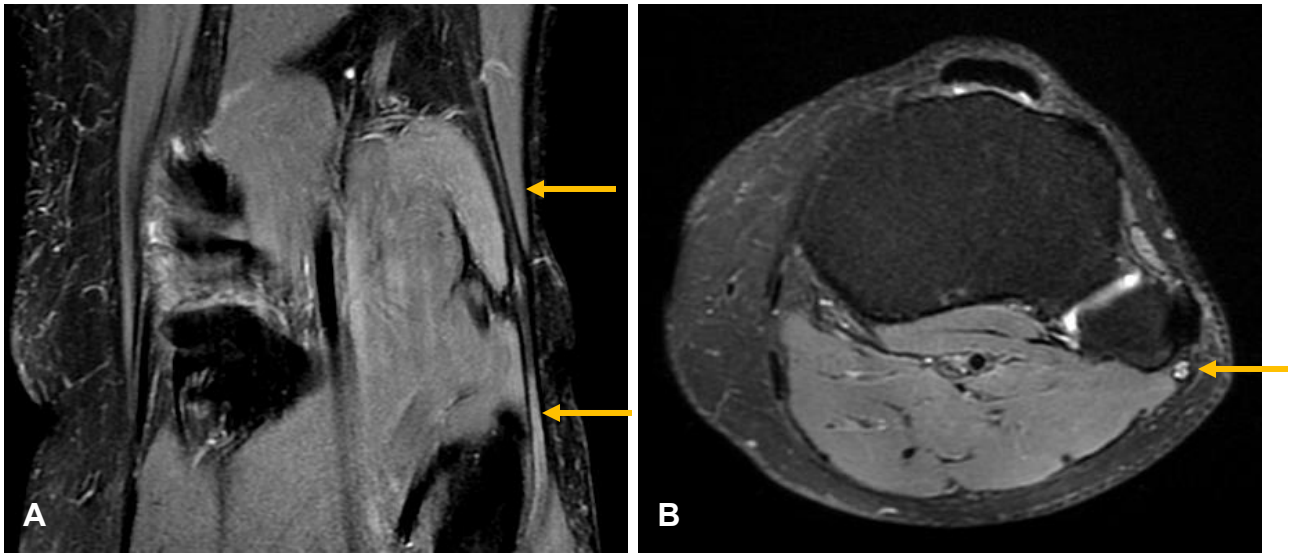

Figure 68. Neurogram of peroneal nerve demonstrating a focal area of neuritis or nerve injury. (A) Coronal STIR of the knee. Note the grayish signal (upper arrow) of the normal appearance of the nerve at the level of the knee. (B) Axial intermediate PD-weighted image just below the knee. Lower arrow in (A) and arrow (B) demonstrate brighter appearance of the damaged nerve.

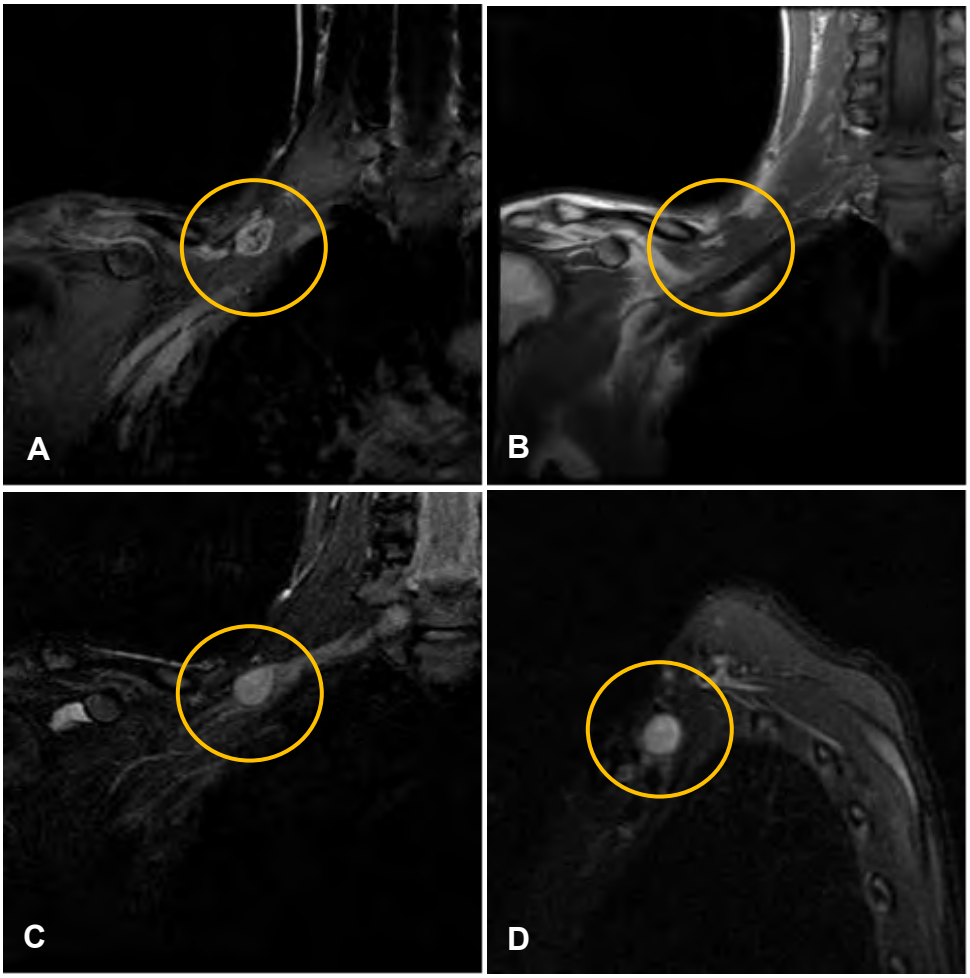

Figure 69. Brachial plexus neurogram demonstrating a 1.7 x 1.3 x 1.3cm lesion. The lesion has the signal characteristics of a schwannoma or enlarged lymph node. (A) Coronal postcontrast SPGR. (B) Coronal T1. (C) Coronal STIR. (D) Sagittal STIR.

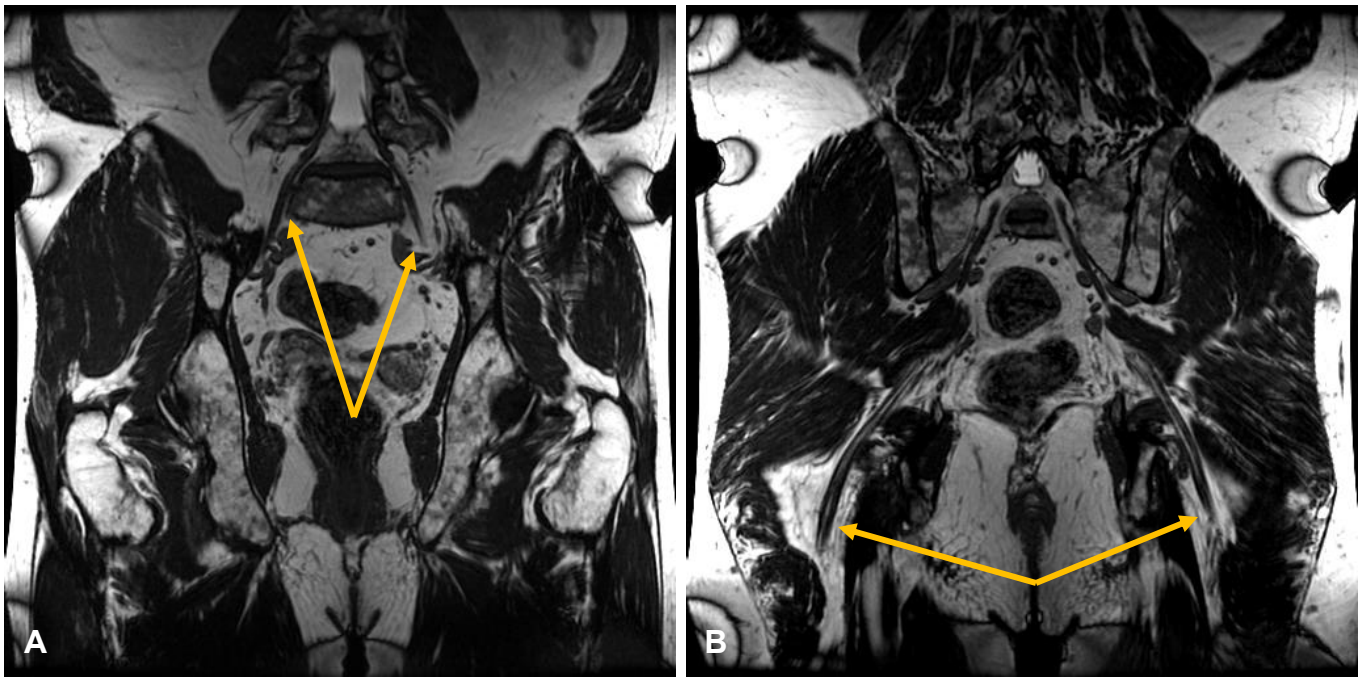

Figure 70. Coronal 3D FIESTA™ neurogram of the lumbosacral plexus. (A) Left and right L5 nerves (arrows). (B) Left and right sciatic nerves (arrows).

MR imaging of the spine is very sensitive for evaluating the spinal cord and its exiting nerve roots within the spinal canal. However, for a subgroup of patients with symptoms of radiculopathy, standard MRI of the cervical, thoracic, or lumbar spine does not reveal the cause of symptoms, such as limb pain, tingling, or weakness. It is in the evaluation of these clinical complaints that high-resolution MR neurography is useful. For these patients, the primary goal of MR neurography is to visualize the structure of the nerve in question, eg, lumbosacral plexus for hip and leg pain or brachial plexus for neck, shoulder, and/or arm pain; locate the site of injury; and determine the cause of the symptom, eg, compression.[5]

MR neurography techniques typically employ high-resolution T1W imaging to visualize the nerve and fat-suppressed T2 or STIR imaging to visualize abnormally high-signal within the nerve. High spatial resolution is obtained through the use of thin 2D or 3D slice thicknesses and carefully positioned high SNR phased array coils. Careful slice orientation is also essential for visualizing the targeted nerve.

3D acquisitions have the advantage of yielding very small and nearly isotropic voxels. Such near-square 3D acquisitions can be reformatted in any plane to optimally lay out the nerve in a single oblique plane. 2D scan planes typically include axial and coronal imaging, although sagittal plane acquisitions may also be helpful.

SUMMARY

Spine MRI has not undergone the vast applications development and advancements that brain MRI has. Nonetheless, spinal MRI has benefited from many of the same technical developments, such as phased array coils, that have resulted in higher signal-to-noise ratio and spatial resolution. Moreover, pulse sequence development and gradient performance improvements have resulted in far fewer artifacts from CSF flow, breathing and cardiac motion, and swallowing motion. The end result is that today MRI of the spine demonstrates a wide range of pathologies from disk herniations to small MS lesions to neurography. MRI has truly revolutionized spinal imaging for indications of radiculopathy and myelopathy. Considerable improvements have been and continue to be made to fine-tune and advance this technology.

MRI is the modality of choice for nearly all spinal imaging.

Protocols for MRI of the Brain

The following protocols list typical planes of acquisition along with recommended coverage and slice thickness as recommended by the American College of Radiology*. Specific parameters such as TR, TE, FOV, and echo train length will vary according to field strength, manufacturer, and individual facility preferences.

* American College of Radiology Clinical Image Quality Guide. May 2017. Refer to ACR MR Accreditation Program Guidelines for specific parameter requirements.

ROUTINE BRAIN PROTOCOL

Axial T1 (pre- and postcontrast if indicated) T2, T2 FLAIR, and DWI	
Coverage:	From foramen magnum to top of the calvarium.
Slice Thickness:	≤ 5.0mm

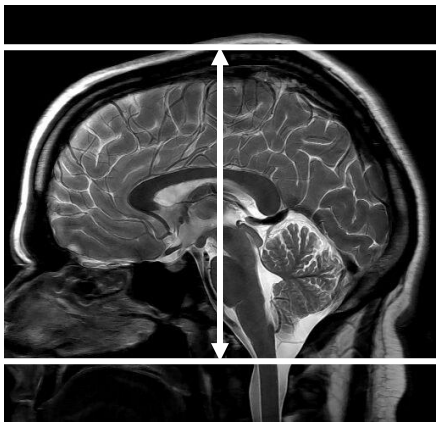

Sagittal T1	
Coverage:	From left side of brain to right side.
Slice Thickness:	≤ 5.0mm

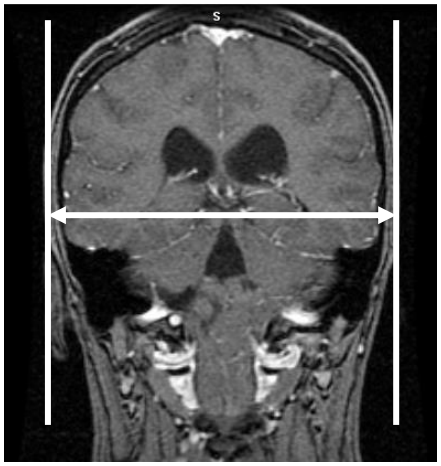

Coronal T1	
Coverage:	From anterior cranial vault to posterior cranial vault.
Slice Thickness:	≤ 5.0mm

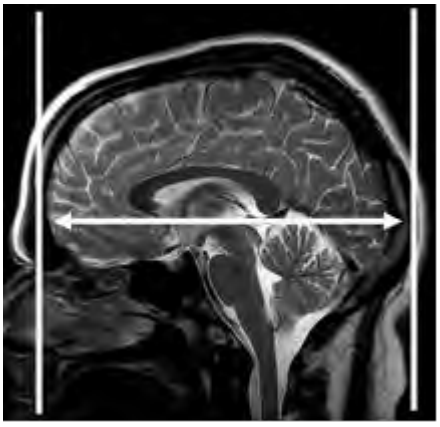

BRAIN PROTOCOL FOR MULTIPLE SCLEROSIS

Axial T1 (pre- and postcontrast if indicated), T2, T2 FLAIR, and DWI	
Coverage:	From foramen magnum to top of the calvarium.
Slice Thickness:	≤ 5.0mm
Sagittal T2 FLAIR	
Coverage:	From left side of brain to right side.
Slice Thickness:	≤ 5.0mm
Coronal T1	
Coverage:	From anterior cranial vault to posterior cranial vault as with routine brain protocol.
Slice Thickness:	≤ 5.0mm

BRAIN PROTOCOL FOR PRIMARY BRAIN TUMORS

Axial T1 (pre- and postcontrast), T2, T2 FLAIR, and DWI	
Coverage:	From foramen magnum to top of the calvarium as with routine brain protocol.
Slice Thickness:	≤ 5.0mm
If positive, thinner slice acquisition and fat suppression post IV-contrast may be necessary	

BRAIN PROTOCOL FOR SELLA TURCICA

Axial T1 (pre- and postcontrast), T2, T2 FLAIR, and DWI	
Coverage:	From foramen magnum to top of the calvarium.
Slice Thickness:	≤ 5.0mm
Sagittal T1	
Coverage:	From medial temporal lobe to medial temporal lobe.
Slice Thickness:	≤ 3.3mm
Coronal T1 IV contrast	
Coverage:	Cover entire pituitary gland
Slice Thickness:	≤ 3.3mm
Scan 5-6 dynamic phases at 25-30 seconds per phase	

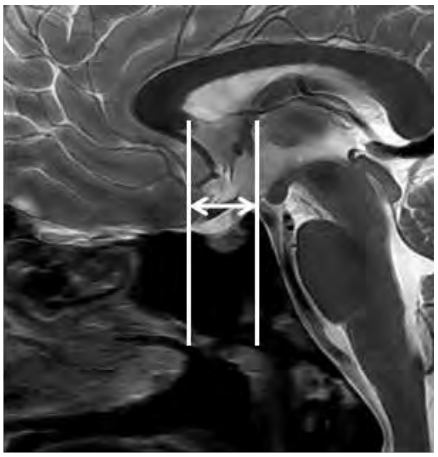

BRAIN PROTOCOL FOR OPTIC NERVES AND ORBITS

Axial T1 whole brain (pre- and postcontrast), T2, T2 FLAIR, and DWI	
Coverage:	From foramen magnum to top of the calvarium.
Slice Thickness:	≤ 5.0mm
Axial T1 thin slices (pre- and postcontrast) with fat suppression	
Coverage:	Through the entire orbit.
Slice Thickness:	≤ 3.0mm
Sagittal T1	
Coverage:	From left side of brain to right side.
Slice Thickness:	≤ 5.0mm
Coronal T1 (pre- and postcontrast) and T2 both with fat suppression	
Coverage:	From anterior dorsum sella to eyelids.
Slice Thickness:	≤ 5.0mm

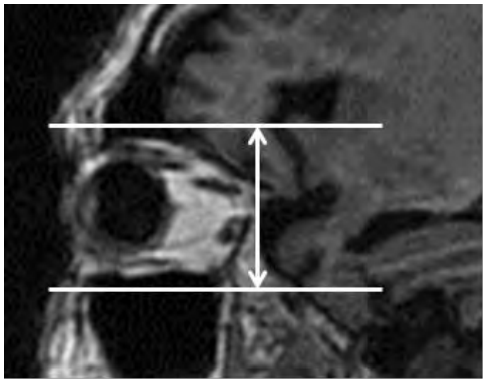

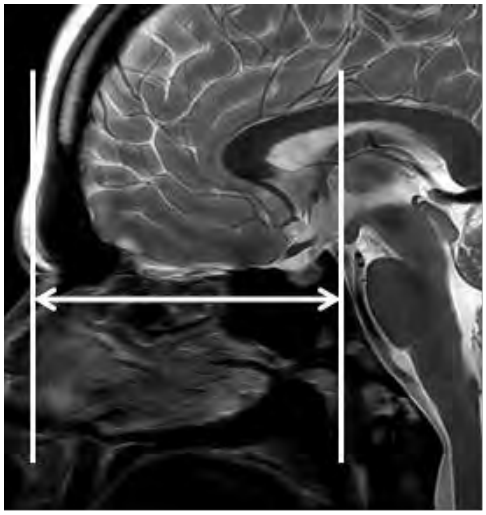

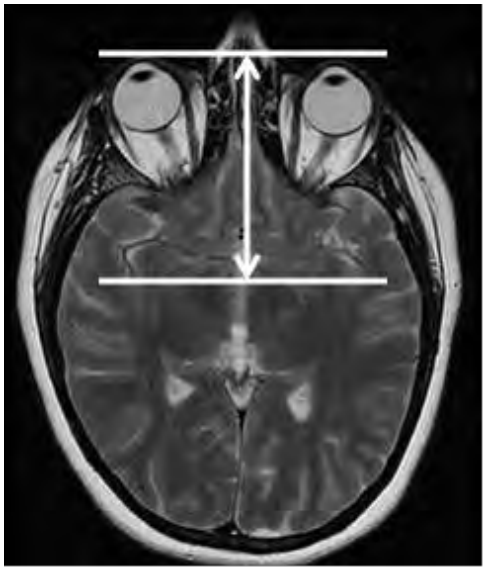

BRAIN PROTOCOL FOR IACS

Axial T1 whole brain (pre- and postcontrast if indicated), T2, T2 FLAIR, and DWI	
Coverage:	From foramen magnum to top of the calvarium.
Slice Thickness:	≤ 5.0mm
Axial T1 thin slices (pre- and postcontrast) with fat suppression	
Coverage:	Must cover top of IACs to cervico-medullary junction.
Slice Thickness:	≤ 3.0mm
Axial 3D bright fluid ultra-thin slice	
Coverage:	Must cover top of IACs to cervico-medullary junction.
Slice Thickness:	≤ 2.0mm
This series can be reformatted to run perpendicular through the semicircular canals through the entire 7th and 8th nerves.	
Sagittal T1	
Coverage:	From left side of brain to right side.
Slice Thickness:	≤ 5.0mm
Coronal T1 (pre- and postcontrast) with fat suppression	
Coverage:	Must cover pituitary to 4th ventricle.
Slice Thickness:	≤ 3.0mm

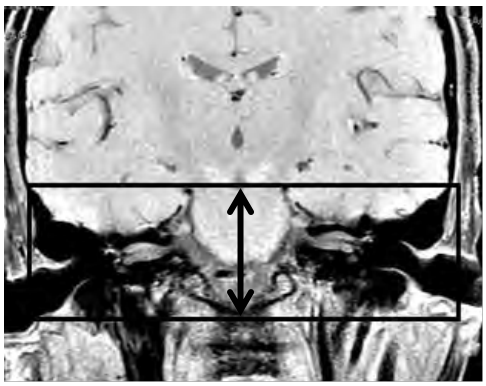

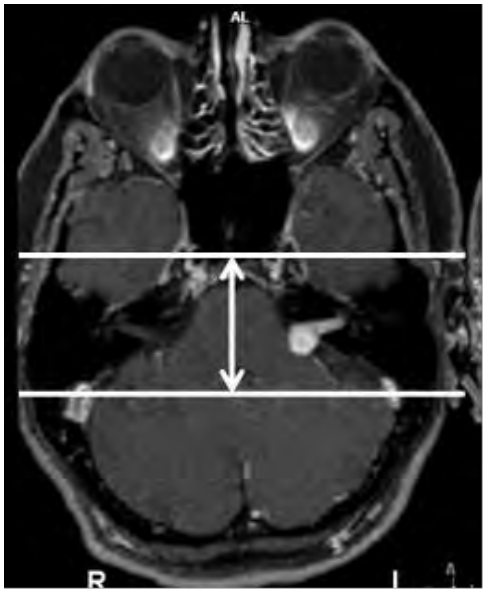

BRAIN PROTOCOL FOR HEMORRHAGE OR TRAUMA

Axial T1 whole brain (pre- and postcontrast if indicated), T2, T2 FLAIR, and DWI	
Coverage:	From foramen magnum to top of the calvarium as with routine brain protocol.
Slice Thickness:	≤ 5.0mm
Axial susceptibility weighted	
Coverage:	From foramen magnum to top of the calvarium as with routine brain protocol.
Slice Thickness:	≤ 5.0mm
This series is typically a GRE pulse sequence or a specific EPI-based sequence sensitized to magnetic susceptibility	
Sagittal T1	
Coverage:	From left side of brain to right side as with routine brain protocol.
Slice Thickness:	≤ 5.0mm
Coronal T1	
Coverage:	From anterior cranial vault to posterior cranial vault as with routine brain protocol.
Slice Thickness:	≤ 5.0mm

MR ANGIOGRAPHY OF THE BRAIN PROTOCOL

Axial 3D TOF multi-slab	
Coverage:	From foramen magnum to the top of the corpus callosum.
Slice Thickness:	≤ 1.5mm

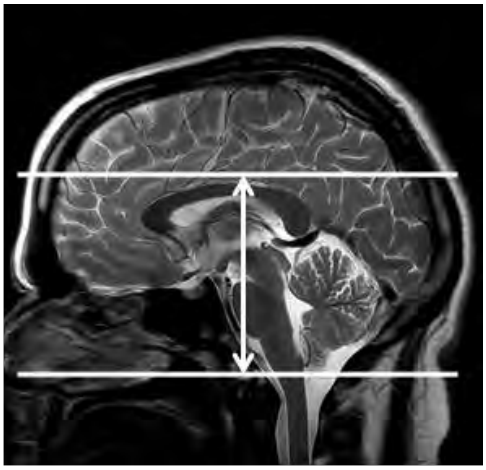

MR ANGIOGRAPHY OF THE NECK PROTOCOL

Coronal 3D contrast-enhanced	
Coverage:	From aortic arch to the Circle-of-Willis. Include basilar and vertebral arteries through carotid siphon.
Slice Thickness:	≤ 1.5mm

In this exam, some form of bolus timing technique is performed.

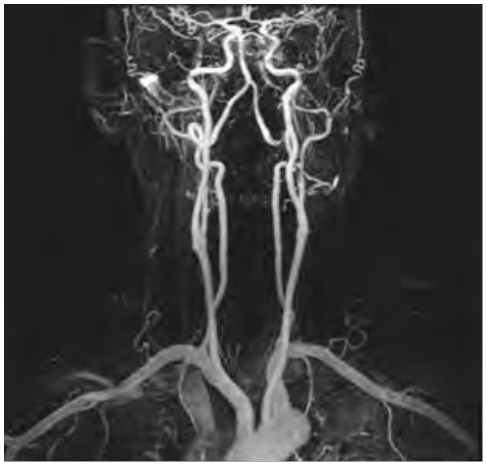

Protocols for MRI of the Spine

The following protocols list typical planes of acquisition along with recommended coverage and slice thickness as recommended by the American College of Radiology*. Specific parameters such as TR, TE, FOV, and echo train length will vary according to field strength, manufacturer, and individual facility preferences.

* American College of Radiology Clinical Image Quality Guide. May 2017. Refer to ACR MR Accreditation Program Guidelines for specific parameter requirements.

CERVICAL SPINE

Sagittal T1, T2, and STIR	
Coverage:	Left-Right coverage: neural foramen-to-neural foramen. Superior-Inferior coverage: foramen magnum to T1.
Slice Thickness:	≤ 3.0mm
Axial	
Coverage:	Contiguously from C3-T1. Slices can be either orthogonal or angled to the majority of the disk spaces.
For cord lesions such as multiple sclerosis, cover from foramen magnum to T1 (see sagittal image below for example)	
Slice Thickness:	≤ 3.0mm

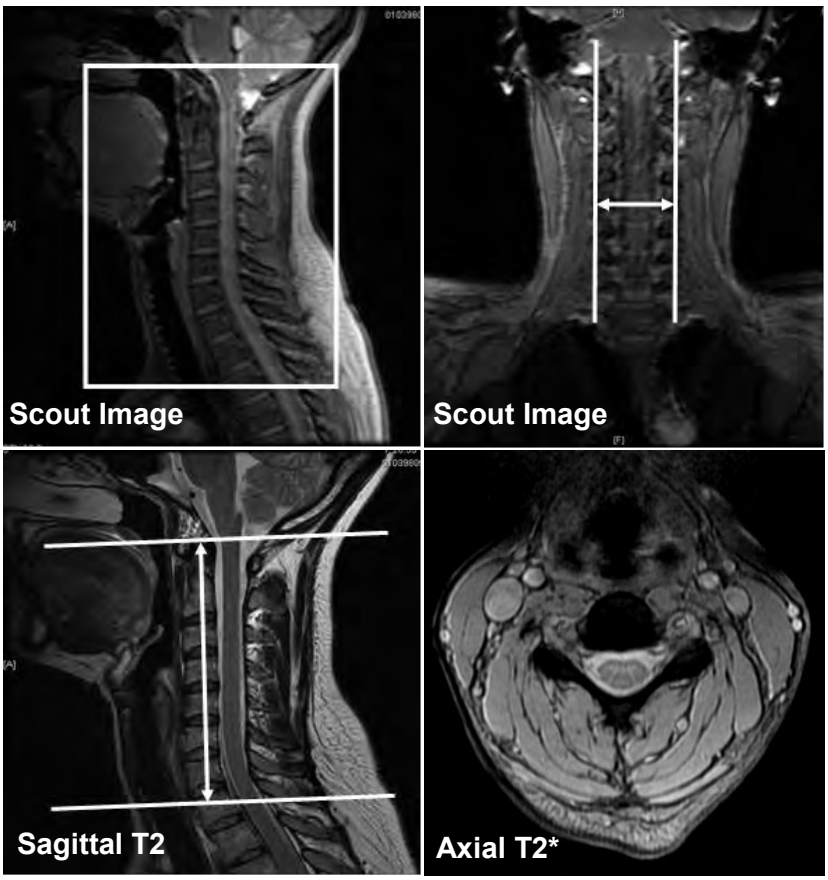

THORACIC SPINE

Note: A large FOV scout or localizer sagittal series is required to ensure accurate vertebral body count from C2 down into the thoracic spine.

Sagittal T1, T2, and STIR	
Coverage:	Left-right coverage: neural foramen-to-neural foramen. Superior-inferior coverage: C7 TO L1.
Slice Thickness:	≤ 3.0mm

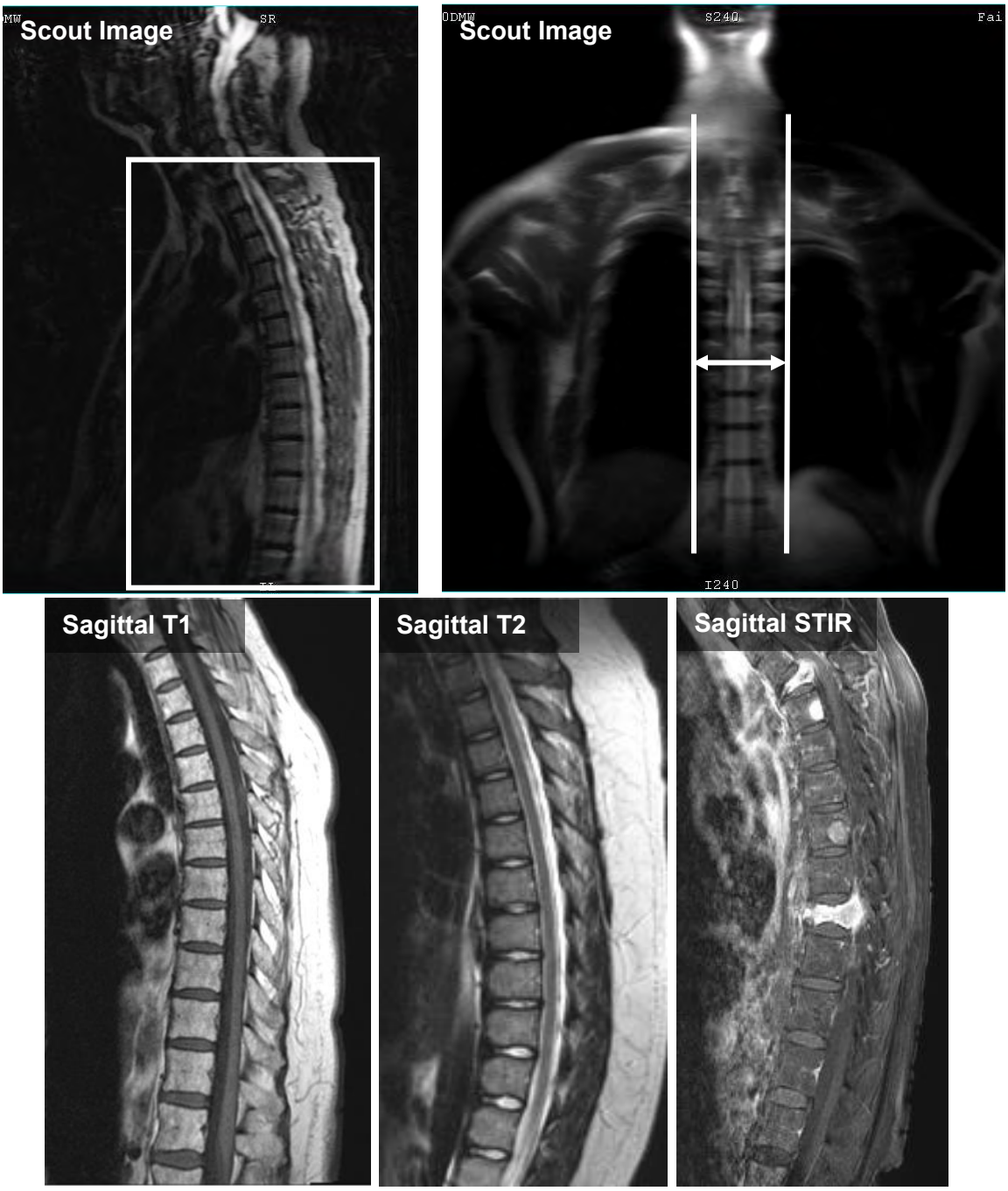

Courtesy of Forsythe Technical Community College, Health Technologies Division, Winston-Salem, NC

THORACIC SPINE

Axial T1 or T2	
Coverage:	Slices may be contiguous or angled. Contiguous slices through at least 6 vertebral bodies and intervertebral disk spaces. Angled slices must have at least 3 slices through intervertebral disk spaces with the center slice in the middle of the disk space.
Slice Thickness:	≤ 4.0mm

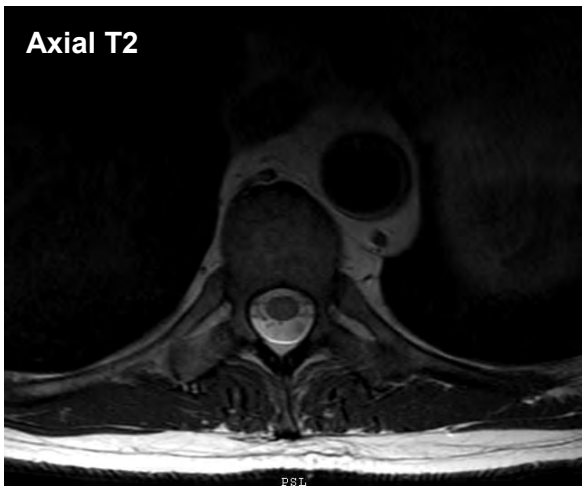

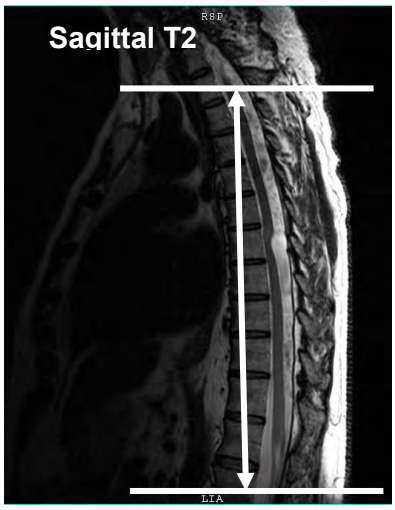

Optional coronal T1 or T2 for severe scoliosis	
Coverage:	In cases of severe scoliosis, a coronal series may be useful. Anterior-posterior coverage is from the most posterior spinous process through the anterior portion of the most anterior vertebral body.
Slice Thickness:	≤ 5.0mm

Courtesy of Fairfax Technical Community College, Health Technologies Division, Winston-Salem, NC

LUMBAR SPINE

Sagittal T1, T2, and STIR	
Coverage:	Left-right coverage: complete pedicle to complete opposite pedicle. Superior-Inferior coverage: T12-S2.
Slice Thickness:	≤ 5.0mm

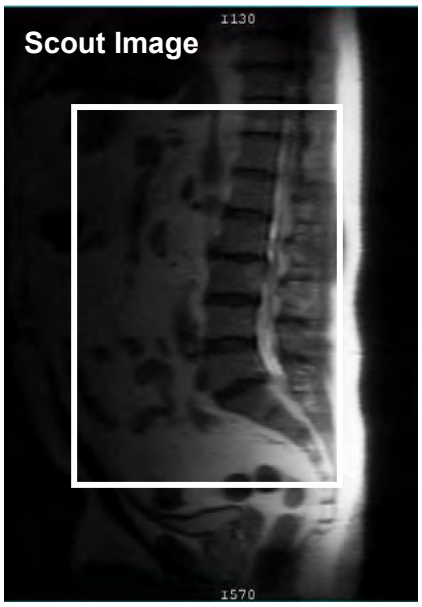

Courtesy of Fairfax Technical Community College, Health Technologies Division, Winston-Salem, NC

LUMBAR SPINE

Axial T1 or T2	
Coverage:	Slices may be contiguous or angled. Must cover L3-L4, L4-L5, and L5-S1. Angled slices should completely traverse the intervertebral disk space.
Slice Thickness:	≤ 4.0mm

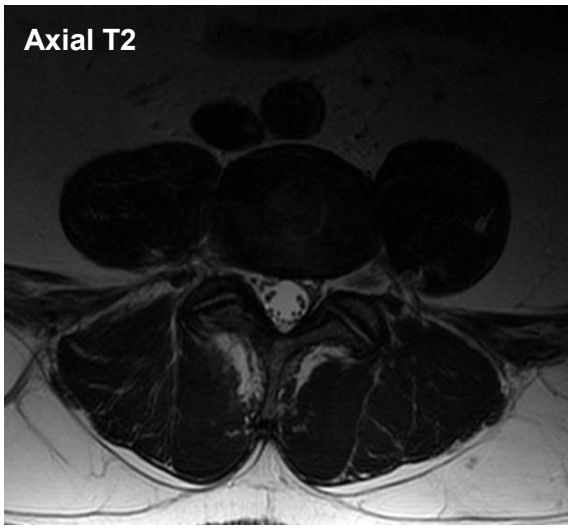

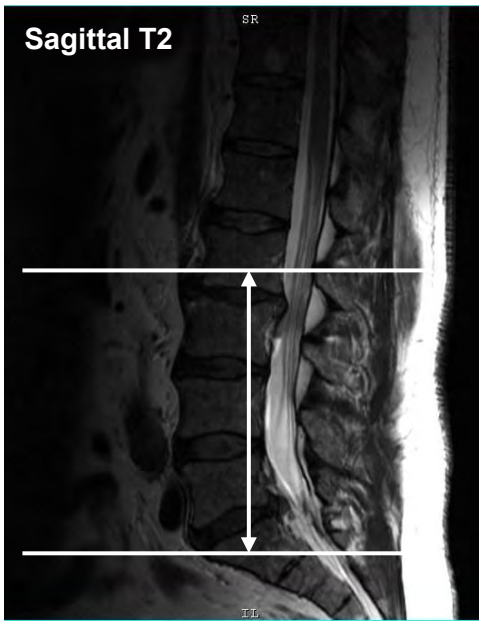

Optional Coronal T1 or T2 for severe scoliosis	
Coverage:	In cases of severe scoliosis, a coronal series may be useful. Anterior-posterior coverage is from most posterior spinous process through the anterior portion of the most anterior vertebral body.
Slice Thickness:	≤ 4.0-5.0mm

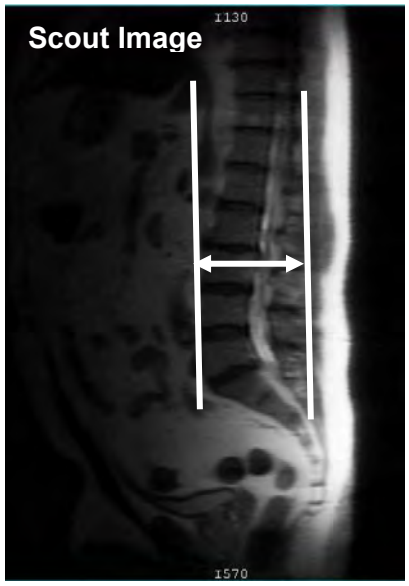

SACRUM, COCCYX, and SACROILIAC JOINTS

Sagittal T1, T2, and STIR	
Coverage:	From and including each sacro-iliac (SI) joint and from L5 to below the coccyx
Slice Thickness:	4.0mm

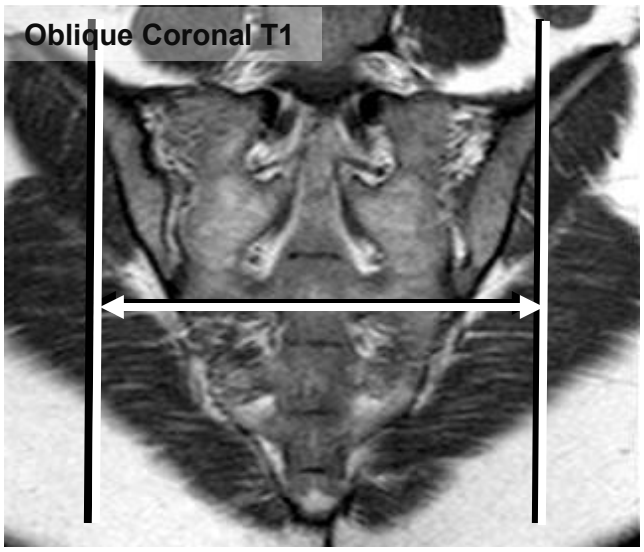

Oblique Coronal T1, T2, and STIR or proton-density with fat suppression	
Coverage:	Parallel from posterior aspect of the sacrum through the anterior aspects of the coccyx and the L5-S1 vertebral disk space
Slice Thickness:	3.0-4.0mm

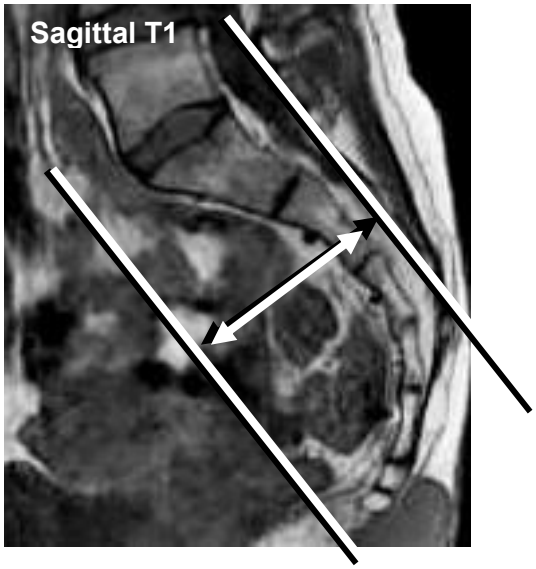

SACRUM, COCCYX, and SACROILIAC JOINTS

Oblique Axial, T2 and T1	
Coverage:	Parallel from posterior aspect of the sacrum through the anterior aspects of the coccyx and the L5-S1 vertebral disk space.
Slice Thickness:	4.0mm

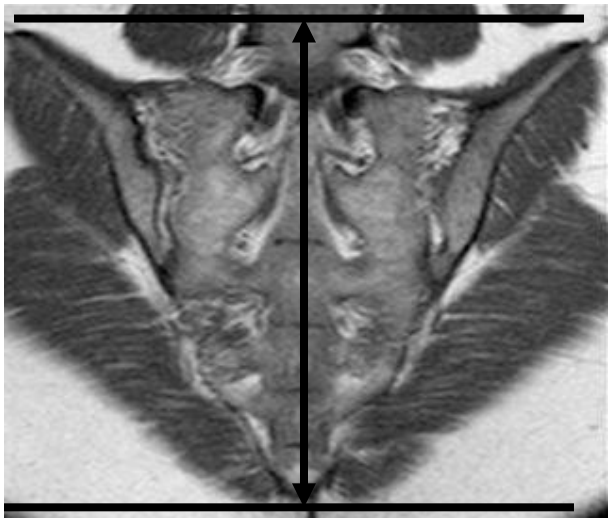

REFERENCES

1. Bridging the Blood-Brain Barrier: New Methods Improve the Odds of Getting Drugs to the Brain Cells That Need Them. Ferber D PLoS (Public Library of Science) Biology Vol. 5, No. 6, e169 doi:10.1371/journal.pbio.0050169.

2. FDA Safety Alert: MRI Related Death of Patient with Aneurysm Clip issued on November 25, 1992. Available at https://wayback.archive-it.org/7993/20170111190819/http:/www.fda.gov/MedicalDevices/Safety/AlertsandNotices/PublicHealthNotifications/ucm242613.htm.

3. Garel C. MRI of the Fetal Brain: Normal Development and Cerebral Pathologies. Berlin Heidelberg, Germany: Springer-Verlag, 2004.

4. Garel C. MRI of the Fetal Brain: Normal Development and Cerebral Pathologies. Berlin Heidelberg, Germany: Springer-Verlag, 2004.

5. Moore KR, Tsuruda JS, Dailey AT. The value of MR neurography for evaluating extraspinal neuropathic leg pain: a pictorial essay. AJNR Am J Neuroradiol. 2001;4:786-794.

GLOSSARY AND ABBREVIATIONS OF TERMS

agenesis
lacking or failing to develop, eg, agenesis of the corpus callosum

amplitude
the magnitude or intensity of change in an oscillating variable; the width of a wave form. In MR, the amplitude of the gradient field is measured in mT/m.

aneurysm
ballooning out of a segment of a vein or artery resulting from disease or weakness of the vessel wall

annulus fibrosus
the tough covering on the outside of the intervertebral disk

atlas
the first cervical vertebrae

axonal
nerve-cell process that usually transmits impulses away from the cell body

B_0 or B-zero
the main magnetic field that represents the direction and strength of magnetic force; measured in tesla

bifid
double, split

blood-brain barrier (BBB)
a naturally occurring barrier that separates the circulating blood and brain extracellular fluid in the central nervous system. Occurs along the capillaries and consists of tight junctions around capillaries that do not exist in normal circulation outside of the brain. Inhibits passage of certain materials from the blood into brain tissue.

caput medusae
appearance of distended or engorged veins

cauda equina
the end of the spinal cord near the L1 level; also known as the conus

cerebritis
an inflammation of the cerebellum that often leads to the formation of an abscess within the brain itself

cerebrospinal fluid (CSF)
the serum-like fluid that circulates through the ventricles of the brain, the cavity of the spinal cord, and the subarachnoid space

cervical spine
the first seven vertebrae just below the skull

cine
in MR, the recording of images in such a rapid fashion that the images can be displayed in a movie-loop to demonstrate real-time movement or function as with cardiac imaging or rapid contrast-up-take imaging

coalesce
to come together in a single mass or body

coccyx
most distal part of the vertebral spine and made up of typically four small fused vertebral bodies, though having one less or one more is not uncommon

demyelination
destruction of the normal nerve myelin sheath

deoxyhemoglobin
reduction of hemoglobin in venous blood through normal cellular processes or certain disease processes such as hemorrhagic stroke

dephasing
the loss of phase coherence in the transverse plane due to T2 processes

dural space
the outermost layer of the meninges (the system of membranes that envelope the central nervous system) surrounding the brain and spinal cord; the dural space is the area between the dura mater and the arachnoid space

echo time (TE)
also time-to-echo and echo delay time; time interval between the initial RF pulse and the first echo of a pulse sequence

empyemas
accumulation of pus in a body cavity

encephalitis
inflammation of the brain

ependymal
pertaining to the membranes lining the ventricles of the brain and the central canal of the spinal cord

extraaxial
outside the brain tissue in the dural space, sinuses, along the vasculature, or in the skull itself

exudates
the protein-rich fluid that flows from injured or diseased tissues

field-of-view (FOV)
area of tissues to be imaged. Decreasing FOV (all other parameters remaining the same) increases spatial resolution but reduces signal-to-noise ratio.

foramen/foramina
in the spine, the opening or canal through which the spinal cord runs; begins at C1 and continues inferior to L5

Gauss (G)
unit of magnetic field strength. 10,000 G is equivalent to 1.0 tesla

hematoma
an area of blood collection, often clotted

hemosiderin
an insoluble form of intracellular storage iron

herniate, herniation
in the spine, when a bulging or tear in the annulus fibrosus of an intervertebral disc allows the nucleus pulposus to bulge out beyond; commonly referred to as a "slipped disk"

heterotopia
the displacement of an organ from its normal position

infarct/infarction
a necrotic area of tissue caused by loss of blood flow

inhomogeneity
absence of homogeneity or uniformity; inhomogeneity in a magnetic field may occur as one area of the field deviates from the average magnetic field strength. Lack of magnetic field homogeneity is a major cause of poor image quality in MRI.

intraaxial
occurring inside the brain tissue itself

isointense
low signal contrast between tissues such that they are difficult to distinguish

inversion time (TI)
the time interval from the execution of the 180^0 RF excitation pulse to the initial 90^0.
k-space the domain in which the information from each phase-encoding step is placed during a pulse sequence prior to Fourier Transform. Each "filled in" line of k-space corresponds to each phase-encoding step; once the required amount of k-space is filled, image reconstruction with a Fourier Transform can begin.

lentiform
lenticular; convex on both sides

lumbar spine
the five vertebrae that support most the weight of the body above the waist

lumbosacral plexus
four pairs of foramina in the sacrum allow spinal nerves to pass through to the sacrum

lyse
to break up or disintegrate, as in the breakdown of red blood cells

magnetization transfer imaging (MTI)
the transfer of longitudinal magnetization from the hydrogen nuclei of water that have restricted motion to the hydrogen nuclei of water that move with many degrees of freedom

mass effect
usually described in the brain, it is the visualization of brain tissue being displaced by some invading disease process such as a malignant tumor

metastasis/es
tumor growth arising because of the transfer of cells from the primary tumor to an unrelated body area; all malignant tumors are capable of metastasis. Also called secondary tumor

methemoglobin
a compound formed from hemoglobin by oxidation. A small amount is found in the blood normally, but injury or toxic agents convert a larger proportion of hemoglobin into methemoglobin, which does not function as an oxygen carrier.

myelomeningocele
a birth defect in which the bony spine and spinal canal do not close before birth. The condition is a type of spina bifida.

myelopathy
any disease of the spinal cord itself, eg, multiple sclerosis

necrosis
cellular or tissue death due to disease or trauma

non-ferrous
not related to or containing iron

nucleus pulposus
jelly-like material in the middle of the spinal disk

number of excitations (NEX)
or number of signal averages (NSA) number of image acquisitions per tissue slice that occur during an MRI scan; also known as averaging (AVG)

oblique
any plane used in MR imaging that is not orthogonal to the x, y, or z axes

orthogonal
pertaining to or involving right angles. In MRI, any imaging plane that is parallel to the x, y, or z planes

osteomyelitis
a bone infection usually caused by bacteria

odontoid process
protuberance of bone projecting superiorly from the body of the 2nd cervical vertebrae

oxyhemoglobin
combination of oxygen and hemoglobin in arterial blood

parenchyma
the functional tissue of any organ vs. its structural (supporting or connective) tissue

patency
the state or quality of being open, expanded, or unblocked, as in a patent vessel

pathognomonic
characteristic or diagnostic of a particular disease

petechial
pertaining to tiny red or purple spots caused by discharge of blood into the tissue

petrous
the very dense, hard portion of the temporal bone that forms a protective case for the inner ear

punctate
characterized by dots or points

quiescent
being quiet, still, or at rest

radiculopathy
any disease of the spinal nerves roots and characterized by pain “radiating” away from the source, eg, herniated vertebral disk

repetition time (TR)
time interval from the beginning of one pulse sequence to the beginning of the next. Used to control the amount of T1 contrast desired in the resultant image.

retrograde
moving or tending backward

rise time
the time for a gradient field to move from the equilibrium point to the desired amplitude; typically measured in milli-seconds

sacrum
five large fused vertebral bodies (S1-S5) just distal to the lumbar spine that form a singular large triangular bone that is widened at the superior end and gradually narrows to an apex; inferior to the lumbar spine

scar tissue
in the spine, the formation of epidural tissue as part of the healing process following spinal surgery; can be a cause of recurrent spinal symptoms if scar tissue impinges on the spinal cord of exiting nerve roots

scoliosis
lateral curvature of the spine

sella turcica
saddle-shaped depression in the sphenoid bone of the human skull that contains the pituitary gland

sequelae
an abnormal condition resulting from a previous disease

shear injury
the stretching and/or tearing of individual axons caused by traumatic brain injury

signal-to-noise ratio (SNR)
amount of true signal relative to the amount of background signal (noise) on an image

slew rate
the calculated slope of a gradient field with regard to its amplitude and rise time. Calculated by the amplitude divided by the rise time and usually reported in units of mT/m/sec.

specific absorption rate (SAR)
the RF power absorbed per unit of mass of an object, measured in watts per kilogram (W/kg). Current FDA SAR limits for the head are 3 W/kg averaged over the head for any 10-minute period, 4 W/kg for the body over a 15 min period, and 8 W/k for extremities over a 5 minute period.

spina bifida
a range of malformations that includes deformities of the certain parts of the vertebrae, the spinous process, and vertebral arch; a failure of those bones to fuse during early fetal development and the most common congenital spine abnormality

stenosis
abnormal narrowing of a vessel

syrinx
an abnormal collection of fluid within the spinal cord

Tesla (T)
the preferred (SI) unit of magnetic field strength. One tesla equals 10,000 Gauss, the older, conventional unit. Current range for patient is imaging is 0.3T – 3.0T. Named for the “Father of Physics,” Nicola Tesla (1856-1943) from Croatia, for his contributions to the field of electricity and magnetism.

thoracic spine
the 12 vertebrae inferior to the cervical spine and just superior to the lumbar spine

thrombosis
the formation of a blood clot

tinnitus
a sensation of ringing or roaring caused by disturbance of the auditory nerve

turbid
clouded or opaque

vortex flow
a complex flow pattern caused by turbulence along the path of the flow; a spiral flow of fluid

ABBREVIATIONS OF TERMS

AVM	arteriovenous malformations	**MS**	multiple sclerosis
BBB	blood-brain barrier	**MTI**	magnetization transfer imaging
B_0	B-zero	**mT**	millitesla
BOLD	blood oxygen-level dependent	**mT/m**	millitesla/meter
CSF	cerebrospinal fluid	**NEX**	number of excitations
DAI	diffuse axonal injury	**NSA**	number of signal averages
DNET	dysembryoplastic neuroepithelial tumors	**PD**	proton density
DTI	diffusion tensor imaging	**PML**	progressive multifocal leukoencephalopathy
DVA	developmental venous anomaly	**rCBF**	relative cerebral blood flow
DWI	diffusion-weighted imaging	**rCBV**	relative cerebral blood volume
EPI	echo planar imaging	**SAR**	specific absorption rate
ESP	echo-spacing	**SE**	spin echo
ETL	echo train length	**SNR**	signal-to-noise ratio
FOV	field-of-view	**SPGR**	spoiled gradient echo
FLAIR	fluid-attenuated inversion recovery	**STIR**	short tau inversion recovery
fMRI	functional MRI	**SWI**	susceptibility-weighted images
FSE	fast spin echo	**T**	tesla
G	Gauss	**T1W**	T1-weighted
GRE	gradient echo	**T2W**	T2-weighted
HNP	herniated nucleus pulposus	**T2'**	T2 prime
IAC	internal auditory canal	**T2***	T2 star
kW	kilowatt	**TBI**	traumatic brain injury
MIP	maximum intensity projection	**TE**	echo time
mm	millimeter	**TI**	inversion time
msec	microsecond	**TOF**	time-of-flight
MRA	magnetic resonance angiography	**TR**	repetition time
MRS	magnetic resonance spectroscopy	**TSE**	turbo spin echo
MRV	magnetic resonance venography	**µs**	micro-second or 1/1000 of a millisecond